Compositions and mobility of major, δD, $\delta^{18}O$, trace, and REEs patterns in water sources at Benue River Basin-Cameroon: Implications for recharge mechanisms, geo-environmental controls and public health

Wilson Y. Fantong[1], Therese L.L. Jokam Nenkam[2], Pierre Nbendah[2], Sharon B. Kimbi[3], Ernest Chi Fru[4], Brice T. Kamtchueng[1], Alain F. Takoundjou[1], Alex R. Tejiobou[5], Gabriel Ngueutchoua[6], Robert Kringel[2,7]

[1]Institute of Geological and Mining Research (IRGM), Hydrological Research Centre, Box 4110 Yaoundé, Cameroon

[2] PRESS NO & SW, P.O. Box 169 Yaoundé, Cameroon

[3] Hiroshima University 1-4-1 Kagamiyama, Higashi-hiroshima, Hiroshima-Japan, 739-8527

[4] School of Earth and Ocean Sciences, Institute of Geochemistry and Geobiology, Cardiff University, Cardiff, Park Place, Wales, United Kingdom

[5]Department of Geography, University of Yaoundé 1, P.O. Box 812, Yaoundé, Cameroon

[6]Department of Earth Sciences, University of Yaoundé 1, P.O. Box 812, Yaoundé, Cameroon

[7]Federal Institute of Geoscience and Natural Resources (BGR), Hanover-Germany

Corresponding author: fyetoh@yahoo.com; fantongy@gmail.com

Hydrogeochemical data are required for understanding of water quality, provenance and chemical composition for the 2117700 km^2 Niger River Basin. This study presents hydrogeochemical analysis of the Benue River Basin, a major tributary of the Niger River. The distribution of, major ions, Si, δD and $\delta^{18}O$, Trace and Rare Earth Elements (TE and REEs, respectively) composition in 86 random water samples, revealed mixing of, groundwater with surface water to recharge shallow aquifers by July and September rains. Equilibration of groundwater with kaolinite, and montmorillonites by, incongruent dissolution imprints hydrochemical signatures that vary from Ca+Mg-NO_3 in shallow wells to Na+K-HCO_3 in boreholes and surface waters, with undesirable concentrations of fluoride identified as major source of fluorosis in the local population. Our results further indicate non-isochemical dissolution of local rocks by water, with springs, wells and borehole waters exhibiting surface water-gaining, weakest water-rock interaction, and strongest water-rock interaction processes, respectively. Poorly mobile elements (Al, Th and Fe) are preferentially retained in the solid residue of incongruent dissolution, while alkalis, alkaline earth and oxo-anion-forming elements (U, Mo, Na, K, Rb, Ca, Li, Sr, Ba, Zn, Pb) are more mobile and enriched in the aqueous phase, whereas transition metals display an intermediate behaviour. Trace elements vary in the order of Ba > Sr > Zn > Li > V > Cu > Ni > Co > As > Cr > Sc > Ti > Be > Pb > Cd, with Potentially Harmful Elements such as Cd, As, and Pb mobilized in acidic media attaining near undesirable levels in populated localities. With the exception of Y, REEs distribution in groundwater in the order of Eu > Sm > Ce >Nd > La > Gd > Pr > Dy > Er > Yb > Ho > Tb > Tm, differ slightly with surface water composition. Post-Archean Average Australian Shale normalized REEs patterns ranging from 1.08-199, point to the dissolution of silicates as key sources of trace elements to groundwater, coupled to deposition by eolian dust.

Keywords: *Recharge periods; Relative mobility of elements; Water-rock interaction; Public health; REEs; Benue River Basin.*

Compositions and mobility of major, δD, $\delta^{18}O$, trace, and REEs patterns in water sources at Benue River Basin-Cameroon: Implications for recharge mechanisms, geo-environmental controls and public health

Wilson Y. Fantong[1], Therese L.L. Jokam Nenkam[2], Pierre Nbendah[2], Sharon B. Kimbi[3], Ernest Chi Fru[4], Brice T. Kamtchueng[1], Alain F. Takoundjou[1], Alex R. Tejiobou[5], Gabriel Ngueutchoua[6], Robert Kringel[2,7]

[1]Institute of Geological and Mining Research (IRGM), Hydrological Research Centre, Box 4110 Yaoundé, Cameroon

[2] PRESS NO & SW, P.O. Box 169 Yaoundé, Cameroon

[3] Hiroshima University 1-4-1 Kagamiyama, Higashi-hiroshima, Hiroshima-Japan, 739-8527

[4] School of Earth and Ocean Sciences, Institute of Geochemistry and Geobiology, Cardiff University, Cardiff, Park Place, Wales, United Kingdom

[5]Department of Geography, University of Yaoundé 1, P.O. Box 812, Yaoundé, Cameroon

[6]Department of Earth Sciences, University of Yaoundé 1, P.O. Box 812, Yaoundé, Cameroon

[7]Federal Institute of Geoscience and Natural Resources (BGR), Hanover-Germany

Corresponding author: fyetoh@yahoo.com; fantongy@gmail.com

Abstract

Hydrogeochemical data are required for understanding of water quality, provenance and chemical composition for the 2117700 km^2 Niger River Basin. This study presents hydrogeochemical analysis of the Benue River Basin, a major tributary of the Niger River. The distribution of, major ions, Si, δD and $\delta^{18}O$, Trace and Rare Earth Elements (TE and REEs, respectively) composition in 86 random water samples, revealed mixing of, groundwater with surface water to recharge shallow aquifers by July and September rains. Equilibration of groundwater with kaolinite, and montmorillonites by, incongruent dissolution imprints hydrochemical signatures that vary from Ca+Mg-NO_3 in shallow wells to Na+K-HCO_3 in boreholes and surface waters, with undesirable concentrations of fluoride identified as major source of fluorosis in the local population. Our results further indicate non-isochemical dissolution of local rocks by water, with springs, wells and borehole waters exhibiting surface water-

gaining, weakest water-rock interaction, and strongest water-rock interaction processes, respectively. Poorly mobile elements (Al, Th and Fe) are preferentially retained in the solid residue of incongruent dissolution, while alkalis, alkaline earth and oxo-anion-forming elements (U, Mo, Na, K, Rb, Ca, Li, Sr, Ba, Zn, Pb) are more mobile and enriched in the aqueous phase, whereas transition metals display an intermediate behaviour. Trace elements vary in the order of Ba > Sr > Zn > Li > V > Cu > Ni > Co > As > Cr > Sc > Ti > Be > Pb > Cd, with Potentially Harmful Elements such as Cd, As, and Pb mobilized in acidic media attaining near undesirable levels in populated localities. With the exception of Y, REEs distribution in groundwater in the order of Eu > Sm > Ce >Nd > La > Gd > Pr > Dy > Er > Yb > Ho > Tb > Tm, differ slightly with surface water composition. Post-Archean Average Australian Shale normalized REEs patterns ranging from 1.08-199, point to the dissolution of silicates as key sources of trace elements to groundwater, coupled to deposition by eolian dust.

Keywords: *Recharge periods; Relative mobility of elements; Water-rock interaction; Public health; REEs; Benue River Basin.*

Introduction

Scientific background and objectives

The 1400 km long Benue River Basin (BRB) located in the Sahel zone of Northern Cameroon is a major tributary of the Niger River (NR) (Fig.1) marked by a mean aridity index (log [potential evapotranspiration/mean annual rainfall]) of 0.47, and a budyko aridity ratio (solar radiation/amount of rainfall) Budyko (1951) of 2.8. These semi-arid climatic conditions cause surface water scarcity, leaving an estimated 2,500,000 inhabitants to depend on groundwater resources and ephemeral streams for domestic and irrigation purposes. Hence the present study is focused on understanding dry season hydrogeochemical dynamics as the main driver of physical water scarcity-related problems in the BRB. Moreover, the location of the BRB at the upstream of the 2117700 km^2 Niger River Basin, makes Cameroon to be a strategic riparian state for integrated and transboundary water resources management amongst the stakeholders of the Niger Basin Authority (NBA).

In order to make useful contributions to the NBA, Cameroon has to furnish comprehensive spatial and temporal data on the chemistry and quantity of water resources in the BRB. In response to the need of generating such data, research work in the BRB has led to exploration of stable environmental isotopes (δD and $\delta^{18}O$) and chloride

content in rainwater (Njitchoua et al. 1995), geochemistry, origin and recharge mechanisms of groundwaters in the Garoua Sandstone aquifer in Northern Cameroon (Njitchoua et al. 1997) and climate hydrology and water resources in Cameroon (Molua 2006). Despite increased knowledge on water resources in the study area, the existing data still present the gaps related to (i) major ions and stable environmental isotope data for δD and $\delta^{18}O$ generated more than 15 years ago, which fall short of presenting an up-to-date information on water chemistry and groundwater recharge periods, respectively. (ii) There is total absence of data on trace elements (TE) and rare earth elements, thus, obscuring important information on hydrogeochemical and geo-environmental dynamics. (iii) The available data are only on the Garoua sedimentary basin, excluding the other five sedimentary basins (Babouri Figuil, Mayo Oulou Lere, Hamakoussou, Benue, and Koum), which are all in the BRB (Fig. 1).

To underscore the feasibility of generating data on water chemistry and its applications, major ions have been used to elucidate groundwater chemistry as a function of water-rock interaction processes (Thomas et al. 1989; Petrides et al. 2006; Srinivasamoorthy et al. 2008), usability for drinking (Nagaraju et al. 2006), and sources of health problems such as fluorosis (e,g., Fantong et al. 2010b). Reporting these characteristics on a river basin scale has also been useful in groundwater supply planning in semi-arid regions (Goni 2006). For surface and groundwater resources to be managed sustainably in semi-arid regions, their origin (e.g., Scalon et al. 2006) and renewability (Leduc et al. 1996; Houston 2007; Shivanna et al. 2008) are important requirements, which can be determined by using the isotopic compositions of oxygen and hydrogen in rain, surface and groundwater (e.g., Azzaz et al. 2008; Goni 2006; Fantong et al. 2010a; Tsujimura et al. 2007; and Edmunds et al. 2002).

In the recharge pathway from rain to groundwater, water molecules interact with minerals that circulate as dust particles in the atmosphere and those within the lithosphere by water-rock interaction, which can also alter the water chemistry by adding TE and REEs (e.g., Rollinson 1993, Vazquez-Ortega et al. 2015; Migaszewski and Galuszka, 2015). Interestingly, "Rare Earths" is a misnomer because they are neither 'earths' nor 'rare', especially as the Earth's upper crust contains 0.015% REEs (Taylor and McLennan 1985), which are referred to as lithophile group 3 lanthanide with atomic numbers 57 (Lanthanum) to 71(Lutetium) and two additional elements, Yttrium (Z=39) and Sc (Z=21). However, most Earth scientists exclude Sc from this group due to its small ionic radius, and classify only lanthanides and Y (with ionic radius similar to that of the REE Ho) into the REEs. Except for Ce (Ce^{3+}, Ce^{4+}) and Eu (Eu^{2+}, Eu^{3+}), the REEs are trivalent, and their ionic radii decrease with increase of atomic number, from 103 pm in La^{3+} to 86 pm in Lu^{3+} ("well known as the lanthanide contraction"). This attribute governs the subtle differences in the REEs geochemical behavior as their respect for the Oddo-Harkins rule provides the basis for dividing the REEs into the following groups: (i) light REE (LREE) including La through Eu or Gd, (ii)

85 medium REE (MREE) that comprises Sm through Ho , and (iii) heavy REE (HREE) from Gd or Tb to Lu including
86 Y (Migaszewski et al. 2014).

87 The diagnostic conservative characteristics of the REEs have made them the most useful of all trace elements in
88 igneous, sedimentary and metamorphic petrology (e.g., Migaszewski and Galuszka 2015; Johannesson and Lyon
89 1995; Gimeno et al. 2000; Gammons et al. 2005b; Rollinson 1993; Ndjigui et al. 2014; Houketchang Bouyo et
90 al. 2015), and also in characterizing surface and groundwater geochemistry (e.g., Rollinson 1993; Vazquez-Ortega
91 et al. 2015; Liu et al. 2016; Migaszewski et al. 2014; Chen and Gui 2017; Guo et al. 2010; Munemoto et al. 2015;
92 Pignotti et al. 2017; Zhuravlev et al. 2016; Ferreira et al. 2015; Sultan and Shazili 2009; Censi et al. 2017). Some
93 of the hydro-geochemical signatures that have been underpinned by the REEs include; geo-environmental controls
94 of REEs patterns in surface and groundwater, paleoclimatic conditions, redox and pH conditions, groundwater
95 flow paths, mixing between surface and groundwater, geogenic and anthropogenic inputs into water resources,
96 and water-rock interaction processes.

97 To underpin water-rock interaction processes, the work of Ferreira et al. (2015), and associated references, have
98 shown that groundwater exhibits signatures that closely resemble those for the rocks through which they flow,
99 whereas other investigations (e.g., Masuda et al. 1987; Takahashi et al. 2002) found that REEs pattern in
100 groundwater exhibits the W-type tetrad effects, while the rocks through which they flow exhibit M-type tetrad
101 effects. Despite such usefulness of REEs in hydro-geochemistry, only the work of Ndjigui et al. (2014), has so far
102 attempted to use REEs to characterized water resources in Cameroon**.** Furthermore, still as a results of water-rock
103 interaction, it has just been over two decades that the International Working Group on Geomedicine (IWGG),
104 now reconstituted into the International Medical Geology Association (IMGA), formalized the study of medical
105 geology as a research discipline, which has continued to develop into a fast-evolving scientific field on the global
106 scene. This is because a tremendous upsurge in research efforts is leading to the decipherment of hitherto “new
107 correlation”, spurring fresh promise for success of this science.

108 Consequently, collaboration between geoscientists and medical researchers has led to the identification of
109 potential environmental health problems. In Cameroon, for instance, a link between the chemistry of groundwater
110 for drinking and human health, seems highly plausible, given that majority of the country’s population still lives
111 close to the land, subsisting largely on water obtained from their immediate surroundings (Davis 2013 and
112 references there-in). This has caused water-borne diseases such as fluorosis (Fantong et al. 2009; 2010b), whose
113 science and management still require upscaling in Cameroon. Although, the German-Cameroon project code

named “PRESS NO and SW”, presents a pilot study on pollution of surface and groundwater in the study area (Jokam Nenkam et al. 2019), the data are only as a technical report.

Against this backdrop, the overall objective of this study is to evaluate the characteristics of water resources in the Benue River Basin in Northern Cameroon, by using a combination of major ions, δD, $\delta^{18}O$, TEs and REEs. The specific objectives include (1) assessing water chemistry and suitability for drinking, (2) identify groundwater recharge periods and pathways, and (3) characterize REEs patterns for the water resource management in the BRB, with a wider implications for sustainable livelihoods and ecosystem services management in the Niger River Basin (NRB).

Location, drainage, relief and climate of study area

The study area (Fig. 1) is administratively located in the Cameroon’s Northern Region, which is bordered to the north, south, east, and west by the Far Northern Region, the Adamawa Region, the Republic of Chad, and the Federal Republic of Nigeria, respectively. Geographically, the study area is located between latitudes 8° and10°N and longitudes 12° and 16°E, with a surface area of 66 263 km². Hillocks by the Mandara, Adamawa Plateaux, and Poli - Alantika Mountains in the north, south and west, respectively, culminate in a maximum height of 1189 m.asl, and drops of 165 m.asl. Such a topographic gradient permits the tributaries of river Benue to rise and flow dendritically towards the west to Nigeria (Hervieu 1969). The hydrological network of the Benue River Basin in Cameroon (Fig. 2), is an upstream catchment of River Niger (Fig. 1) . The principal streams that drain BRB are the Mayo Rey and Mayo Godi in the west, the Mayo Louti, Mayo Kebi and Mayo Tiel in the north, and the Faro and Mayo Deo in the south. At the basin midstream is the artificial Lagdo dam that occupies a surface area of about 700 km^2 and has a capacity to retain 7.7 billion m^3 of water for irrigation and hydro-electricity (Blanken and Pecher 2013). During dry months, the surface of the draining channels of almost all the tributaries (except for the Faro and Kebi) run dry, but with underflow at depths of about 0.5 m. Such ephemeral characteristic of the streams obliges the population to depend and rely on groundwater resources for domestic and subsistent agriculture for most part of the year.

With respect to climate, the study area is situated in a semi-arid Soudano-Sahelian climatic zone, with a mean annual temperature of 28°C, maximum atmospheric temperature of 45°C that drops to about 19°C in December (Molua 2006). The area is characterized by a rainy and dry season. The rainy season lasts for about 5 months (May to September), and seven months (October-April) for the dry season. The mean annual rainfall has reduced from 1018 mm of rain between 1951-1989 (Njitchoua et al. 2005) to 950 mm in 2000-2014, with about 70 %

concentrated between July and September. Rainfall occurs either as low altitude monsoon rains or as occasional high altitude squally showers. Despite the high amount of annual rainfall, contribution to groundwater recharge remains limited because of the incidence of high annual evapotranspiration of 1800 mm, about twice the mean annual rainfall. During the dry season, the harmattan winds blow from the Sahara in the north, causing an estimated 48 % low humidity, and cloud of harmattan eolian dust (Fig. 3). During the rainy season, moisture-laden winds blow from the Gulf of Guinea in the south, bringing higher humidity and rain which flows as runoff into rivers, draining the basin dendritically.

Geological and hydrogeological settings

The Benue River Basin, which is an extension of the Cretaceous to Quaternary marine and continental sediments in Benue trough, constitutes six (Koum, Benue, Garoua, Babouri Figuil, Mayo Oulo-Léré, and Hamakoussou) sub sedimentary basins of carbonated, ferruginous, siliceous and phosphatic sandstones, mudstones, limestone, conglomerates, and alluvial deposits (Nolla et al. 2015; Zaborski et al. 2004; Bessong 2012; Schwoerer 1965; Ntsama et al. 2014; Maurin and Guiraud 1989; Eyong et al. 2013; Brunet et al. 1988; Tillement 1972; Ntsama et al. 2014), that are intruded by basaltic rocks, and they unconformably overlay Neo-Proterozoic basement (Fig. 1) (Ntsama 2013). A N-S cross section of the Mayo-Oulo sedimentary basin is presented in Fig. 4a. The dominant geochemical processes that occur in the basin are compaction, inter-grain pressure, fracturing, precipitation of calcite and hematite cements, kaolinization, and quartz overgrowth (Fig. 4b), which to an extend affects the hydrogeology of the basin by decreasing sediment porosity and permeability together with low groundwater recharge, reduces aquifer yields. According to Bouyo et al. (2015), chondrite normalized plots show enrichment in LREE relative to HREE with an almost flat pattern and slight negative Eu anomaly.

To the southwestern border of the study area is the Adamawa massif from where some of the first order tributaries of river Benue originate, and according to Ndjigui et al. (2014), the rock types on this massif do not only exhibit positive Eu anomaly, but are also rich in vivianite ($Fe_3(PO_4)_28H_2O$ (Fodoue et al. 2015).

In the plains of the Benue river and its tributaries, Quaternary alluvial deposits (sand, gravel and clay) of the Garoua sedimentary basin, with some description in Tillement (1972) and Njitchoua et al. (1995), constitute shallow and unconfined aquifers with transmissivities of 10^{-1} to 10^{-5} m^2/s in the upper horizon, which also provides surfaces on which the harmattan aeolian dust from the Sahara desert accumulates.

Materials and methods

171 Sampling campaign was undertaken in January (dry season period), during which 86 water samples were
172 randomly collected as shown in Figure 1. The number of samples included 37 from open wells with depths to
173 water ranging from 0.3 to 16.5 m, 34 from sealed wells and boreholes, 12 from surface water, including wadis
174 with depths to underflow from 0.5 to 1 m, and two from lakes. The samples were collected from the Garoua,
175 Benue, Hamakoussou, Mayo-Oulo Lere, and Babouri Figuil sedimentary basins (Fig. 1). Latitudal and longitudal
176 locations of the sample sites were predetermined in the entire catchment with the use of Google Earth, to enable
177 good spatial coverage of the basin for high-resolution hydrogeochemical analysis. Location and altitude were
178 determined on the field using a 3 m precision Garmin 64 Global Positioning System (GPS). Open wells were
179 sampled using drawing buckets anchored by ropes. Hand pump wells and boreholes were pumped for 5 - 15
180 minutes before sampling. The waters were collected into a collector after thorough rinsing with large volume of
181 sample water. Water from the collector was filled into four new 100 ml polyethylene bottles after rinsing with the
182 sample and one filtered through 0.45 µm cellulose filters and preserved unacidified for the determination of the
183 dissolved anions of SO_4^{2-}, Cl^-, F^-, Br^-, NO_3^-, NO_2^-, and PO_4^{3-} from each site. The second bottle was filled with
184 filtered and acidified water that was used for cations (Ca^{2+}, Mg^{2+}, Na^+, K^+, NH_4^+, and H_4SiO_4) and trace elements
185 (Fe^{2+}, Mn^{2+}, Al^{3+}, Pb, Cd, Ni, Zn, Cu, Ti, Sn, Mo, As, Co, Sb, Ba, U, Sr , La, Ce, Pr, Nd, Sm, Eu, Gd, Tb, Dy, Ho,
186 Er, Tm, Yb, Lu, and Y) determination. Acidification was done to pH~2 with supra-pure HNO_3 for the sampled
187 water. The third and fourth bottles for ^{18}O and ^{2}H and alkalinity determination were properly corked to avoid
188 evaporation. while the fourth bottle contained water that was used for alkalinity measurement. Electrical
189 conductivity (EC), pH, and water temperature were measured immediately in the field before sample collection,
190 using a Hanna made pH meter model HI 991001, pH/EC waterproof meter and a custom CT-450WR thermometer,
191 respectively. Atmospheric temperature was measured with a custom CT- 450WR thermometer. Land use, human
192 activities and rock type were noted at each sampling site using a mobile Open Data Kit (ODK) smartphone
193 application. Alkalinity measurements were carried out within 10 hours of sample collection by acid titration from
194 the volume of 0.02 N HCl added to the sample to reach the end -point titration, which was marked by a pH of 4.5.
195 Samples for anions, cations and TE, and stable environmental isotope determination were labeled, preserved in
196 ice-chilled boxes and dispatched to Federal Institute of Geoscience and Natural Resources (BGR), Hanover-
197 Germany for analyses.

198 Major elements (anions and cations) were quantified using a Spectro Ciros ICP-AES and a DIONEX ICS 3000
199 ion chromatography. Silica (H_4SiO_4) was analyzed by the molybdenum-blue method using spectrophotometry.
200 Stable environmental isotopes ratios were determined on a PICARRO cavity ringdown spectrometer (CRDS

model L2120-i), following the procedures described by Brand et al. (2009) and Lis et al. (2008).Trace elements, including the REEs content were measured on an Agilent 7500ce ICP-MS. Details on the analytical instrumentation and methods can be found in Birke et al. (2010). For the major elements, reliabilities of the chemical measurements were verified by using a charge balance equation (Appelo and Postma 1993), and they were within the limit of less than ±10 % for all the investigated samples. The obtained stable isotope ratios were given in the conventional delta (δ) expression in parts per mil (‰) relative to Vienna Standard Mean Ocean Water (VSMOW) with analytical precisions of ±1‰ for δD and ±1.5‰ for $\delta^{18}O$. For TEs, the analytical accuracy was checked from replicate measurement of several samples and by measuring the certified reference materials (CRM) standard of, River Water (SLRS-4), produced by the National Research Council of Canada. The detection limits were 1 ng/L for all REEs. Analytical precision for the REEs, except for Ce and Pr, was better than 5% relative standard deviation (RSD), with a 10 and 11 % RSD precision for Ce and Pr, respectively.

2.1. Data processing and quantification of REEs anomalies

Box and whisker plots were used to analyze the distribution of observed variables. All statistical analyses were performed with R software. Aquachem software was used to draw Pipers' diagram to identify water facies, and REE patterns and δD versus $\delta^{18}O$ space diagrams were drawn using Microsoft excel, while maps were established with ArcGIS version 10.2 and QGIS 2.18.X softwares.

Although the distribution and geochemical behavior of REEs in natural materials can be illustrated by plotting the relative abundances versus the atomic number, such a plot produces a saw tooth pattern (the Oddo Harkins Rule effects), with decreasing slope toward the highest atomic numbers. Thus, the REEs behavior is better presented if the values are normalized and reported as a relative abundance plot on a logarithmic scale . This means that the concentrations of REEs found in the sample are normalized to their concentrations in a reference material such as Cl chondrite, the chondritic meteorite, and the Post Archaean Australian Shales (PAAS) (Edet 2004). The advantage of this process is that the Oddo Harkins Rule effect is eliminated, and any fractionation that has occurred among the REEs will be detected. Hence, the abundance of positive peaks and negative troughs in the normalized REE pattern reflect the geochemical history of the sample. Generally, the abundance of REEs in natural waters is extremely low in comparison to the levels found in most rocks. In this investigation, the Post-Archean Average Australian Shale (PAAS) (McLennan 1989), was chosen as a reference standard because 'shales' are widely used in hypergene processes and environmental studies (Migaszewski et al. 2014) such as surface and shallow groundwater systems affected by weathering. Detection of anomalies is based on the presence of individual

elements that are higher or lower than the corresponding shale-normalized patterns. For example, Eu and Ce anomalies were quantified, according to Noak et al. (2014), in which the geogenic value of each element was obtained by interpolation of the neighbor normalized REE elements of Ce and Eu, by using the equations presented in equations (1) and (2), respectively.

$$Ce/Ce^* = Ce_{PAAS}/(La_{PAAS} + Pr_{PAAS})^{0.5} \quad \ldots\ldots(1)$$

$$Eu/Eu^* = Eu_{PAAS}/(Sm_{PAAS} + Gd_{PAAS})^{0.5} \quad \ldots\ldots(2)$$

It is worth mentioning that the last two indexes could be influenced in some situations by anomalies in La and Gd. Nevertheless, their calculation can be useful in discriminating sampled water types.

Results

Geochemistry

The laboratory results for the content of major cations and anions, including EC, pH, water temperature, δD, $\delta^{18}O$, TEs and REEs are presented in Tables 1a, 1b, and 1c, respectively. The elements data for rock in any of the Tables are from Ndjigui et al. (2014).

The data shows that water temperature ranged from 24.1 to 32.2°C and 23.9 to 32.3°C in surface and groundwater, respectively. In decreasing order, water temperature followed the pattern boreholes > hand dug wells > lakes > rivers > springs, with a mean value of 31°C, similar to groundwater temperature reported 22 years ago by Njitchoua et al. (1997). pH values ranged from acidic (5.7) to basic (8.9), declining according to the following trend, lake water > rivers > springs > boreholes > dug wells. Electrical conductivity (EC) showed a wide range from 35 to 2500 µS/cm, with mean values for surface and groundwater being 106 and 376 µS/cm, respectively, and varied in the observed sample as, dug wells > boreholes > rivers > lakes > springs.

The values of major ions (anions and cations) shows that concentrations are higher in groundwater samples than in surface water samples. Such observation depicts that the observed groundwater has a longer residence time in the aquifer than surface water (Kazemi et al. 2006), and that the hydrological regime is dominantly a stream loosing system by surface water recharging the groundwater aquifer. The concentration of anions were distributed in the order of $NO_3^- > HCO_3^- > Cl^- > SO_4^{2-} > F^- > PO_4 > Br^-$ in groundwater, compared to $HCO_3^- > NO_3^- > Cl^- > SO_4^{2-} > PO_4 > NO_2 > F^- > Br^-$ in surface water. Relative concentration of cations in both groundwater and surface water was in the order of $Ca^{2+} > Na^+ > Mg^{2+} > K^+ > NH_4$. Piper's diagram (Piper 1944) plots (Fig. 5) suggest,

that the hydro-chemical facies evolved predominantly from Ca+Mg-NO_3 rich water in shallow wells to Na+K-HCO_3 rich water in boreholes, and surface waters.

Stable environmental isotopes distribution

The δD values in ‰ ranged from -42 to -18 in boreholes, -32 to -16 in hand dug wells, -18 to 3 in rivers, and -27 in the only spring sample analysed. The $\delta^{18}O$ values in ‰ ranged from -6.62 to -2.94 in boreholes, -5.37 to -2.94 in hand dug wells, -3.37 to 0.55 in rivers, and -5.10 in the spring. The δD and $\delta^{18}O$ cross plots of these values are presented in the delta space (Fig. 6a). The Global Meteoric Water Line (GMWL) of Craig (1961), was used for comparative purposes because of the acute lack of regular rainfall measurements in the BRB. Deuterium excess (d-excess) values were more than 10 ‰ in ca.70 % groundwater (hand dug wells and boreholes) samples, with only the exception of one borehole that was > 15 ‰, whilst all surface waters were < 10 ‰ (Fig. 6b).

Trace elements (TEs and REEs) distribution

Selected trace elements concentrations are in the order of Ba > Sr >Zn > Li > V > Cu > Ni > Co > As > Cr > Sc > Ti > Be > Pb > Cd, in both groundwater and surface water samples, with relatively higher concentrations in groundwater compared to surface water. Figure 7 is a scatter plot of the average concentration of each metal in water and in BRB sandy clay. As purported by Aiuppa et al. (2000), a good correlation between the two variables suggests that composition of local sediments contribute to the water chemistry. Figure 7 also indicates that metal partitioning between the sediments and solution depends on the chemical behaviour of the elements. With respect to the general trend, Al, Fe, Ti, Ta, Hf, Ga, Y, Cr, and Zr appear to be depleted in water, due probably to their concentration in secondary product of weathering such as oxides and clays. On the contrary, the alkalis, alkaline earth and lithophile elements (Na, Mg, Ca, Sr) are shifted towards the lower axis, depicting their preferential solution during weathering. A similar trend is also observed for U and Mo, called "oxo-hydroxo anion forming elements" (indicated as OHA elements), due to their tendency to form water soluble anion complexes (Aiuppa et al. 2000). Transition metals plot in an intermediate position.

Individual REEs, total REEs, LREEs, HREEs, MREEs concentrations, as well as LREEs/HREEs ratios, selected raw data, and PAAS-normalized values presented in Table 1c, suggest REEs concentrations are generally low, and broadly consistent with circumneutral pH waters (e.g., Johannesson et al. 1999; Guo et al. 2010). Total REEs (ΣREEs) varied widely from 0.007 to15.02 µg/L with concentrations in boreholes, hand dug wells, rivers and spring from 0.044 to 2.12 µg/L , 0.086 to 0.36 µg/L, and 0.149 µg/L, respectively. With the exception of Y, the concentrations of REE in groundwater (boreholes and hand dug wells) followed the order Eu > Sm > Ce >Nd >

La > Gd > Pr > Dy > Er > Yb > Ho > Tb > Tm and these differed from the surface water rivers and spring trends with concentrations in the order of Eu > Sm > Ce > Nd > La > Gd > Pr > Dy > Tb > Er > Yb > Ho. The MREE (Sm-Ho) were the most abundant elements, followed by the LREE (La-Gd), with the HREE (Tb-Lu) being the least abundant

PAAS normalized REEs patterns

To enable comparison across the full suite of sample types, the REE concentrations were normalized with respect to Post-Archean Average Australian Shale (PAAS) (Fig. 8 a-g), employed extensively in groundwater studies (e.g., McLennan 1989; Sholkovitz et al. 1994; Tang and Johannesson 2006; Rollinson 1993). With exception of samples from boreholes 25 (BO 25) and 37 (BO 37) (Fig. 8b), which show a relatively monotonous flat pattern, all the waters mostly exhibit enrichment in the HREEs relative to the LREEs. Positive Eu anomalies ($Eu/Eu^* = Eu_{PAAS}/(Sm_{PAAS} + Gd_{PAAS})^{0.5}$) with values of 1.08-199 in boreholes, 6.26-171 in the hand dug wells, 72.9-107.6 in rivers and 30.58 in spring, impose a distinctly steep roof - shaped PAAS-normalized REE patterns, masking the commonly observed "W and M" types tetrad REE patterns.

Interpretation and discussion

Groundwater recharge mechanisms and period

With the low temperature (~24-32^{o}C) of water samples in the study area (Table 1a), the observed $\delta^{18}O$ and δD values can be regarded as conservative during water-rock interaction reaction (e.g., Gat 2010;Taylor and Howard 1996). Thus, the δ-values of the groundwater would be expected to be almost similar to that of the recharging meteoric water. Factors that can affect the recharging rainfall are soil-zone processes and direct heterogeneous/diffuse or localized/focused rainfall infiltration (Taylor and Howard 1996). The clustering of observed groundwater and surface water along the GMWL (Global Meteoric Water Line) in Fig. 6a indicates that soil-zone evaporation prior to rainfall infiltration is not a significant process in the area. However, a few surface water samples plot to the right of the GMWL, indicating that within the rainwater-surface water-groundwater system, the incidence of evaporation prior to groundwater recharge was not totally absent. Such a pattern suggests that in the study area, the mechanism of preferential flow pass (e.g. Tsujimura et al. 2007, Asai et al. 2010) dominates groundwater recharge after localized evaporation (Edmunds et al. 2002, Tsujimura et al. 2007, Fantong et al. 2010a). The suggestion of a preferential flow pass hypothesis indicates that irrespective of reduced porosity in the study area as (Fig. 4b) illustrates, local occurrences of effective porosity in the sand-rich sediment, which favors rapid infiltration of rainwater into the aquifer, cannot be totally denied. Similar recharge mechanism was

identified in part of the study area by Njitchoua et al. (1995), and in the Lake Chad (Fantong et al. 2010a), coastal (Fantong et al. 2016) sedimentary basins of Cameroon, and also in the semi-arid sediments in Mongolia (Tsujimura et al. 2007). The high d-excess in groundwater (with ca. 75 % of the groundwater samples having values above 10 ‰) does not only confirm direct infiltration of rainwater into the shallow aquifer (Kebede et al. 2005), but also suggests that groundwater recharge occurred under low relative humidity conditions (Kendall and Doctor 2011). The implications from the δ-space diagram (Fig. 6a) and d-excess (Fig. 6b) indicate hydraulic connectivity within the shallow aquifer that favors mixing between surface and the shallow groundwater over the entire region. A comparison of isotopic compositions between monthly local rainfall and groundwater on a δ-space can be employed to identify the period(s) of groundwater recharge (e.g., Mbonu and Travi 1994; Nkotagu 1996; Taylor and Howard 1996; Deshpande et al. 2003). The δ values for monthly rainfall co-opted from Njitchoua et al. (1995) and plotted together with measured (Fig. 6a) and as observed, the $\delta^{18}O$ and δD in groundwaters clustered between those of July and September abundant monsoon rains, indicating that the groundwater is predominantly recharged in the months of July and September. This groundwater recharge period is similar to that in the Lake Chad basin (Fantong et al. 2010a), but differs from the recharge period of June to August in the Lakes Monoun and Nyos volcanic aquifer (Kamnctueng et al. 2014), May to June in the Quaternary sediment in Ndop plain (Wirmvem et al. 2015), and May to September in the volcano-sedimentary aquifers of Mt. Cameroon and Douala (Fantong et al. 2016). As the rainwater circulates to recharge the groundwater, water-rock interaction occurs, which result in geogenic sources of ions in water (e.g., Faure 1991; Fantong et al. 2009; Fantong et al. 2010b) .

Geogenic controls on the chemical composition of water

Gibbs (1970) used the chemical composition of freshwater to identify major processes controlling dissolved ions in water based on the concentration of total dissolved solids (TDS) and $(Na^+ + K^+)/(Na^+ + K^+ + Ca^{2+})$ and $Cl^-/(Cl^- + HCO_3^-)$ ratios. Similarly, Gibbs diagram (Fig. 9) for sites dominantly within the rock domain, suggests incongruent dissolution of silicates as the provenance of Ca, Mg, Na, K, and HCO_3 to groundwater according to the following reactions (3), (4) and (5) (Nesbitt and Wilson 1992; Subramani et al. 2010; Faure 1991), which could be promoted by root respiration (Fantong et al. 2009):

$$CaAl_2SiO_2O_8 + 2CO_2 + 3H_2O = Al_2SiO_5\,(OH)_4 + Ca^{2+} + 2HCO_3 \quad \text{.....(3)}$$

$$2NaAlSi_3O_8 + 2H_2CO_3 + 9H_2O = 2Na^+ + 2HCO_3^- + Al_2Si_2O_5(OH)_4 + 4H_4SiO_4 \quad \text{.....(4)}$$

$$2KAl\,Si_3\,O8 + 2H^+ + 2H_2O = Al_2\,Si_2\,O_5\,(OH)_4 + 4SiO_2 + 2K^+ \quad \text{.....(5)}$$

Although such incongruent dissolution depicts that weathering of rock-forming minerals is a controlling factor for the major ion chemistry of groundwater in the area, the Ca and Na systems stability diagrams (Fig. 10 a-b) further clarify the equilibrium states between the secondary minerals and the circulating water (Tardy 1971; Appelo and Postma 1993). For example, the stability of albite, anorthite, kaolinite, and montmorillonite in the waters was evaluated in this study by plotting log (aNa^+/aH^+) vs Log (aH_4SiO_4) and Log ($a\ Ca^{2+}/a2H^+$) versus log (aH_4SiO_4). The diagrams were drawn with the assumption that Al was preserved in the weathering product (Appelo and Postma 1993; Faure 1991). End member compositions were also assumed using equilibrium relationship for standard temperature (25^{o}C) and pressure (1 atmosphere), which approximately reflect the groundwater conditions. Constituents' activities computed using Phreeqc for Windows version 2.1 (Appelo and Postma 1993), show that groundwater and surface water from the study area span the stability fields of Na-montmorillonite (Fig.10 a), Ca-montmorillonite (Fig.10 b), kaolinite and amorphous silica. These observations do not only concur with the occurrence of clay minerals in the study area, but are also similar to findings from areas such as the Lake Chad basin (e.g., Fantong et al. 2009) and the Lake Nyos catchment (e.g., Fantong et al. 2015), where granites constitute the fresh rock suites. Moreover, with saturation index (SI) it is possible to predict the reactive mineralogy of the subsurface from groundwater data without collecting the samples of the solid phase and analyzing the mineralogy (Deutsch 1997). The saturation index (SI) of a given mineral is defined in Eq. (6) (Garrels and Mackenzie, 1967) $SI = \log_{10}(IAP/Ksp)$……(6)

IAP is the ion activity product of the solution and Ksp is the solubility product at a given temperature (the thermodynamic equilibrium constant adjusted to the temperature of a given sample). The thermodynamic data used in this computation are those contained in the default database of the 'Phreeqc for Windows'. Supersaturation ($SI > 0$) indicates that precipitation is thermodynamically favorable. On the other hand, undersaturation ($SI < 0$) signifies that dissolution is favored. Using this guideline, a plot of SI against TDS indicates that all the samples were undersaturated with respect to gypsum and anhydrites relative to some crossing the undersaturation threshold into the supersaturation zone for the carbonates of calcite, aragonite, and dolomite (Fig. 10 c). This may reflect the incongruent re-dissolution of calcium carbonates that commonly occur as cementing material within the sediments as shown in Fig. 4b. However, the strong evidence for incongruent dissolution, imply favorable environmental conditions such as pH, reduction, oxidation, residence time, enabled the selective enrichment of water with major cations, Si, trace elements and REEs.

Geo-environmental controls and implications for REEs patterns

As shown in Figure 8, the REE patterns in groundwater (boreholes and hand dug wells) fall within the same range and are spatially the same as for surface waters (rivers, springs), where both show distinct but similar positive Eu positive anomalies. This similarity suggests that hydraulic connectivity between groundwater and surface water result in mixing. Further the generally flat PAAS normalized REEs pattern of samples BO37 and BO25 (Fig. 8b), is interpreted as groundwater sourced from deeper aquifer that do not mix with the surface water. Moreover, the clustering of groundwater $\delta^{18}O$ and δD values with surface waters (Fig. 6a) and their similar water chemistries support spatial mixing enabled by aquifer interconnectivity (Fig. 5). To further verify such aquifer interconnectivity, the log-log plots for trace elements in different types of waters in boreholes (BO) that showed absence and presence of EU anomaly, and for a hand dug well and borehole are presented in Fig. 11a and 11b, respectively. According to Taran et al. (2008), such correlation plots can be used for the estimation , at least , qualitative, whether waters from different sources originate from the same aquifer or not. The two plots show very good correlation between major and trace elements, suggesting that irrespective of slight differences in REE patterns of sample BO25 and BO37, all waters are from the same aquifer or a part of a bigger aquifer.

Such a mixing-based REEs pattern has been reported in the North China plain (Liu et al. 2016), and Australian catchment (Duvert et al. 2015). The characteristic steep-roof-shaped PAAS normalized pattern may hints that MREEs are more easily leached from parent rocks (Migaszewski et al. 2014), through preferential dissolution of feldspars (Guo et al. 2010), because, bivalent Eu (an MREE) is selectively enriched and incorporated into primary tectosilicates. For example, MREE enrichment in K-felspars and plagioclases is achieved by preferential substitution into Ca^{2+}, Na^{+}, and K^{+} sites. Moreover, preferential dissolution of feldspars relative to other REE-bearing primary minerals, should result in positive aqueous Eu-anomalies (Ma et al. 2011; Brioschi et al. 2013). Such positive Eu anomaly in freshwater has also been attributed to dissolution of phosphate mineral and eolian deposition (Vazquez-Ortega et al. 2015).

Considering that phosphate-Feldspar-rich minerals (e.g., vivianite) have been located in the western upstream of our study area (Fodoue et al. 2015; Bouyo et al. 2015), and that the fresh granitoids in the study area have similar positive Eu anomalies (Ndjigui et al. 2014), while the sediments express negative Eu anomalies (Ndjigui et al. 2014; Bouyo et al. 2015), point to incongruent dissolution of silicates, followed by enrichment in water and depletion in sediments. It has also been reported that influent atmospheric aeolian dust contains substantial total phosphorous, which can be associated with phosphate and alkali feldspars (Nash 1984). Hence, dust inputs may contribute significantly to the near surface REEs measurements. As shown in Fig. 3, the study area is markedly

influenced by eolian dust storm, and eventually deposited as sediments in which the shallow groundwater and surface water circulates to acquire a positive Eu anomaly.

It is worth noting that the observed positive Eu anomalies in freshwater within the study area contradicts observations in high temperature hydrothermal waters (Rollinson 1993; Bau 1991) and in fresh water from the Terengganu River basin, Malaysia (Sultan and Shazili 2009) and Tono in central Japan (Munemoto et al. 2015). However, the patterns are similar to freshwater from New Northern Mexico, South central Poland, Northern Anhui Province in China, Ukraine, Israel, Romagna in Italy, North China plain, and Inner Mongolia |(Vazque-Ortega et al. 2015; Migaszewski et al. 2014; Chen and Geu 2017; Zhuravlev et al. 2016; Censi et al. 2017; Pignotti et al. 2017; Liu et al. 2016; and Guo et al. 2010). Although most of the latter work attributed their REEs patterns to redox conditions, our investigation did not measure the Eh of sampled waters, thus falling short of defining the precise redox conditions that controlled REEs concentrations in the BRB. However, the biplots of La/Yb ratio against HCO_3 (Fig. 12), show that La/Yb ratio in surface water increased at low HCO_3 concentration, while the ratio dropped significantly in groundwater as HCO_3 concentration increases. Such plots suggest that acidic conditions most likely favoured the enrichment of HREEs and MREEs concentrations in surface waters, while enriching LREEs under alkaline conditions. This observation, however, is in disagreement with the suggestion of Johannesson and Hendry (2000) that higher carbonate ion concentrations would promote greater stability of the REEs in solution, and lead to their elevated concentrations.

Potentially Harmful Elements (PHEs) and health impacts

An interplay of geogenic and anthropic factors is suggested to mobilize potentially harmful elements (PHEs) such as fluoride (F^-), cadmium (Cd), lead (Pb), and arsenic (As) to water reaching levels that expose the local population to various unhealthy clinical phenomena.

Contextually, PHEs are elements whose concentrations in water are toxic to consumers (Davies 2013), for example F^-, Cd, Pb, and As. Most fluoride-related health studies pay more attention to endemic fluoride exposure from drinking water because that is the easiest pathway to quantify the impact on a community served by public water supply. Considering that the maximum permissible level of fluoride in drinking water is set at 1.5 mg/L by WHO (WHO 2004) and an optimum level of 0.7 mg/L for the semi-arid Northern regions of Cameroon (Fantong et al. 2010b), the concentrations of fluoride measured in the water samples (Table 1a; Fig. 13) show an undesirable concentrations of fluoride in drinking water sources from both the sedimentary basins (Garoua, Hamakoussou, Mayo Oulo Lere, and Babouri Figuil) and the granitic Precambrian basement, where children from these localities

(Barnake, Garoua, Pitoa, and Figuil) manifest chronic incidences of fluorosis (pitted teeth with white horizontal striations, pitted brown teeth, and unpitted teeth with black, brown, and chalky coats). Considering that the study area is just to the south of the Mayo Tsanaga River Basin, where Fantong et al. (2010b), identified alkaline-mobililized geogenic (mica and fluorapatite) provenance of fluoride in groundwater exploited for drinking, it is most likely that similar geochemical factors control the origin and mobilization of fluoride in the Benue River basin. However, a site-specific investigation is hereby proposed to underpin the origin and factors that mobilize fluoride in groundwater within the study area.

With respect to metalloids and heavy metals such as As, and Cd, and Pb, respectively, which have been found to cause lung and bladder cancers (Silvera and Rohan 2007), kidney damage (Davies 2013), and blockage of the large intestine (Tayie 2004), respectively, their concentrations in the study area (Table 1b) were found to be below, but close to the WHO (2004) threshold limits in some of the drinking water sources observed (Fig. 14). Although, the values of As, Cd and Pb (Fig. 14a-c), increase in the populated locality of Garoua, relative to sites with limited human influence, suggest a more likely anthropogenic origin for As, Cd and Pb, for instance from smelting, open-air burning of E-waste, and poorly disposed batteries (Davies 2013), a positive correlation of As, Cd, and Pb with HCO_3 in some samples (Fig. 15 a, b, and c), still suggests contribution from water-rock interaction processes. Evidence for anthropogenic input into the observed water samples can also be observed by a positive correlation between As, Cd and Pb versus NO_3 in some samples (Fig. 15 d, e and f), and a sturdy positive correlation between nitrate and chloride (Fig. 16), as explained in Fantong et al. (2016 and references there-in). Thus, a combination of conditions for water-rock interaction and anthropogenic input mobilizes elements in water, and determines the degree to health impacts on the population within the BRB.

Relative Mobility of metals in waters within the Benue River Basin

The extend to which major and trace elements enter the aqueous phase during weathering is called " relative mobility" (RM), which was computed from Eqn. 7 (Meybeck 1987; Gislason et al. 1996).

$$RM = (X/Mg)_w/(X/Mg)_r \quad \ldots\ldots 7$$

Where w and r refer to the solution and the rock, respectively. Considering that this approach has been successfully applied to rivers draining basaltic terrains in Iceland (e.g., Louvat 1997), Mt. Etna-Sicily (Aiuppa et al. 2000), and Mount Vesuvius volcanic aquifer in Italy (Aiuppa et al. 2005), in this study, the relative mobility of elements was calculated for 10 samples (representing boreholes (BO), hand dug wells (W), rivers (R), Spring (Sp), no EU anomaly samples (BO 25; and 37), and EU anomaly samples (e.g., BO 53)) from their water/rock concentration

460 ratio, normalized to magnesium, because of its strong chemical mobility during weathering. The results, which
461 are presented in Table 2, are plotted in Figure 17 a, b, in which elements are ranked with RMs increasing from
462 left to right with the groupings (1), (2), (3), and (4) representing the OHA (oxo-hydroxo anion) elements, alkalis
463 and alkaline earths, transition metals, and immobile metals, respectively. The main information therefrom are
464 summarized as follows:

465 (i) The spike-shaped data pattern reveals that the dissolution of BRB lithology is not isochemical with
466 relative mobility values ranging from 0.01-2.48 for OHA elements; 0.01-24.3 for alkalis and alkaline
467 earths; 0.01 to 76.33 for transition metals, and 0.01-0.15 for immobile metals.
468 (ii) Aqueous mobility of redox-sensitive elements such as Mn and Fe is weak, disagreeing with the
469 findings of Aiuppa et al. (2005), in the volcanic aquifer of Versuvius, where their mobility was
470 significantly enhanced.
471 (iii) The mean mobility sequence for alkalis is Na > K >Rb, and that for alkaline earth elements is Ca >
472 Ba. In agreement with the observation of Aiuppa et al. (2005), both sequences are similar to the
473 Hofmeister series, which refer to the relative affinity of cations for clay minerals and oxides (e.g.,
474 Stumm and Morgan 1996). Thus, water-rock interaction is a controlling factor for the distribution of
475 these elements between the aqueous and solid phase in the BRB, probably enriching the aqueous
476 phase in lithogenic fluoride that is consumed via drinking water sources and leading to observed
477 fluorosis.
478 (iv) Lead, Cu, Zn, Mo, U, Ca, and Sr are among the most mobile elements in the BRB.
479 (v) Aluminum is shown to be the most immobile element , probably because it is retained in the product
480 of incongruent dissolution such as hydroxides and clay minerals. Moreover, Cr, Mn, Rb, and V are
481 among the least mobile elements in the BRB.
482 (vi) For the only spring source that was sampled (Sp001), the analyzed elements show relative mobility
483 values ranging in between those of hand dug wells and boreholes, indicating that the spring water
484 was more or less draining an aquifer, thus a "surface water gaining system".
485 (vii) The hand dug wells (W028; W038), are characterized by lowest elements mobility, suggesting that
486 among the selected samples, they harbor the weakest water-rock interaction (WRI) process.
487 (viii) The boreholes (B025 and B037), on the other hand are characterized by highest elements mobility
488 (Fig. 17a), suggesting that they harbor the strongest water-rock interaction processes. This trend

supports the speculation that their flat REE patterns (Fig. 8b) may be attributed to deeper aquifer sources.

When these heavy metal (loid)s dissolve in water bodies, their mobility and dispersion are partly controlled by pH. To check this assertion, the sum of Pb, Cd, Cu, Zn, and Co was plotted against pH (Fig. 18), which depicts that in acidic pH < 6, condition the concentration of the heavy metal (loid)s increased in groundwater. On the other hand, a pH > 6, causes the concentrations to drop below 250 µg/L in both groundwater and surface waters.

Conclusions

In the Benue River Basin, Cameroon, one of the major upstream catchments of river Niger, groundwater is recharged by monsoon rainwater from July to September via a permeable clayey sandy lithology that favours hydraulic connectivity, preferential flow pass mechanism, but minimizes evaporation. High d-excess values (>10 ‰) in groundwater indicate that the recharge occur under low relative humidity conditions. Major ions plots on a Piper`s diagram, δD versus $\delta^{18}O$ plots, and PAAS normalized REEs patterns, depict mixing of surface and groundwater within a shallow aquifer system. The aquifer minerals interact with the circulating water incongruently, in an acidic-basic media, resulting in equilibrium between secondary clay minerals (kaolinite, Ca-montmorillonite, and Na-montmorillonite) and the groundwater, which becomes loaded with dissolved major ions, TEs and REEs. The results further indicate non-isochemical dissolution of local rocks by water, with springs, wells and borehole waters exhibiting surface water-gaining, weakest water-rock interaction, and strongest water-rock interaction processes, respectively. Poorly mobile elements (Al, Th and Fe) are preferentially retained in the solid residue of incongruent dissolution, while alkalis, alkaline earth and oxo-anion-forming elements (U, Mo, Na, K, Rb, Ca, Li, Sr, Ba, Zn, Pb) are more mobile and enriched in the aqueous phase, whereas transition metals display an intermediate behaviour. The dominantly geogenic processes imprint hydro-chemical signatures that varied from Ca+Mg-NO_3 type in shallow wells to Na+K-HCO_3 type in boreholes, and surface waters, with undesired concentrations of fluoride along the southwest-northeast corridor of the study area, where children manifest fluorosis in the localities of Barnake, Garoua, Pitoa, and Figuil. In addition to the fluoride-based health impacts, geogenic and anthropogenic concentrations of potentially harmful Cd, Pb and As are mobilized in acidic media attaining near-undesirable levels in and around populated localities. The data suggest that these localities should be actively monitored for As, Cd and Pb vulnerability linked to chronic toxicity, which could turn acute along the Niger river following population expansion and industrialization. The observed surface and groundwater samples had acidic-mobilized, low REEs concentrations with a wide range (0.007 to15.02 µg/L) in total REEs

(ΣREEs), and "steep roof-shaped" PAAS normalized positive Eu anomalies that could be attributed to preferential dissolution of feldspars relative to other REE-bearing primary minerals, the dissolution of phosphate-rich minerals, and the deposition of eolian dust. This work suggests important tenets for sustainable management of groundwater resources in other headwater basins in Sub-Saharan Africa.

Acknowledgements

This study was financially supported by the Federal Ministry for Economic Cooperation and Development (BMZ)-Germany as BMZ N°: 2014.2472.0, through the PRESS NO-SW project in Cameroon that was implemented by the Federal Institute of Geoscience and Natural Resources (BGR)-Germany as BGR N°: 05-2388, and the Institute of Geological and Mining Research (IRGM), Yaoundé.

References

Asai, K., Satake, H., and Tsujimura, M. (2010). Isotopic approach to understanding the groundwater flow system within the andesitic strato-volcano in a temperate humid region: case study of Ontake volcano, Central Japan. Hydrological Processes, 23, 559–571.

Appelo, C.A.J., & Postma, D. (1993). Geochemistry, groundwater, and pollution. Balkema, Netherlands, p 536.

Aiuppa, A., Allard, P., D'Alessandro, W., Michel, A., Parello, F., Trueil, M., and Valenza, M. (2000). Mobility and fluxesof major, minor and trace metals during basalt weathering and groundwater transport at Mt. Etna volcano (Sicily). Geochemica et Cosmochimica Acta. Vol. 64, No. 11, 1827-1841.

Aiuppa, A., Federico, C., Allard, P., Gurrieri, S., and Valenza, M. (2005). Trace metal modelling of groundwater-gas-rock interactions in a volcanic aquifer: Mount Vesuvius, Southern Italy. Chemical Geology. 216, 289-311.

543 Azzaz, H., Cherchali, M., Meddi, M., Houha, B., Puig, J.M., Achachi, A. (2008). The use of environmental
544 isotopic and hydrochemical tracers to characterize the functioning of karst systems in the Tlemcen
545 Mountains, northwest Algeria. Hydrogeol J. 16, 593– 607.

546 Bau, M. (1991). Rare-earth element mobility during hydrothermal and metamorphic fluid-rock interaction and the
547 significance of the oxidation state of europium. Chem. Geol. 93, 219–230.

548 Bessong, M. (2012). Paléoenvironnements et diagenèse dans un réservoir gréseux d'âge crétacé du fossé de la
549 Bénoué au Nord Cameroun : les grès de Garoua. Thèse de Doctorat, Université de Poitiers, 197 p.

550 Birke, M., Reimann, C., Demetriades, A., Rauch, U., Lorenz, H., Harazim, B., Glatte, W. (2010). Determination
551 of major and trace elements in European bottled mineral water—analytical methods. J Geochem Explor
552 107:217–226. doi:10.1016/j.gexplo.2010.05. 005

553 Blanken, J., and Pecher, S. (2013). Programme "changements climatiques, gestion des ressources naturelles et
554 securite alimentaire dans le bassin versant de la Bénoué" Technical Report.

555 Bouyo, M. H., Zhao, Y., Penaye, J., Zhang, S.H., Njel, U.O. (2015). Neoproterozoic subduction-related
556 metavolcanics and metasedimentary rocks from the Rey Bouba Greenstone Belt of north-central Cameroon
557 in the Central African Fold Belt: New insights into a continental arc geodynamic setting. Precambrian
558 Research. 261, 40-53.

559 Brand, W.A., et al. (2009). Cavity ring-down spectroscopy versus high temperature conversion isotope ratio mass
560 spectrometry; a case study on $\delta^{2}H$ and $\delta^{18}O$ of pure water samples and alcohol/water mixtures. Rapid
561 Communication in Mass Spectrometer, 23, 1879-1884. doi:10.1002/rcm.4083

562 Brioschi, L., Steinmann, M., Lucot, E., Pierret, M.C., Stille, P., Prunier, J., Badot, P.M. (2013). Transfer of rare
563 earth elements (REE) from natural soil to plant systems: implications for the environmental availability of
564 anthropogenic REE. Plant Soil 366, 143–163.

565 Brunet, M., Dejax J., Brillanceau ,A., Congleton, J ., Downs, W., Duperon-Laudoueneix M., Eisenmann V.,
566 Flanagan, K., Flynn, L., Heintz, E., Hell, J., Jacobs, L., Jehenne, Y., Ndjeng, E., Mouchelin, G., et Pilbeam,
567 D. (1988). Mise en évidence d'une sédimentation précoce d'âge Barrémien dans le fossé de la Bénoué en
568 Afrique occidentale (Bassin du Mayo Oulo Léré, Cameroun), en relation avec l'ouverture de l'Atlantique
569 Sud. C.R. Acad. Sci. Paris, 306 (II), pp. 1125-1130).

570 Budyko, M.I. (1951). On climate factors of runoff. Prob. Fiz. Geogr. 16 in Russian Canadian Council of Ministers
571 of the Environment (2001a) Canadian water quality guidelines for the protection of aquatic life. CCME
572 water quality index 1.0, Technical report. http://www.ccme.ca

573 Censi, P., Raso, M., Yechieli, Y., Ginat, H., Saiano, F., Zuddas, P., Brusca, L., D'Alessandro, W., and
574 Inguaggiato, C. (2017). Geochemistry of Zr, Hf, and REE in a wide spectrum of Eh and water
575 composition: The case of Dead Sea Fault system (Israel), Geochem. Geophys. Geosyst., 18, 844–857,
576 doi:10.1002/2016GC006704.

577 Chen, S., and Gui1, H. (2017). Hydrogeochemical characteristics of groundwater in the coal-bearing aquifer of
578 the Wugou coal mine, northern Anhui Province, China. Appl. Water Sci. 7, 1903-1910.

579 Craig, H. (1961). Isotopic variation in meteoric water. Science. 133,1702–1703.

580 Davies, T.C. (2013). Geochemical variables as plausible aetiological cofactors in the incidence of some common
581 environmental diseases in Africa. Journal of African Earth Sciences. 79, 24-49.

582 Deshpande, R.D., Bhattacharya, S.K., Jani, R.A., Gupta, S.K. (2003). Distribution of oxygen and hydrogen
583 isotopes in shallow groundwaters from southern India: influence of a dual monsoon system. J Hydrol. 271,
584 226–239.

585 Deutsch, W.J.(1997). Groundwater geochemistry: fundamentals and applications to contamination. Lewis, New
586 York, p 221.

587 Duvert, C., Cendón, D.I., Raiber, M., Seidel, J., Cox, M.E. (2015). Seasonal and spatial variations in rare earth
588 elements to identify inter-aquifer linkages and recharge processes in an Australian catchment. Chem. Geol.
589 369, 83–97.

590 Edet, A.E. (2004). A preliminary assessment of the concentrations of rare earth elements in an acidic fresh
591 groundwater (south-eastern Nigeria), Applied Earth Science, 113, 100-109.

592 Edmunds, W.M., Carrillo-Rivera, J.J., Cardona, A. (2002). Geochemical evolution of groundwater beneath
593 Mexico city. J Hydrol. 258,1–24.

594 Eyong, J.T., Bessong. M., Hell, J.V., Mfoumbeng, M.P., Ntsama, A.J., Ngjeng, E. (2013). Lithostratigraphy of
595 the Mayo Oulo-Lere basin Northern Cameroon (W. Africa). Journal of Geological Resource and
596 Engineering. 1, 2328 – 2193.

Fantong, W.Y., Satake, H., Ayonghe, S.N., Aka, F.T., Kazuyoshi, A.(2009). Hydrogeochemical controls and usability of groundwater in the semi-arid Mayo Tsanaga River Basin: Far north province, Cameroon. J. Environ. Geol. 58, 1281–1293.

Fantong, W.Y., Satake, H., Aka, F.T., Ayonghe, S.N., Asai, K., Mandal, A., Ako, A.A. (2010a). Hydrochemical and isotopic evidence of recharge, apparent age, and flow direction of groundwater in Mayo Tsanaga River Basin, Cameroon: bearings on contamination. Environ. Earth Sci. 60, 107–120.

Fantong, W.Y., Satake, H., Ayonghe, S.N., Suh, C.E., Adelana, S.M.A., Fantong, E.B.S., Banseka, S.H., Gwanfogbe, C.D., Woincham, L.N., Uehara, Y., Zhang, J. (2010b). Geochemical provenance and spatial distribution of fluoride in groundwater of Mayo Tsanaga River Basin, Far North Region, Cameroon: implications for incidence of fluorosis and optimal consumption dose. Environ Geochem Health. 32,147–163.

Fantong, W.Y., Kamtchueng, B.T.,Yamaguchi, K.,, Ueda, A., Issa., Ntchantchoa, R., Wirmvem, M.J., Kusakabe, M.,Ohba, T., Zhang, J., Aka, F.T., Tanyileke, G., Joseph V. Hell, J.V. (2015). Characteristics of chemical weathering and water–rock interaction in Lake Nyos dam (Cameroon): Implications for vulnerability to failure and re-enforcement. Journal of African Earth Sciences. 101, 42-55.

Fantong, W.Y., Fouepe, A.T., Ketchemen-Tandia, B., Kuitcha, D., Ndjama, J., Fouepe, T.A., Takem, G.E., Issa Wirmvem, M.J., Bopda Djomou, S.L., Ako, A.A., Nkeng, G.E., Kusakabe, M., Ohba, T. (2016). Variation of hydrogeochemical characteristics of water in surface flows, shallow wells, and boreholes in the coastal city of Douala (Cameroon). Hydrol. Sci. J. http://dx.doi.org/10.1080/0262666720161173789.

Faure, G. (1991). Principles and Applications of Inorganic Geochemistry. Macmillan publishing, New York, pp. 626.

Ferreira, C.A., Helena, E. L., Palmieri., Maria Ângela de B. C. M. (2015). Rare Earth Elements And Uranium In Fountain Waters From Different Towns Of The Iron Quadrangle, Mg, Brazil. International Nuclear Atlantic Conference. Associação Brasileira De Energia Nuclear - ABEN ISBN: 978-85-99141-06-9

Fodoue, Y., Nguetnkam, J.P., Tchameni, R., Basga, S.D., and Penaye, J. (2015). Assessment of the Fertilizing effect of Vivianite on the growth and yield of the Bean “Phaseolus vulgaris” on oxisoils from Ngaoundere (central North Cameroon). International Research Journal of Earth Sciences. 3 (4), 18-26.

624 Garrels, R.M., Mackenzie, F.T. (1967). Origin of the chemical composition of some springs and lakes. In: Gould
625 RF (ed) Equillibrium concepts in natural water systems. American Chemical society, Washington, DC, pp
626 222–242.

627 Gammons, C. H., Wood, S. A., Pedrozo, F., Varekamp, J. C., Nelson, B. J., Shope, C. L., & Baffico, G. (2005b).
628 Hydrogeochemistry and rare earth element behavior in a volcanically acidified watershed in Patagonia,
629 Argentina. Chemical Geology, 222, 249–267.

630 Gat, J.R. (2010). Isotope hydrology: a study of the water cycle. Series on environmental science and
631 management, vol 6. Imperial College Press, London

632 Gibbs, R.J. (1970). Mechanisms controlling World water chemistry. Science, 170, 1088–1090. American
633 Association for the Advancement of Science, Washington DC. doi:10.1126/science.170.3962.1088.

634 Gimeno, M. J., Auqué, L. F., & Nordstrom, D. K. (2000). REE speciation in low-temperature acidic waters and
635 the competitive effects of aluminium. Chemical Geology, 165, 167–180.

636 Gislason, S.R., Arnorsson, S., Armannsson, H. (1996). Chemical weathering of basalts in southwest Iceland:
637 effects of runoff,, age of rocks and vegetative/glacial cover. Am. J. Sci. 296, 837-907

638 Goni, I.B. (2006). Tracing stable isotope values from meteoric water to groundwater in the south western part of
639 the Chad basin. Hydrogeol. J. 14, 4331–4339.

640 Guo, H.M., Zhang, B., Wang, G.C., Shen, Z.L. (2010). Geochemical controls on arsenic and rare earth elements
641 approximately along a groundwater flow path in the shallow aquifer of the Hetao Basin, Inner Mongolia.
642 Chem. Geol. 270, 117–125.

643 Herczeg, A.L., Simpson, H.J., Mazor, E. (1993). Transport of soluble salts in a large semiarid basin. River
644 Murray, Australia. J Hydrol. 144, 59–84.

645 Houston, J. (2007). Recharge to groundwater in the Turi basin, northern Chile: an evaluation based on tritium and
646 chloride mass balance techniques. J Hydrol. 334, 534-544.

647 Johannesson, K. H., & Lyons, W. B. (1995) . Rare-earth element geochemistry of Colour Lake, an acidic
648 freshwater lake on Axel Heiberg Island, Northwest Territories, Canada. Chemical Geology, 119, 209-223.

649 Johannesson, K.H., Farham, I.M., Guo, C.X., and Stetzenbach, K.J.(1999). Rare earth element fractionation and
650 concentration variations along a groundwater flow path within a shallow, basin-fill aquifer, southern
651 Nevada, USA. Geochemica et Cosmochima Acta. 63, 2697-2708.

652 Johannesson, K.H., Hendry, M.J. (2000). Rare earth element geochemistry of groundwaters from a thick till and
653 clay-rich aquitard sequence, Saskatchewan, Canada. Geochim. Cosmochim. Acta 64 (9), 1493–1509.

654 Jokam Nenkam, T. L. L., Nbendah, P., Fantong, W.Y., Takoundjou, A. F. (2019). Etude Pilote sur la Pollution
655 des Eaux de Surface et Souterraines a Garoua et ses environs et son Impact sur la Sante des Populations
656 Riveraines (EPESS Garoua). Federal Institute for Geosciences and Natural Resources (BGR) Technical
657 Report No. 05-2388. Edited by Kringel Robert, Vassolo Sarah, and Wilczok Charlotte. 125 pages.

658 Kamtchueng, B.T., Fantong, W.Y., Ueda, A., Tiodjio, E.R., Anazawa, K., Wirmvem, M.J., Mvondo, J.O.,
659 Nkamdjou, L.S., Kusakabe, M., Ohba, T., Tanyileke, G., Hell, J.V. (2014). Assessment of shallow
660 groundwater in Lake Nyos catchment (Cameroon, central Africa): Implications for hydrogeochemical
661 controls and uses. Environ. Earth Sci. http://dx.doi.org/10.1007/s12665-014-3278-6.

662 Kazemi, G.A., Lehr, J.H., Perrochet. P. (eds) (2006). Groundwater age. Wiley, Hoboken, New Jersey, 325 pp

663 Kebede, S., Travi, Y., Alemayehu, T., Ayenew, T. (2005). Groundwater recharge, circulation and geochemical
664 evolution in the source region of the Blue Nile River, Ethiopia. Appl Geochem. 20,1658– 1676.

665 Kendall, C., Doctor, D.H. (2011). Stable isotope applications in hydrologic studies. In: Holland HD, Turekian KK
666 (eds) Isotope geochemistry, 1st edn. Academic Press, London, pp 181-220.

667 Leduc, C., Taupin, J.D., Gal La Salle, C. (1996). Estimation de la recharge de la nappe phreatique du Continental
668 Terminal (Niamey, Niger). C R Acad Sci Paris Ser IIa 323, 599-605.

669 Lis, G., Wassenaar, L.L., and Hendry, M.J. (2008). High precision laser spectrometry D/H and $^{18}O/^{16}O$
670 measurements of microliter natural water samples. Analytical Chemistry, 80, 287–293. doi:10.1021/
671 ac701716q

672 Liu, H., Guo, H., Xing, L., Zhan, Y., Li, F., Shao, J., Niu. H., Liang, X., Li, C. (2016). Geochemical behaviours
673 of rare earth elements in groundwater along a flow path in the North China Plain. Journ. Asian Earth
674 Sciences. 117, 33-51.

675 Louvat, P. (1997). Etude geochemique de l`erosion fluviale des iles volcaniques : l`aide des bilans d`elements
676 majeurs et traces. These de doctorat, Universite Paris VII.

677 Ma, L., Jin, L., Brantley, S.L. (2011). How mineralogy and slope aspect affect REE release and fractionation
678 during shale weathering in the Susquehanna/Shale Hills Critical Zone Observatory. Chem. Geol. 290, 31–
679 49.

680 Masuda, A., Kawakami, O., Dohmoto, Y., and Takenaka, T. (1987). Lanthanide tetrad effects in nature: Two
681 mutually opposite types, W and M. Geochemical Journal. 21, 119-124.

682 Maurin, J.C., and Guiraud, R. (1989). Relations entre tectonique et sédimentation dans les bassins barrémo-aptiens
683 du Nord Cameroun. C.R. Acad. Sci. Paris 308, Sér. II, pp. 787-792.

684 Mbonu, M., Travi, Y. (1994). Labelling of precipitation by stable isotopes (^{18}O, ^{2}H) over the Jos Plateau and the
685 surrounding plains (north-central Nigeria). J Afr. Earth Sci. 19, 91-98.

686 McLennan, S.M.(1989). Rare earth elements in sedimentary rocks; influence of provenance and sedimentary
687 processes. In Liplin BR and McKay GA (eds) Geochemistry and mineralogy of rare earth elements.
688 Reviews in Mineralogy and Geochemistry 21. Mineralogical Society of America, pp 169–200.

689 Meybeck, M. (1997). Global chemical weathering of surficial rocks estimated from river dissolved loads. Am. J.
690 Sci. 287, 401-428.

691 Migaszewski, Z.M., Gałuszka, A., Migaszewski. (2014). The study of rare earth elements in farmer's well
692 waters of the Podwiśniówka acid mine drainage area (south-central Poland). Environ Monit Assess.
693 186,1609–1622.

694 Migaszewski, Z. M., and Galuszka, A. (2015). The Characteristics, Occurrence, and Geochemical Behaviour of
695 Rare Earth Elements in the Environment: A Review. Critical Reviews in Environmental Science and
696 Technology. 45, 492-471.

697 Molua, E.L. (2006). Climatic trends in Cameroon: implications for agricultural management. Clim. Res. 30,
698 255–262.

699 Munemoto, T., Ohmori, K., Iwatsuki. (2015). Rare earth elements (REE) in deep groundwater from granite and
700 fracture-filling calcite in the Tono area, central Japan: Prediction of REE fractionation in paleo- to present
701 -day groundwater. Chem. Geol. 417,58-67.

Nagaraju, A., Surresh, S., Killam, K., Hudson-Edwards, K. (2006). Hydrogeochemistry of waters of Mangampeta Barite Mining Area, Cuddapach Basin, Andhra Pradesh, India. Turk J Environ Sci. 30, 203–219.

Nash, W.P. (1984). Phosphate minerals in terrestrial igneous and metamorphic rocks. In: Nriagu, J.O., Moore, P.B. (Eds.), Phosphate minerals. Springer, Berlin Heidelberg, pp. 215-241.

Ndjigui, P.D., Beauvais, A., Fadil-Djenabou, S., Ambrosi, J-P. (2014). Origin and evolution of Ngaye River alluvial sediments, Northern Cameroon: Geochemical constraints. Journal of African Earth Sciences. 100, 164-178.

Nesbitt, H.W., Wilson, R.E. (1992). Recent chemical weathering of basalts. Am J Sci 292:740–777.

Njitchoua, R., Aranyossy, J.F., Fontes, J.C., Michelot, J.L., Naah, E., Zuppi, G.M. (1995). Oxygen-18, deuterium et chlorures dans les precipitations a Garoua (Nord-Cameroon): implications meteorolgiques. CR Acad Sci Paris, t 321, serie IIa: 853–860.

Njitchoua, R., Dever, L., Fontes, J-C., Naah, E. (1997). Geochemistry, origin and recharge mechanisms of groundwaters from the Garoua Sandstone aquifer, northen Cameroon. J Hydrol. 190,123–140.

Nkotagu, H. (1996). Application of environmental isotopes to groundwater recharge studies in a semi-arid fractured crystalline basement area of Dodoma, Tanzania. J Afr Earth Sci. 22, 443–457.

Noak, C.W., Dzombak, D.A., Karamalidis, A.K. (2014). Rare earth element distributions and trends in natural waters with a focus on groundwater. Environ. Sci. Technol. 48, 4317–4326.

Nolla, J.D., Hell, J.V., Ngos, S., Bessong, M., Mfoumbeng, M. P., Eyong, T. J., Dissombo, E.A.N., Mbang, A. R., Engombi, G., Ndjeng, E. (2015). Lithostratigraphy of the Koum Basin (Northern Cameroon). International Journal of Multidisciplinary Research and Development. 2 (6), 103-114.

Ntsama, J.A. (2013). Magnétostratigraphie et sédimentologie des formations crétacées des bassins sédimentaires d'Hamakoussou et du Mayo Oulo-Léré au Nord-Cameroun (Fossé de la Bénoué). Thèse Terre solide et enveloppes superficielles. Poitiers : Université de Poitiers. 193 pp.

Ntsama, A. J., Bessong, M., Hell, J. V., Mbesse, C. O., Nolla, J. D., Dissombo, E. A. N., Eyong, J.T., Mbassa, B.J., Mouloud, B., Vignaud, P., Mfoumbeng, M.P. (2014). The Importance of Diagenetic Processes in Sandstones Facies of the Hamakoussou Sedimentary Basin in North Cameroon: Influence on Reservoir Quality. International Journal of Sciences: Basic and Applied Research. 13, 220-230.

729 Petrides, B., Cartwright, I., Weaver, T.R. (2006). The evolution of groundwater in the Tyrell catchment, south-
730 central Murray Basin, Victoria, Australia. Hydrogeol J. 14,1522-1543.

731 Pignotti, E., Dinelli, E., Birke, M. (2017). Geochemical characterization and rare earth elements anomalies in
732 surface- and groundwaters of the Romagna area (Italy). Rend. Fis. Acc. Lincei. 28, 265-279.

733 Piper, A. M. (1944). A graphic procedure in the geochemical interpretation of water analyses. American
734 Geophysical Union Transactions. 25, 914–923.

735 Rollinson, H. R. (1993). Using Geochemical data: Evaluation, Presentation, Interpretation. Longman Singapore
736 Publishers Ltd. Singapore. 352 pp.

737 Scalon, B.R., et al. (2006). Global synthesis of groundwater recharge in semi-arid and arid regions. Hydrol
738 Process, 20, 3335–3370. doi:10.1002/hyp.6335

739 Schwoerer, P. (1965). Carte de reconnaissance à l'échelle du 1/500 000. Notice explicative sur la feuille Garoua-
740 Est. Direction des Mines et de la Géologie du Cameroun (éd) Yaoundé, 49 p.

741 Shivanna, K., Tirumalesh, K., Noble, J., Joseph, T.B., Singh ,G., Joshi, A.P., Khati, V.S. (2008). Isotope
742 techniques to identify recharge areas of springs for rainwater harvesting in the mountainous region of
743 Gaucher area, Chamoli District, Uttarakhand. Curr Sci. 94,1003–1011.

744 Sholkovitz, E.R., Landing, W.M., and Lewis, B.L. (1994). Ocean particle chemistry: The fractionation of rare
745 earth elements between suspended particles and seawater. Geochimica et Cosmochimica Acta. 58, 1567-
746 1579.

747 Silvera, S., Rohan, T. (2007). Trace elements and cancer risk: a review of the epidemiological evidence.
748 Cancer causes and control. 18 (1), 7-27.

749 Srinivasamoorthy, K., Chindambaram, S., Prasanna, M.V., Vasanthavihar, M., Peter, J., Anandhan, P. (2008).
750 Identification of major sources controlling groundwater chemistry from a hard rock terrain-A case study
751 from Mettur taluk, Salem district, Tamil Nadu, India. J Earth Syst Sci. 117(1), 49–58.

752 Stumm, W., Morgan, J.J. (1996). Aquatic Chemistry: Chemical Equillibria and rates in Natural Waters. Wiley
753 Interscience Publication, New Jersey.

754 Subramani, T., Rajmohan, N., Elango, L. (2010). Groundwater geochemistry and identification of
755 hydrogeochemical processes in hard rock region, Southern India. Environ Monit Assess. 162,123-137.

Sultan, K., Shazilli, A.A. (2009). Rare earth elements in tropical surface water, soil and sediments of the Terengganu River Basin, Malaysia. Journal of Rare Earths. 27, 1073-1078.

Takahashi, Y., Yoshida, H., Sato, N., Hama, K., Yasu, Y., and Shimizu, H. (2002). W-and M- type tetrad effects in REE patterns for water-rock system in the Tono uranium deposit, central Japan. Chemical Geology. 184, 311-335.

Tang, J., and Johannesson, K.H. (2006). Controls on the geochemistry of rare earth elements along a groundwater flow path in the Carrizo Sand aquifer, Texas, USA. Chem. Geol. 225, 156–171.

Taran, Y., Rouwet, D., Inguaggiato, S., Aiuppa, A. (2008). Major and trace element geochemistry of neutral and acidic thermal springs at El Chichon volcano, Mexico: Implications for monitoring of the volcanic activity. Journal of Volcanology and Geothermal Research. 178, 224-236

Tardy, Y. (1971). Characterization of the principal weathering types by the geochemistry of waters from some European and African crystalline massifs. Chem. Geol. 7, 253–271.

Tayie, F. (2004). Pica: motivating factors and health issues. African Journal of Food, Agriculture, Nutrition and Development 4 (1) <http://www.bioline.org.br/ (accessed 18.07.2019).

Taylor, R.G., Howard, K.W.F. (1996). Groundwater recharge in the Victoria Nile basin of East Africa: support for the soil moisture balance method using stable isotope and flow modelling studies. J Hydrol. 180, 31–53.

Thomas, J.M., Welch, A.H., Preissler, A.M. (1989). Geochemical evolution of groundwater in Smith Creek Valley—a hydrologically closed basin in central Nevada, USA. Appl Geochem. 4, 493–510.

Tillement, B. (1972). Hydrogeologie du Nord—Cameroun. Rapport 6, 294p. Direction des Mines et de la Geologie, Yaounde, Cameroon

Tsujimura, M., Abe, Y., Tanaka, T., Shimada, J., Higuchi, S., Yamanaka, T., Davaa, G., Oyunbaatar, D. (2007). Stable isotopic and geochemical characteristics of groundwater in Kherlin River Basin: a semiarid region in Eastern Mongolia. J. Hydrol. 333, 47–57.

Vázquez-Ortega, A., Perdrial, J., Harpold, A., Zapata-Ríos, X., Rasmussen, C., McIntosh, J., Schaap, M., Pelletier, J.D., Brook, P.D., Amistadi, M.K., Chorover, J. (2015). Rare earth elements as reactive tracers of biogeochemical weathering in forested rhyolitic terrain. Chem. Geol. 391, 19–32.

783 WHO (World Health Organization). (2004). Guidelines for drinkingwater quality: training pack. WHO, Geneva

784 Wirmvem, M.J., Mimba, M.E., Kamtchueng, B.T., Wotany, E.R., Bafon, T.G., Asaah, A.N.E., Fantong, W.Y.,
785 Ayonghe, S.N., Ohba, T. (2015). Shallow groundwater recharge mechanism and apparent age in the Ndop
786 plain, northwest Cameroon. Appl Water Sci. doi:10.1007/ s13201-015-0268-0

787 Zaborski, P., Ugodunlunwa, F., Idornigie, A., Nnabo, P., Ibe, K. (1997). Stratigraphy and structure of the
788 Cretaceous Gongola Basin 'N.E. Nigeria). Bulletin des Centres de Recherches Exploitation-Production Elf-
789 Aquitaine 21(1), 153-177.

790 Zhuravlev, A., Berto, M., Arabadzhi,, M., Gabrieli, J., Turreta, C., Cozz, G.m Barbante, C. (2016). Trace and
791 Rare Earth Elements in Natural Ground Waters: Weathering Effect of Water-Rock Interaction. Int. J.
792 Environ. Res. 10 (4), 561-574.

793

794 **Figure Captions**

795 **Fig. 1** Location of study area in the Northern Region of Cameroon and within the River Niger system in Africa.
796 It also shows the spatial locations of the 5 sub sedimentary basins that constitute the extension of the
797 Benue Trough in Cameroon, and sample collection sites

798 **Fig. 2** Topography (Digital Elevation Model) of study area, showing the hydrographic network

799 **Fig. 3** Incidence of Aeolian harmattan dust, which reduce visibility to less than 15 meters

800 **Fig. 4** North-South correlation panel of Mayo-Oulo sedimentary Basin (a), and geochemical diagenetic processes
801 of the Hamakoussou sedimentary Basin (b)

802 **Fig. 5** Pipers` plots of observed water samples, showing Ca+Mg-NO_3 water facies in shallow wells (group1),
803 Na+K-HCO_3 facies in boreholes (group 2), and Na+K-HCO_3 (group 3) type in surface water. The cluster
804 of the plots indicates mixing of the surface and groundwater resources

805

806 **Fig. 6** A $\delta^{18}O$-δD relationship of groundwater, surface water and rainfall in the Benue River basin. There is an
807 almost dominant cluster of observed water samples between July and September rains and along the
808 Global Meteoric Water Line (GMWL) of Craig (1961), indicating groundwater recharge months are

809 mainly July and September, with little or no evaporation. The cluster of the plots are also indicative of
810 mixing between surface and groundwater. The monthly rainfall data are from Njitchoua et al. 1995. Plots
811 of some surface water to the right of the GMWL indicate evaporation effect (a). More than 60 % of
812 groundwater plot show d-excess greater than 10 ‰ indicating recharge under low humidity conditions
813 (b).

814

815 **Fig. 7** Average metal concentrations in water within the Benue River Basin (Cw, µg/l) versus average
816 concentrations in local lithology (sandy clay) (Cs, mg/kg). The abbreviation "OHA" stands for oxo-
817 hydroxo anion forming elements. Water and rock data are presented in Tables 1a, b and c, and original
818 rock data were gotten from Ndjigui et al. (2014).

819 **Fig. 8** PAAS normalize patterns of rare earth elements in observed water samples. (a)-(c) in boreholes, (d)-(f) in
820 hand dug wells, and (g) in spring. All samples, except (BO 25 and 37) show a "steep roof-shaped" positive
821 Eu anomaly

822

823 **Fig. 9** Gibbs plots indicating rock domain (water-rock interaction) as main process controlling groundwater
824 chemistry in the study area

825 **Fig. 10** Stability diagrams for some minerals in the systems Na_2-Al_2O_3-SiO_2-H_2O (a) and CaO-Al_2O_3-SiO_2-H_2O
826 (b) at 25°C and pressure of 1 bar, showing that observed water samples are in equilibrium with
827 montmorillonites and kaolinite, and the plots of saturation index versus TDS (c) showed that some samples
828 were supersaturated with respect to carbonate phases, while all samples were undersaturated with respect
829 to gypsum and anhydrite

830

831 **Fig. 11** Log-log plots for major and trace elements in selected water samples within the Benue River Basin

832 **Fig. 12** Biplots of La/Yb ratio against HCO_3 show that La/Yb ratio in surface water increased at low HCO_3
833 concentration (group 1), suggesting that acidic conditions may favour REEs concentration in surface
834 waters than alkaline conditions will do

Fig. 13 Spatial distribution of mg/l concentrations of fluoride in observed water samples. Sites with high (> 1.5 mg/l) fluoride concentration cause fluorosis on children teeth

Fig. 14 Spatial distributions of Potentially Harmful Elements (PHEs) showed that the values (µg/L) of As (a), Cd (b), and Pb (c) increase in relatively populated locality (Garoua) within the study area. This suggests that their origin may be associated to anthropogenic activities

Fig. 15 Scatter diagrams plotting HCO_3 versus As (a), Cd (b), Pb (c), and NO_3 versus As (d), Cd (e), and Pb (f). The diagrams depict water rock interaction (WRI) and anthropogenic input (AI) as contributing factors to the incidence of As, Cd, and Pb in waters within the Benue River Basin

Fig. 16 Chloride versus nitrate plots, indicate the incident of anthropogenic input into the water resources observed

Fig. 17 Relative mobility of metals in selected groundwater samples in Benue River Basin. RM values were normalized to magnesium and computed from equation 7 (see text). Elements are arranged in four groups based on increasing mobility (1. OHA elements; 2, alkalis and alkaline earths; 3, transition metals; 4, immobile metals). Relative metal mobilities in the selected samples are compared to the average trend

Fig. 18 Biplots of the sum of Pb, Cd, Cu, Zn, and Co against pH, depict that at acidic pH of less than 6, the concentration of the heavy metals increased in groundwater (group (a)), whereas above pH 6, the concentrations drop (group (b))

Table Captions

Table1a Sample location and physico-chemical (majors ions and stable isotopes) results of groundwater (n=72) and surface water (n=14) in the Benue River Basin

Table 1b Sample location and trace elements results of groundwater (n=72) and surface water (n=14) in the Benue River Basin

Table 1c Rare earth elements results of observed water (B=borehole; W= hand dug well; R= rivers; S= spring) (n=86) in Benue River Basin

Table 2 Relative mobility of elements in selected water samples in Benue River basin.

Figure 1

Click here to access/download;Figure;Fig. 1..tif

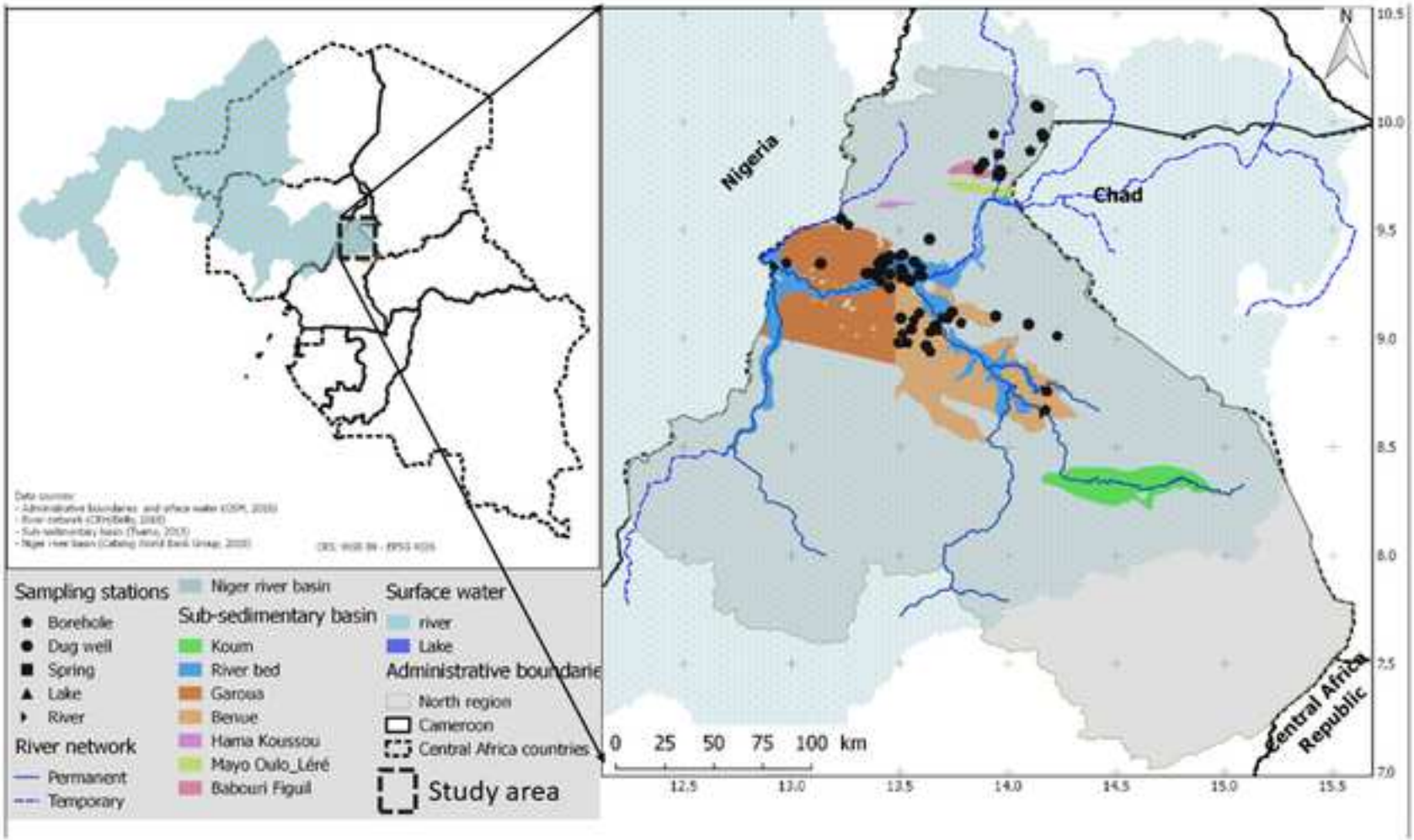

Figure 2

Click here to access/download;Figure;Fig. 2..tif

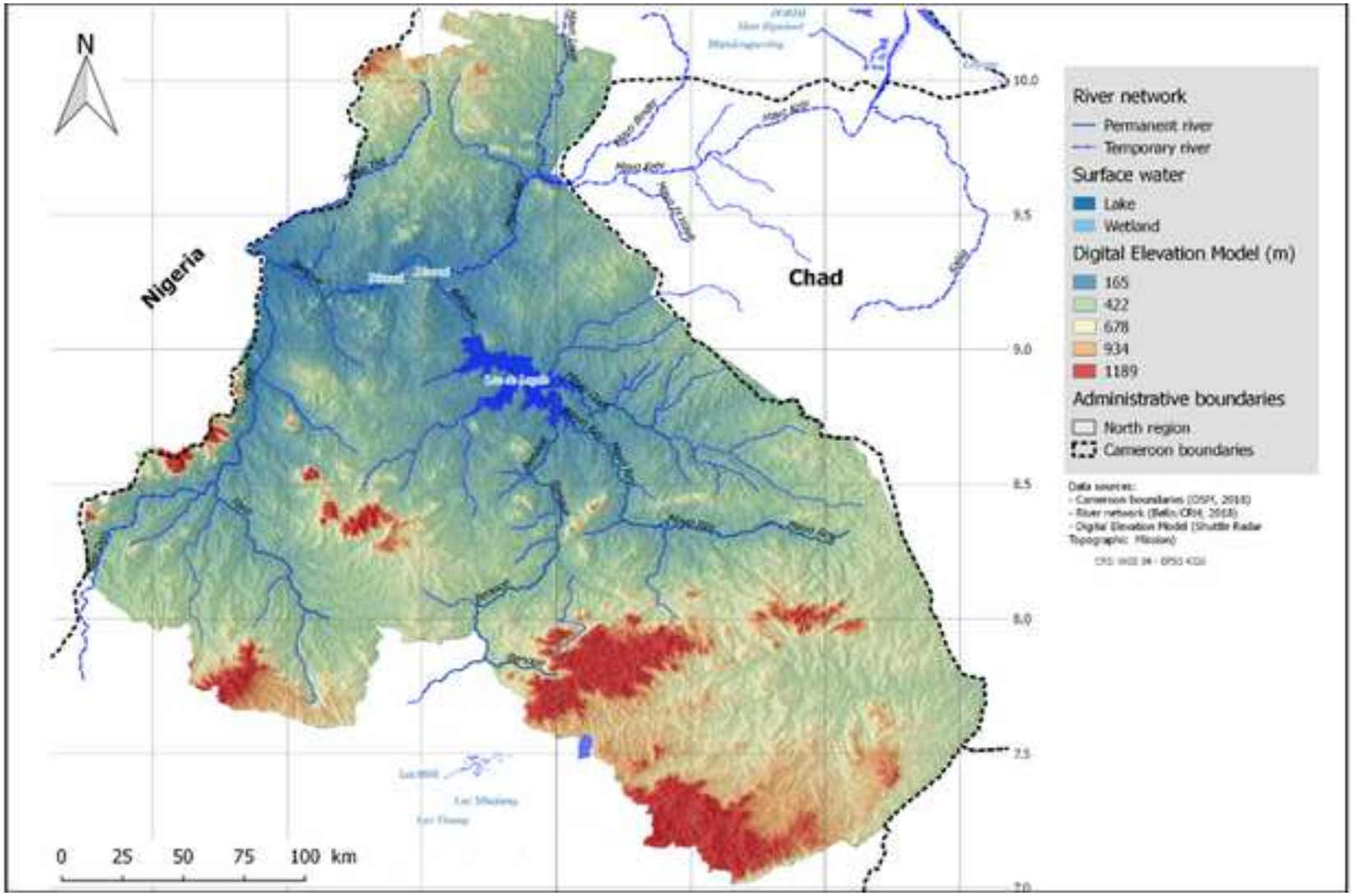

Figure 3

Click here to access/download;Figure;Fig. 3.tif

Figure 4a

Click here to access/download;Figure;Fig. 4a.tif

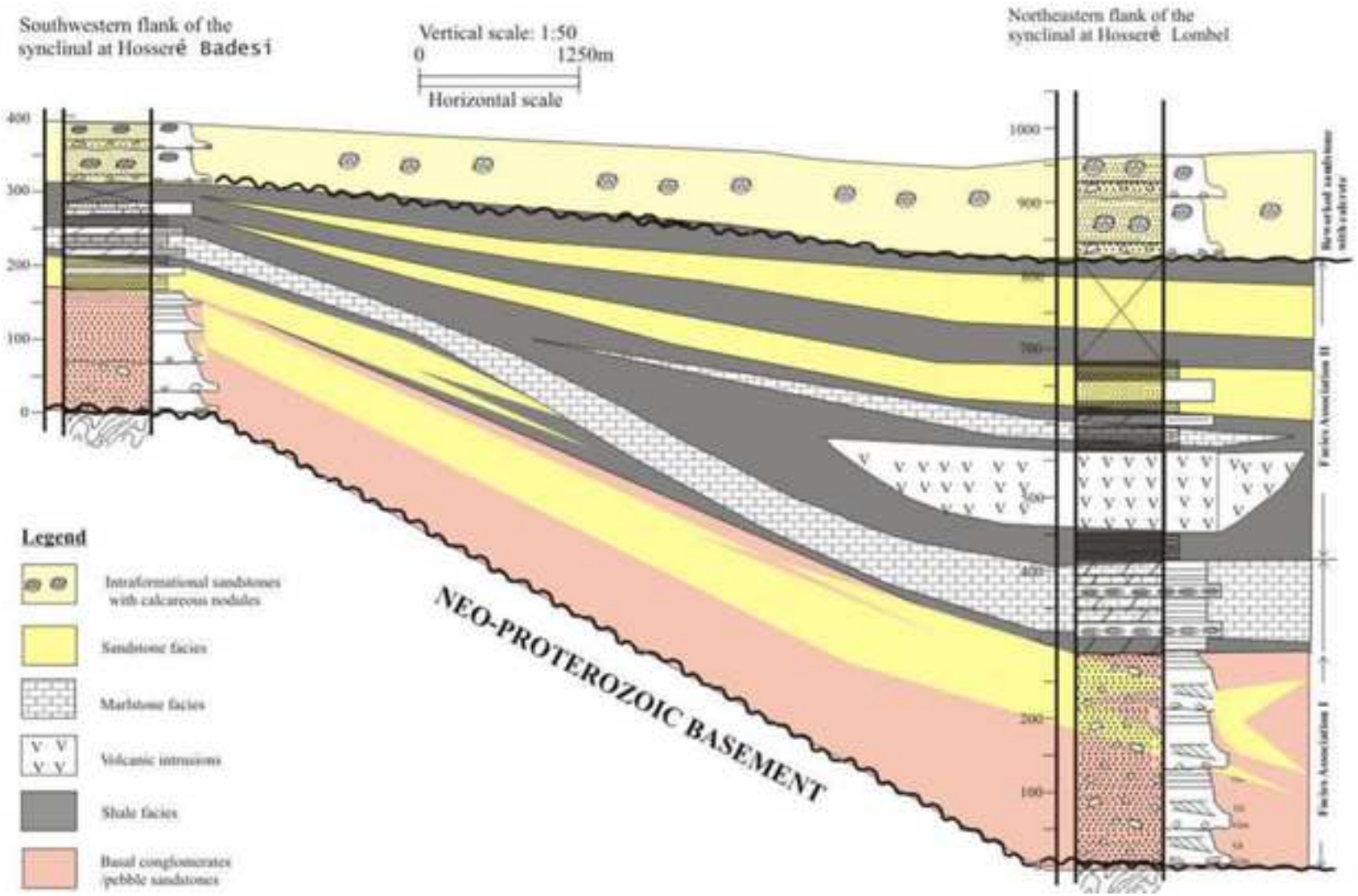

Figure 4b

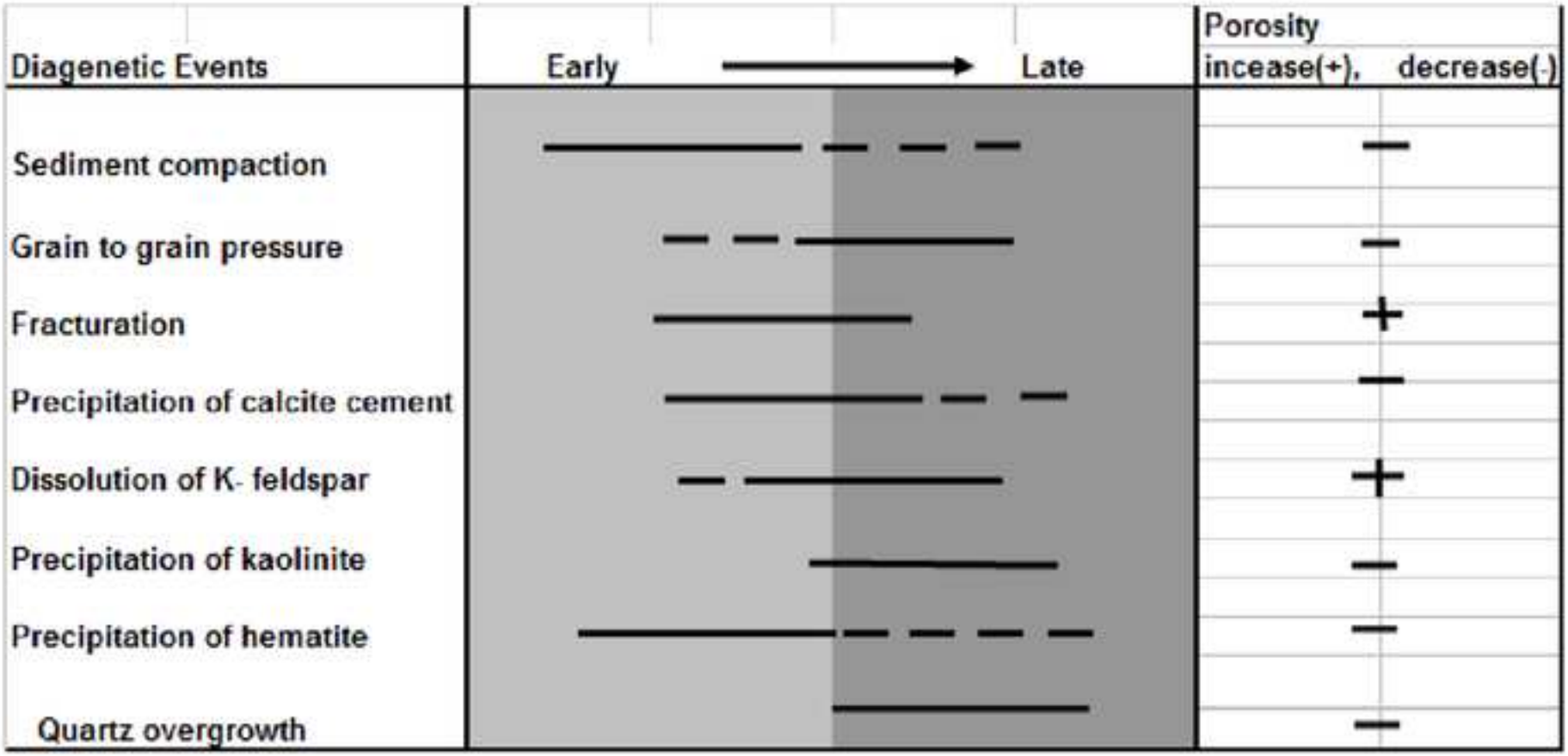

Figure 5

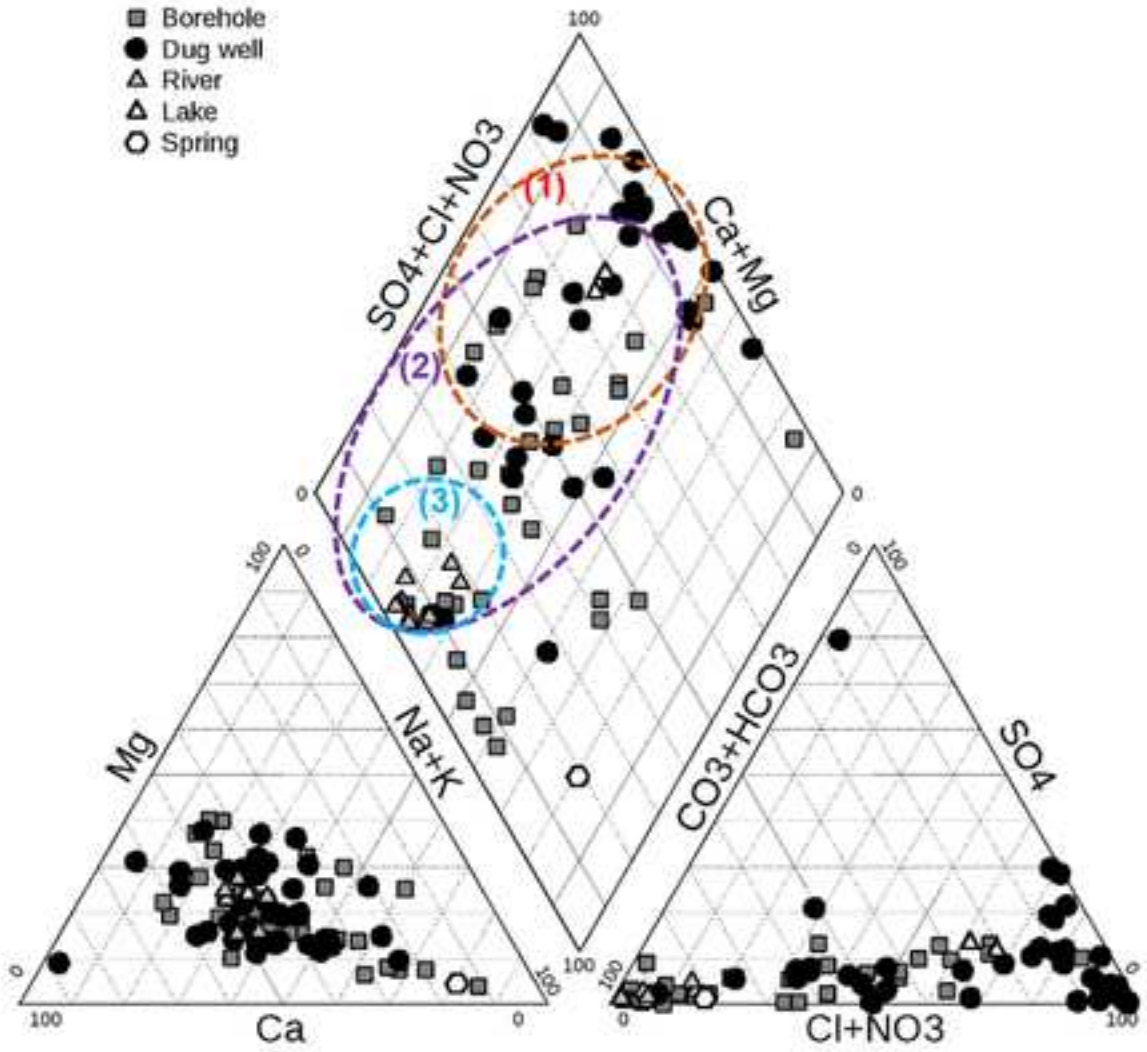

Figure 6a

Click here to access/download;Figure;Fig. 6a.tif

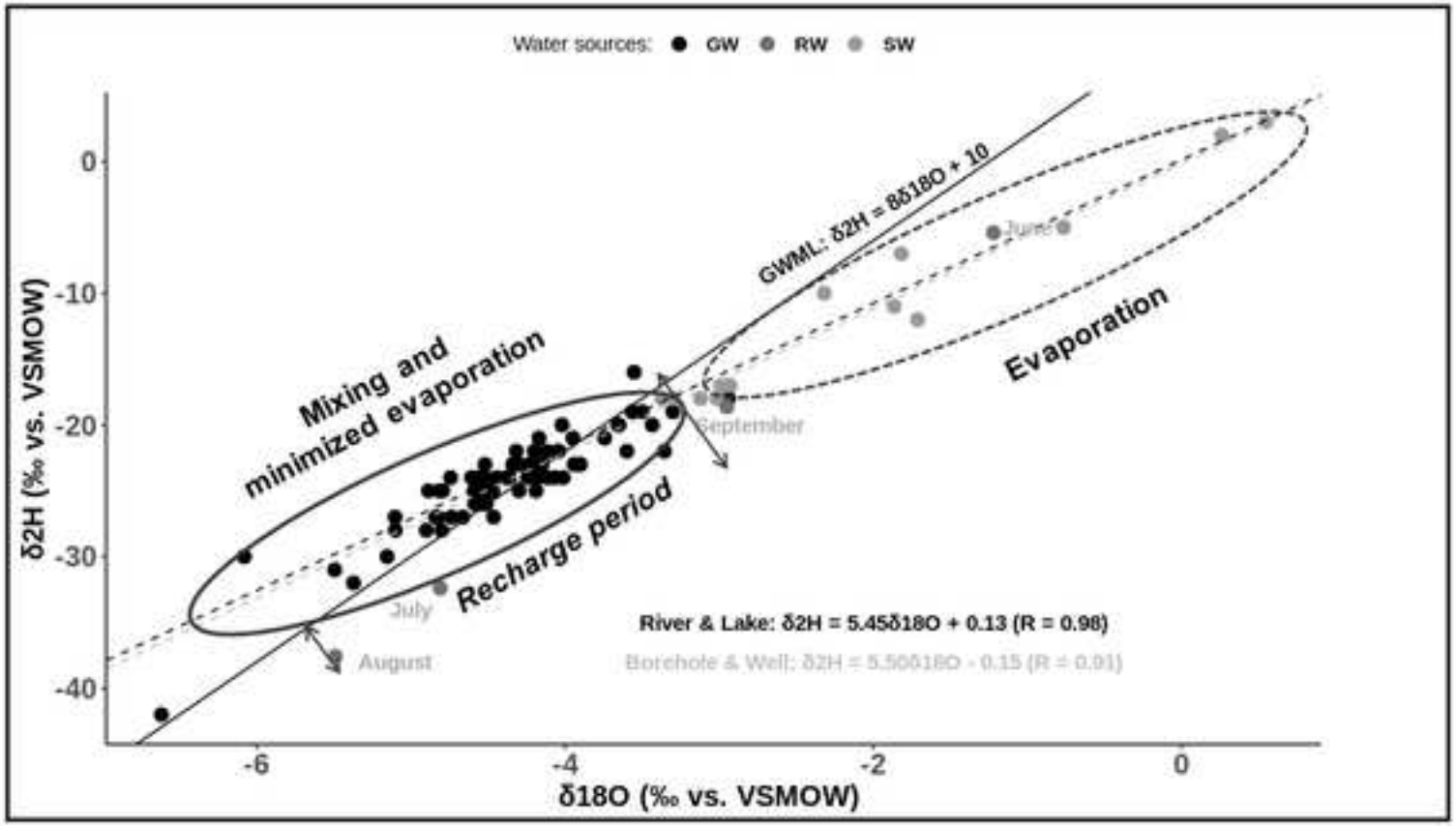

Figure 6b

Click here to access/download;Figure;Fig. 6b.tif

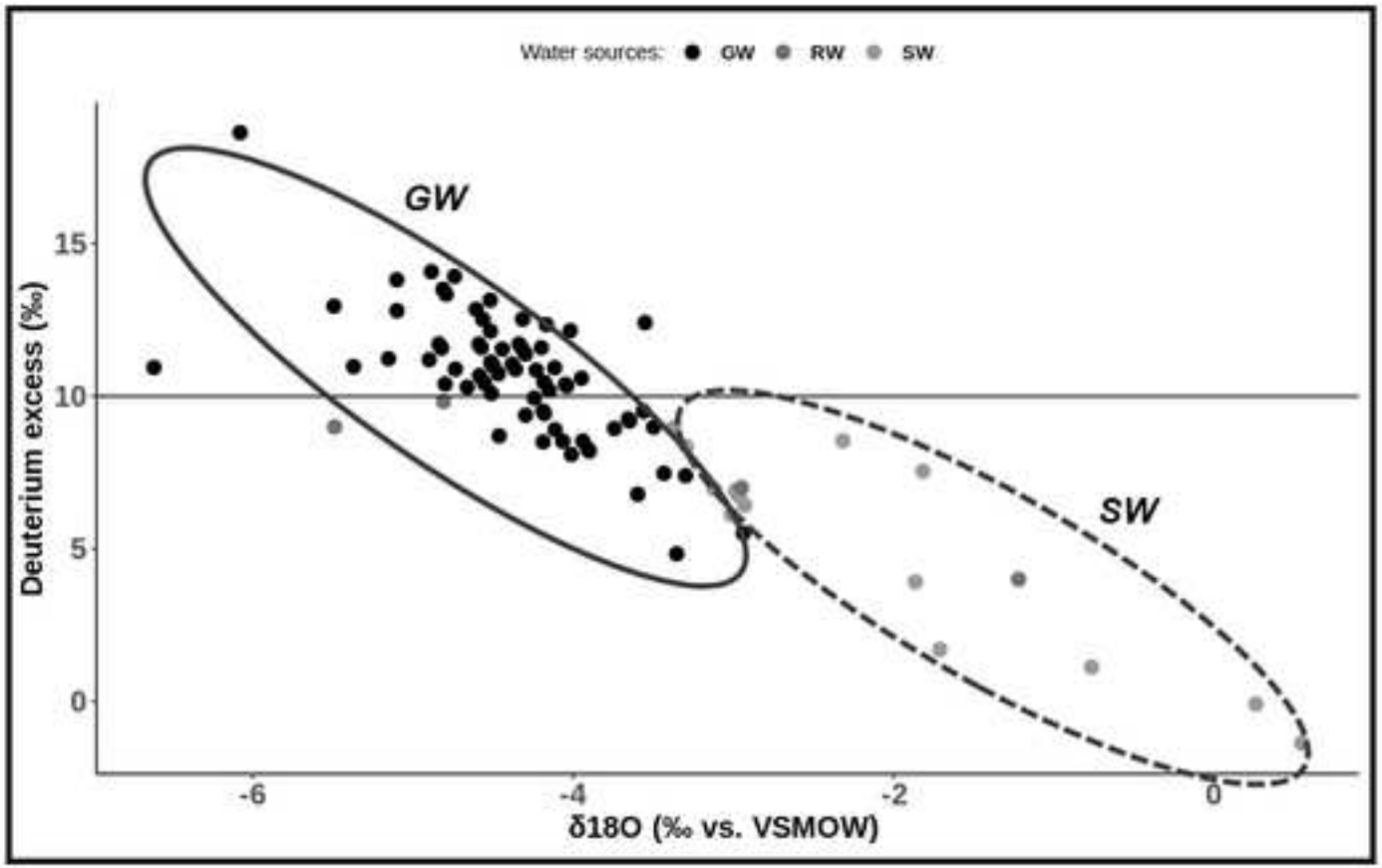

Figure 7

Click here to access/download;Figure;Fig. 7.tif

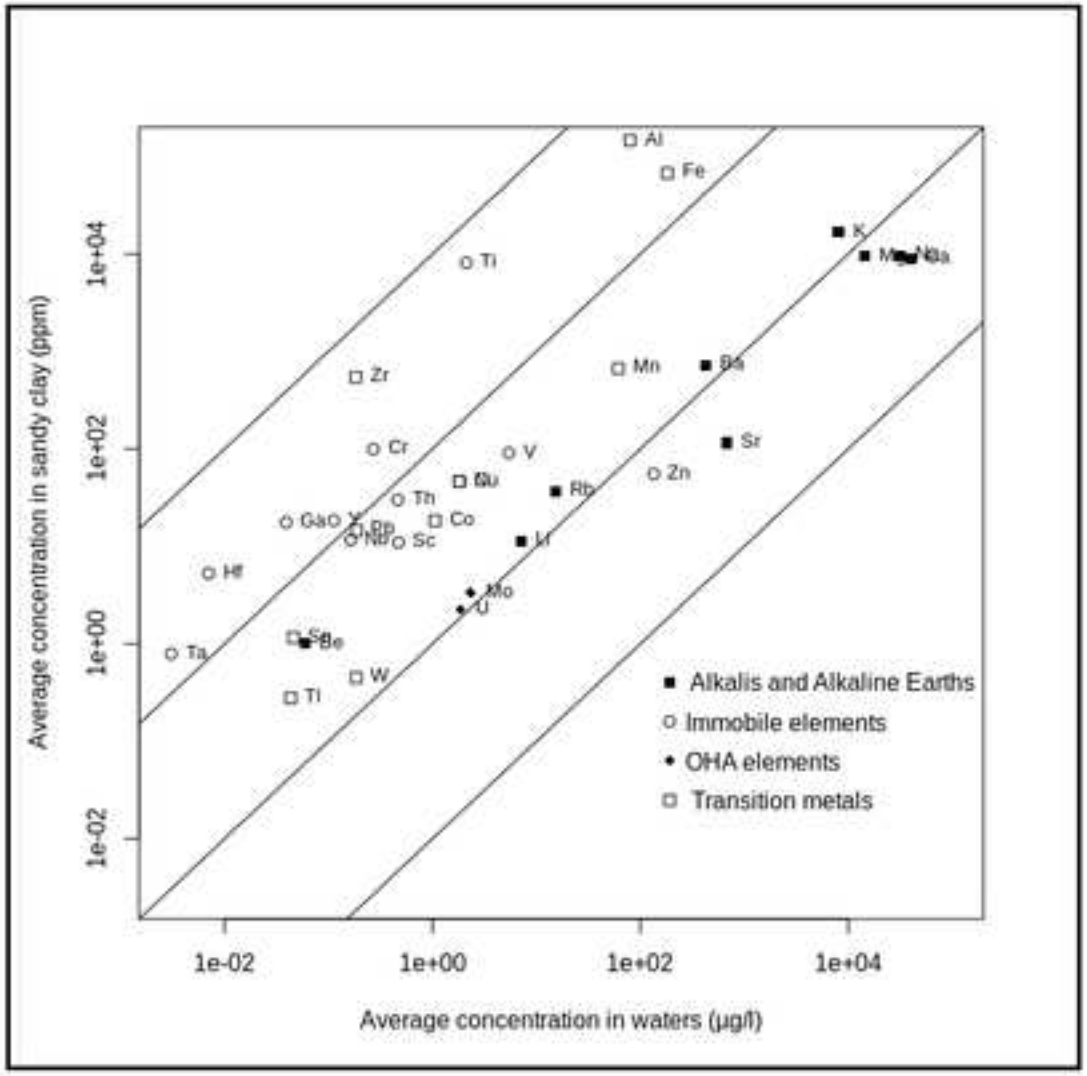

Figure 8

Click here to access/download;Figure;Fig. 8..jpg

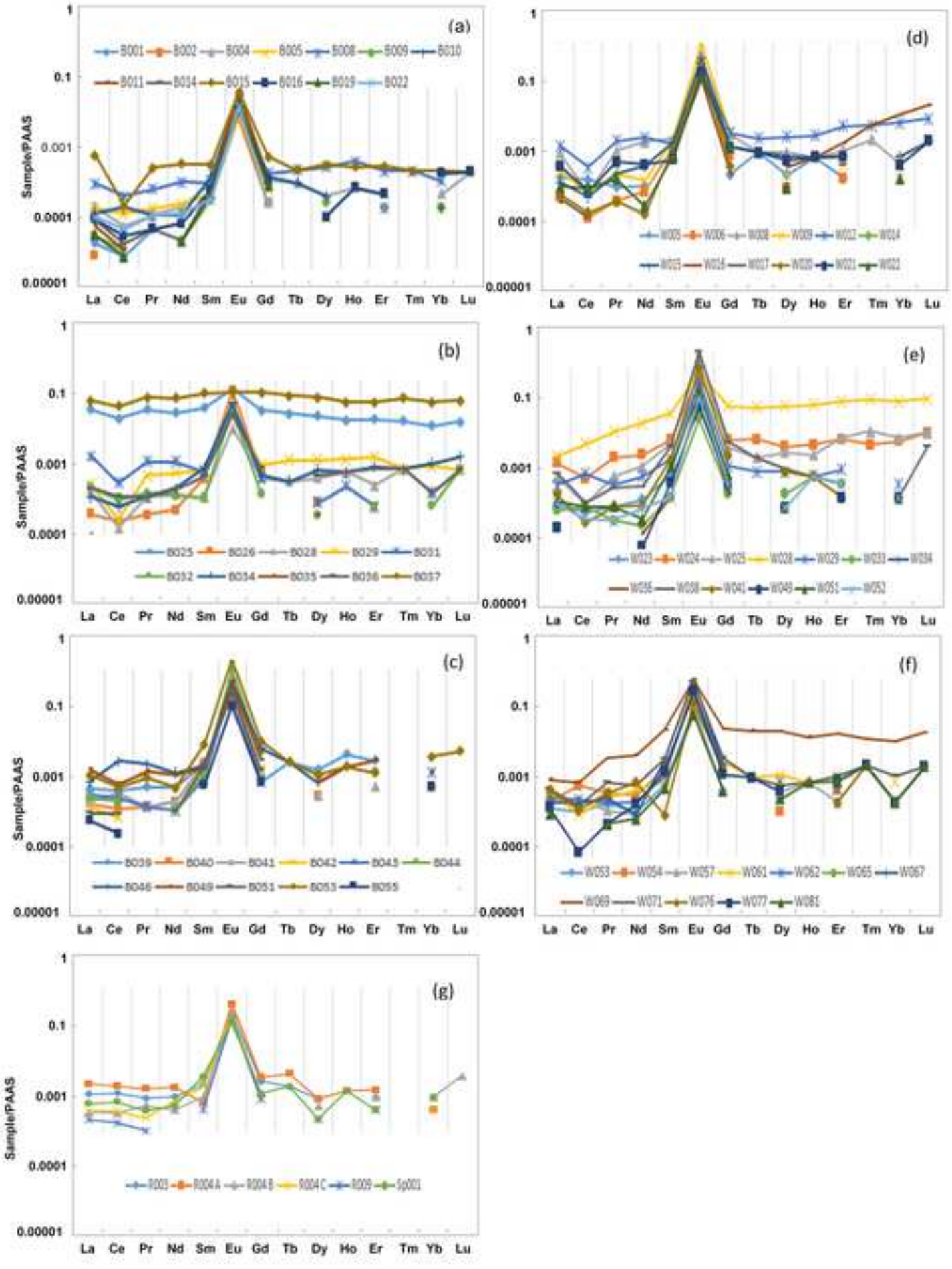

Figure 9

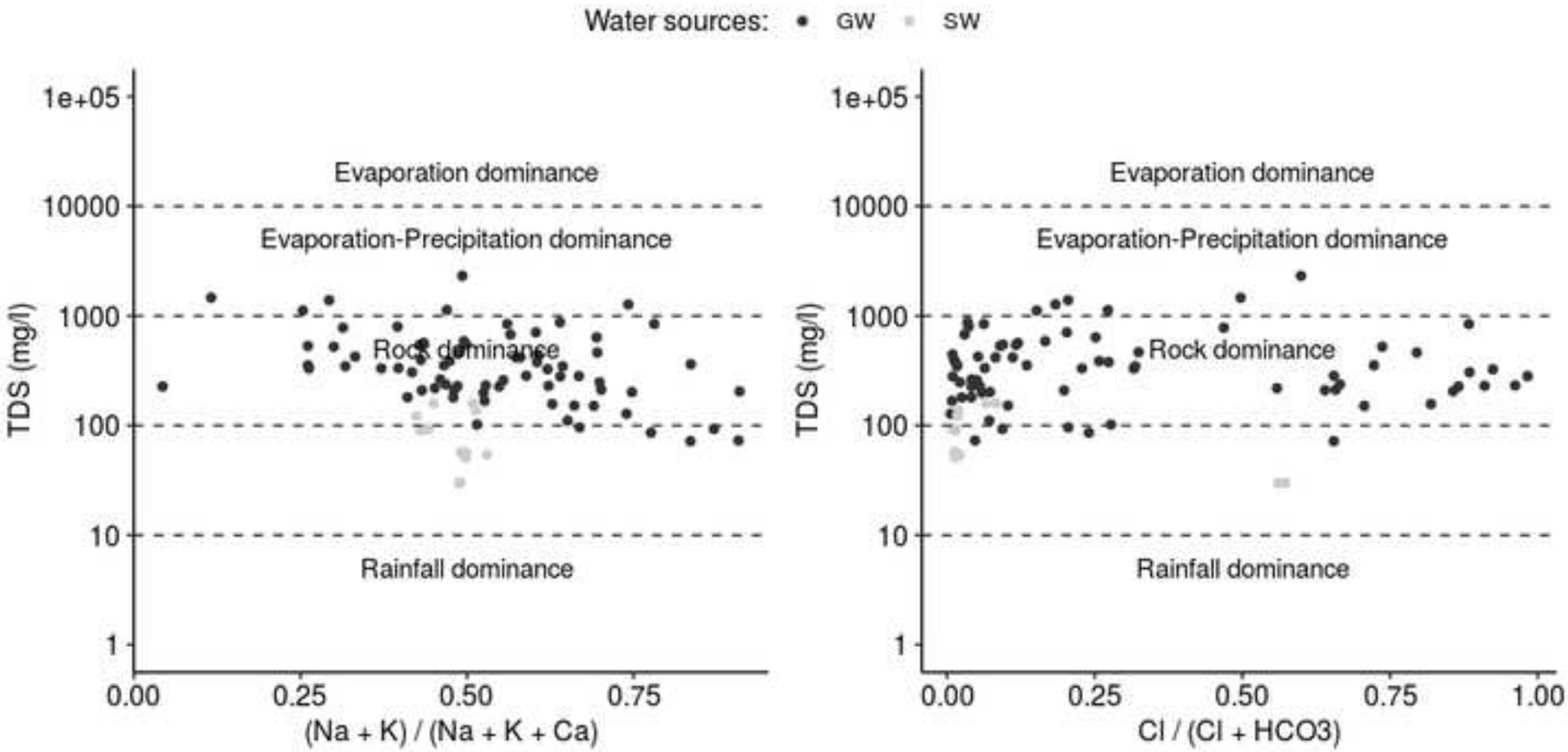

Figure 10

Click here to access/download;Figure;Fig. 10 a and b.tif

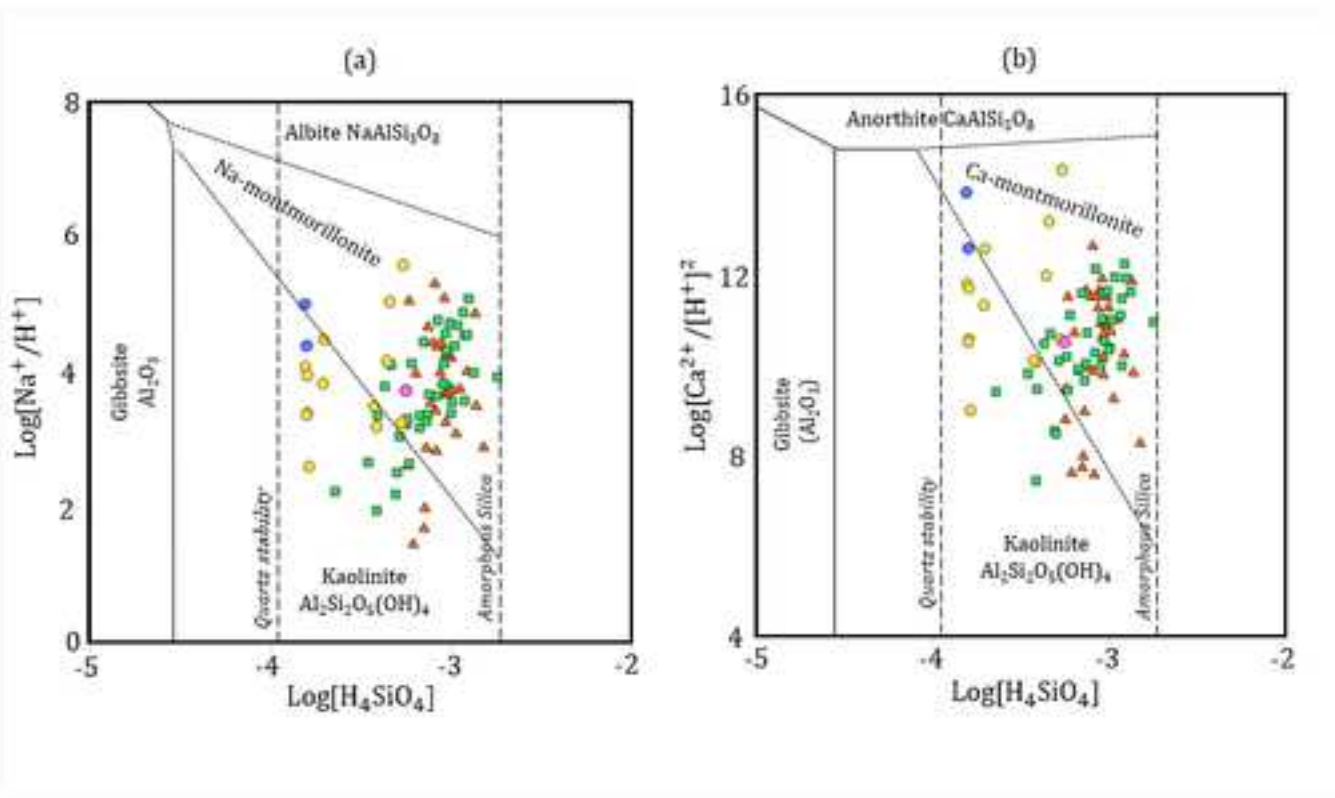

Figure 10c

Click here to access/download;Figure;Fig. 10 c.tif

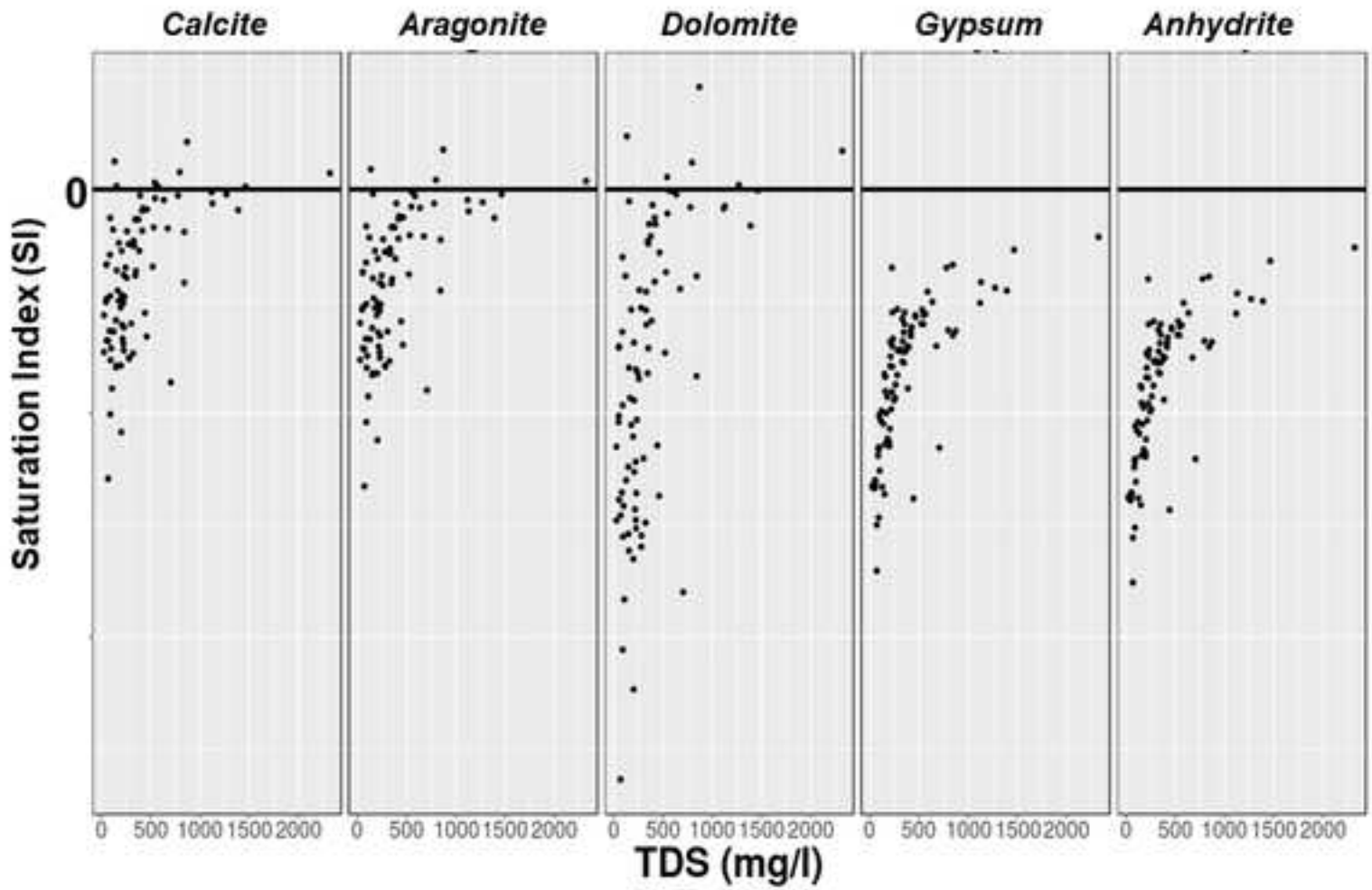

Figure 11

Click here to access/download;Figure;Fig. 11 a and b.tif

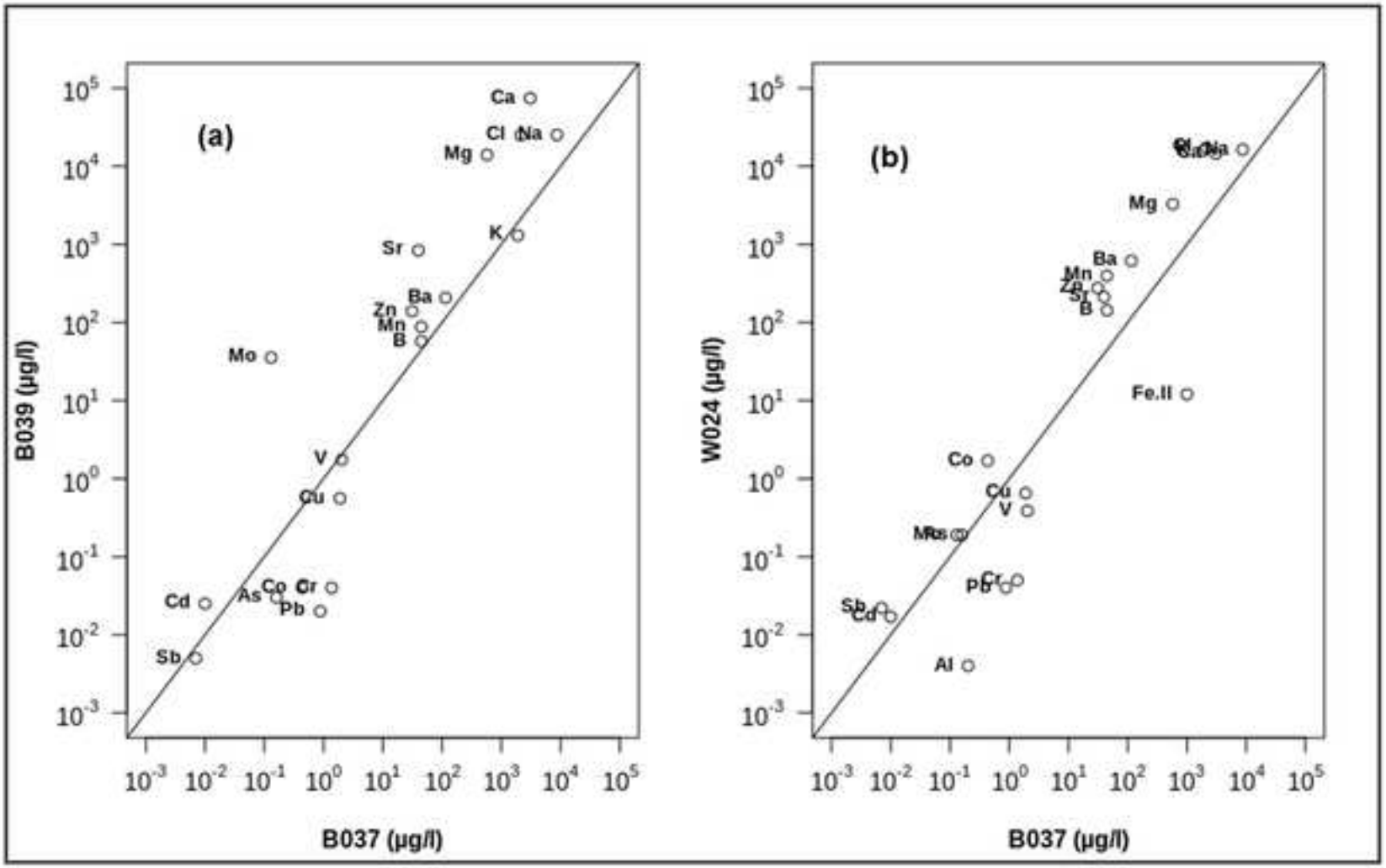

Figure 12

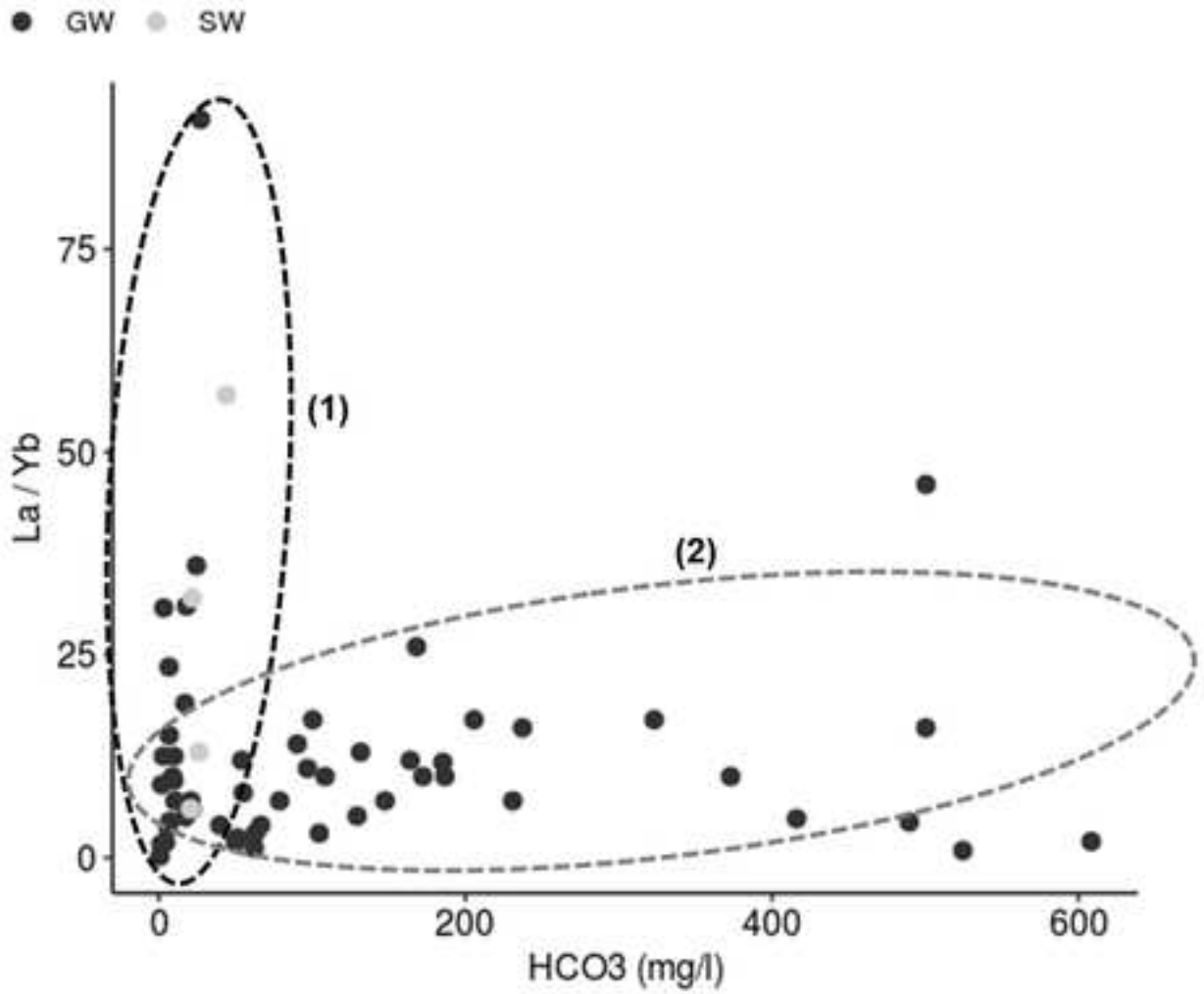

Figure 13

Click here to access/download;Figure;Fig. 13..tif

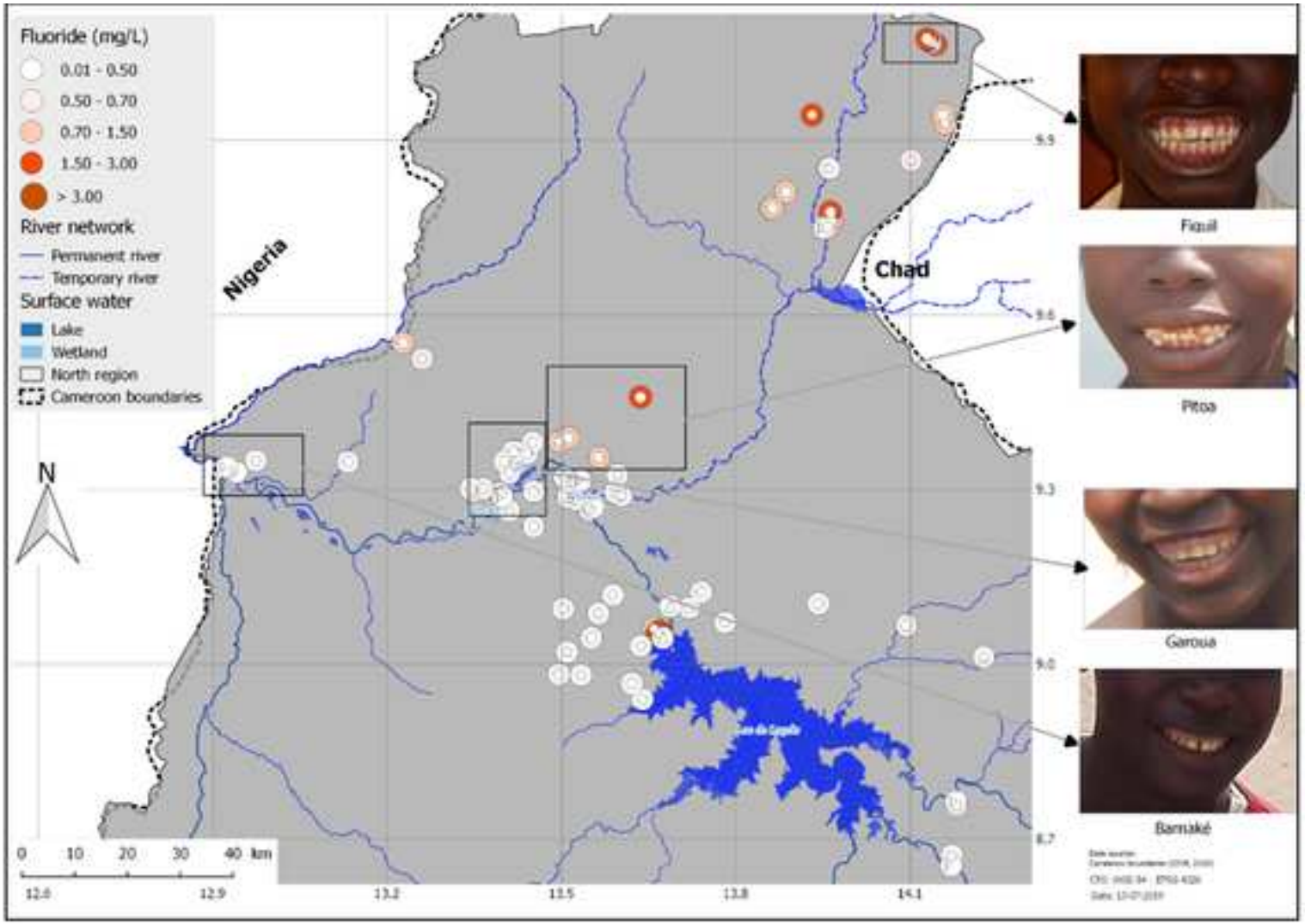

Figure 14

Click here to access/download;Figure;Fig. 14a-c..tif

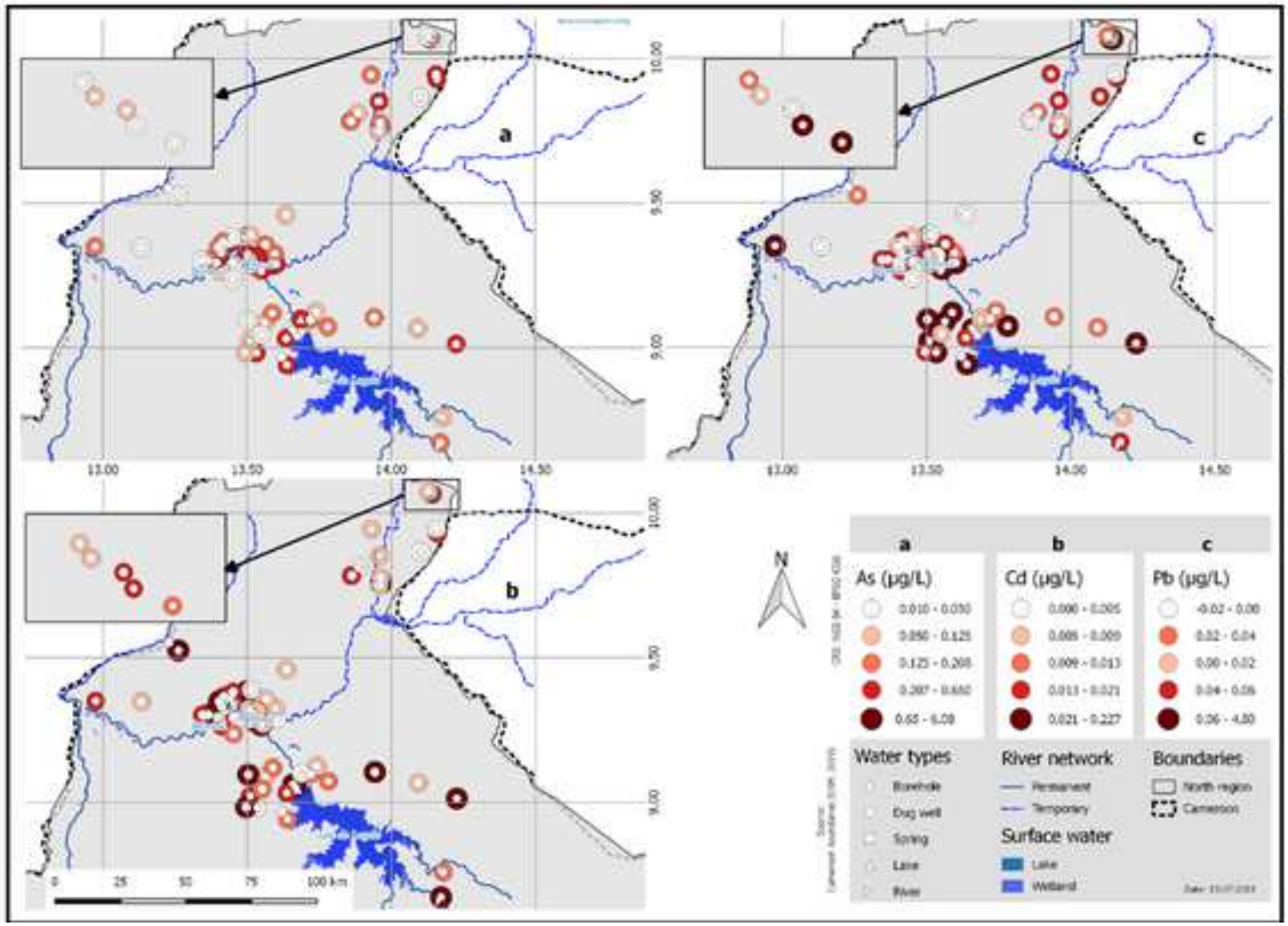

Figure 15

Click here to access/download;Figure;Fig. 15a-f.tif

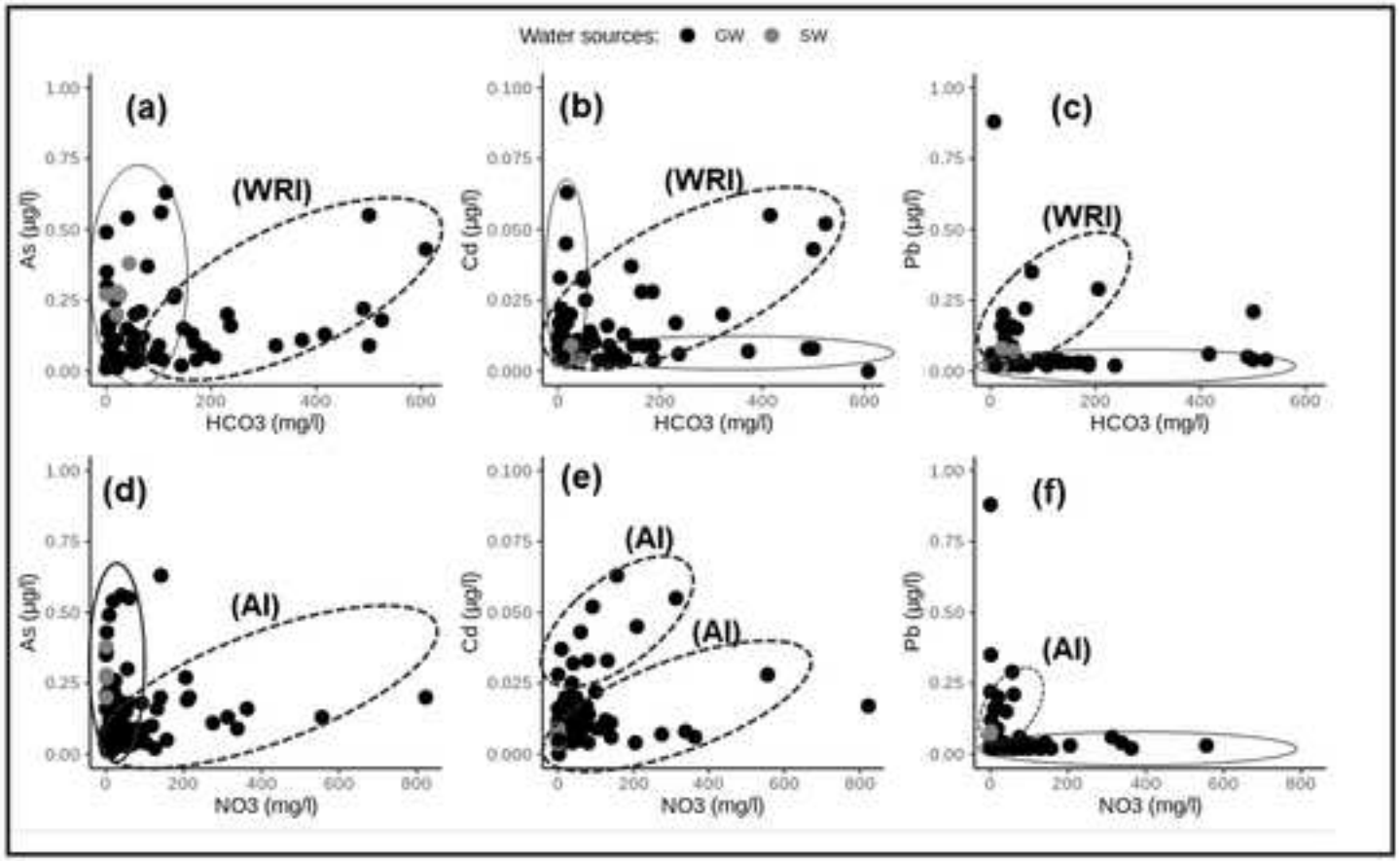

Figure 16

Click here to access/download;Figure;Fig. 16.tif

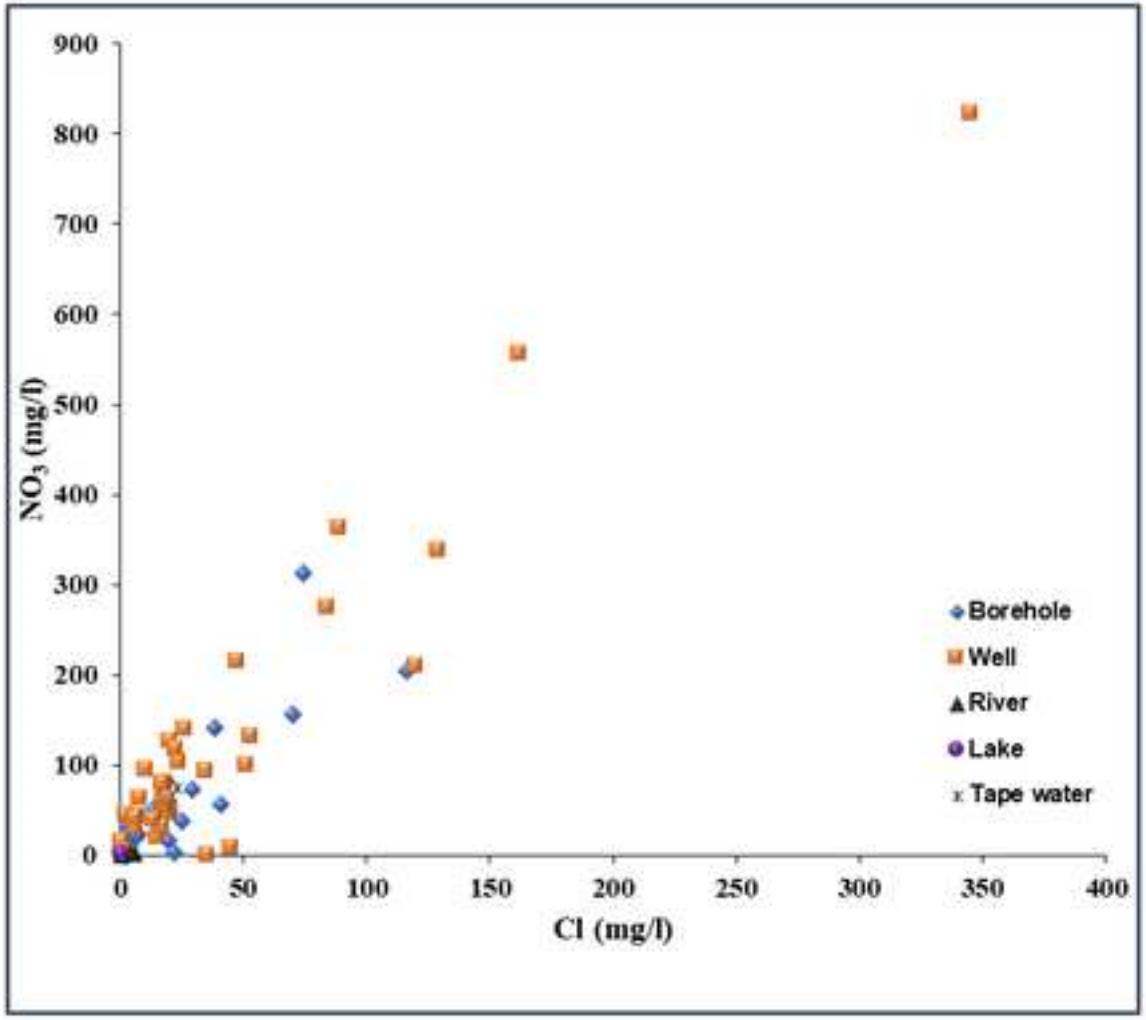

Figure 17

Click here to access/download;Figure;Fig. 17a and b.tif

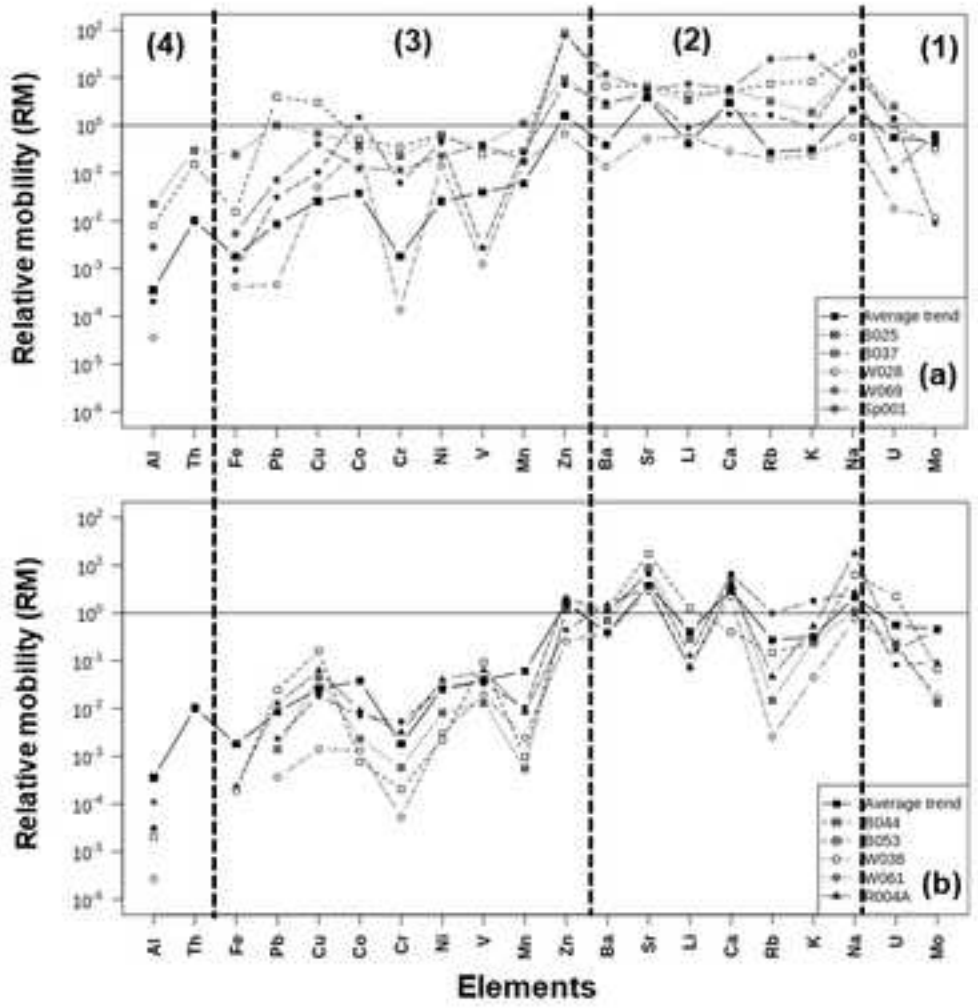

Figure 18

Click here to access/download;Figure;Fig. 18.tif

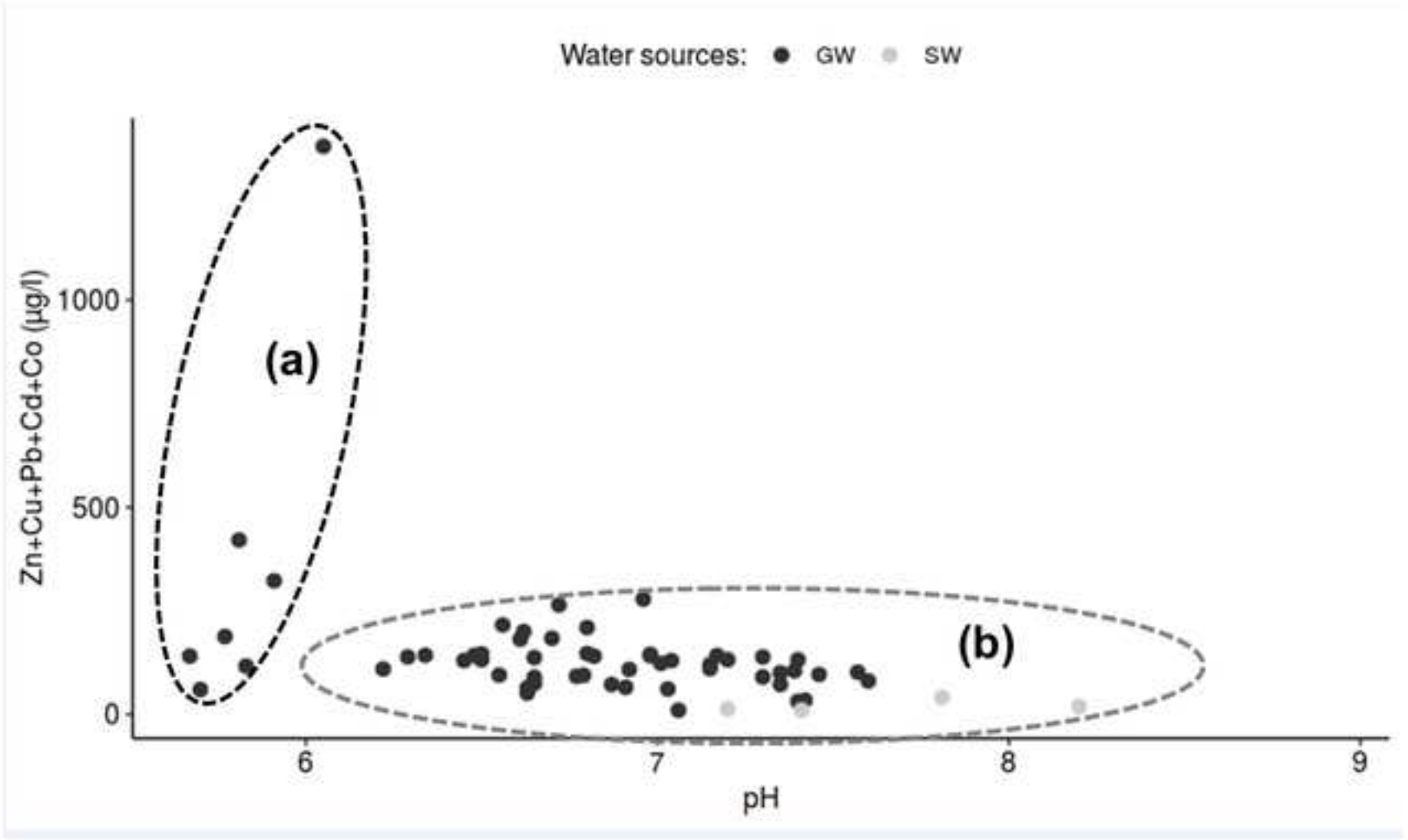

Table 1a:

Sample ID	Long (dd.dd)	Lat (dd.dd)	Temp (°C)	PH	EC (µS/cm)	HCO_3 (mg/l)	K (mg/l)	Na (mg/l)	Cl (mg/l)	Mg (mg/l)	Ca (mg/l)	SO_4 (mg/l)	NO_3 (mg/l)	Br (mg/l)	NH_4 (mg/l)	F (mg/l)	SiO_2 (mg/l)	$\delta^{18}O$ (‰)	$\delta^{2}H$ (‰)	DE (‰)
B001	13.59	9.29	30.2	6.63	214	36.42	1.5	19.5	0.31	5.63	18.9	0.774	4.52	0.009	0.01	0.321	46.4	-2.94	-18	6
B002	13.6	9.29	30.2	6.63	332	40.75	5.1	26.6	2.39	9.09	33.6	3.13	17.9	0.017	0.01	0.498	56.0	-3.43	-20	8
B004	13.6	9.33	30.8	6.8	474	147.62	3.1	52.8	13.2	10.9	40.5	10.2	51.1	0.042	0.03	0.367	55.1	-4.18	-24	10
B005	13.5	9.39	28.3	7.06	1266	131.58	1.7	65.5	116	47.9	147	64.0	205	bdl	0.02	1.10	bdl	-4.17	-21	12
B008	13.5	9.38	31.1	7.17	549	185.26	1.6	44.0	2.28	20.2	60.3	4.59	0.025	0.022	bdl	1.09	47.4	-4.57	-25	12
B009	13.55	9.27	31.1	6.98	378	62.83	7.1	12.5	18.6	19.3	33.2	4.19	81.4	0.040	0.02	0.292	58.1	-4.59	-25	11
B010	13.52	9.28	30.9	7.35	741	108.46	11.8	120	1.82	28.0	25.9	8.83	0.017	0.016	0.01	0.768	35.0	-6.62	-42	11
B011	13.5	9.32	30.7	6.7	71	5.92	8.1	2.0	1.53	1.49	5.00	2.30	14.9	0.010	0.02	0.079	34.3	-5.10	-28	13
B014	13.41	9.26	32	5.7	82	13.24	11.0	1.4	1.02	1.57	6.65	1.43	14.7	0.009	bdl	0.099	37.1	-6.08	-30	19
B015	13.39	9.3	26.9	5.91	648	18.06	39.7	49.1	70.1	10.1	38.9	26.3	156	0.206	0.01	0.090	33.8	-4.24	-24	10
B016	13.42	9.34	30.9	6.5	244	62.22	32.4	20.3	29.1	7.04	29.2	15.5	72.3	0.033	0.01	0.272	49.2	-4.19	-25	8
B019	13.42	9.37	32.3	6.17	50	5.55	10.3	1.6	0.574	0.425	1.77	0.090	4.38	0.005	bdl	0.074	42.7	-4.84	-27	12
B022	13.35	9.3	30.6	6.48	68	38.74	5.7	6.1	0.242	1.21	4.16	0.145	2.01	0.004	0.01	0.152	43.5	-4.90	-28	11
B025	12.97	9.35	31.8	5.81	192	3.23	11.6	25.8	19.3	0.793	3.75	1.95	58.5	0.028	0.02	0.036	49.7	-4.59	-26	11
B026	13.26	9.52	31.1	7.01	383	143.53	5.3	13.2	2.46	21.9	39.8	3.39	9.01	0.007	0.01	0.576	67.3	-5.15	-30	12
B028	14.1	9.87	31.7	7.03	571	90.28	0.5	22.0	14.1	30.0	63.7	11.0	37.7	0.038	0.01	0.632	52.4	-4.79	-25	13
B029	14.16	9.93	31.2	6.98	771	129.32	0.4	40.9	7.17	36.5	83.1	8.03	23.1	0.012	0.01	1.03	59.7	-4.18	-23	10
B031	14.14	10.06	31.5	7.4	285	27.27	1.0	25.9	0.699	6.66	29.2	1.00	1.49	0.017	0.01	1.56	53.2	-3.35	-22	5
B032	14.14	10.07	30.2	7.3	279	24.52	2.0	21.9	6.06	3.54	31.4	3.33	19.9	0.032	0.01	1.14	58.5	-4.34	-23	12
B034	13.93	9.94	31.5	7.39	734	51.24	4.0	70.9	19.3	32.3	48.9	5.85	15.5	0.022	0.01	1.87	81.1	-3.60	-22	7
B035	13.96	9.85	30.7	7.4	840	113.95	3.8	118	38.3	40.9	53.6	37.0	141	bdl	0.01	2.78	54.8	-4.19	-24	10
B036	13.66	9.06	30.7	7.2	840	205.63	4.1	68.9	41.0	25.1	74.4	39.3	55.9	0.039	0.01	1.32	44.5	-4.05	-22	10
B037	13.78	9.07	26.9	7.42	67	6.77	1.9	8.7	2.14	0.575	3.06	0.699	0.007	0.018	0.04	0.051	38.2	-5.49	-31	13
B039	13.67	9.05	29.7	6.82	580	54.11	1.3	25.2	25.0	14.0	74.4	11.7	36.8	0.043	0.01	3.34	53.4	-3.95	-21	11

B040	13.64	9.03	31.8	6.05	130	17.32	1.3	16.5	1.36	1.13	6.02	0.559	9.80	0.005	0.01	0.268	91.0	-4.80	-28	10
B041	13.56	9.09	31.7	6.45	272	21.47	6.0	15.6	0.927	6.75	31.0	0.165	9.08	0.004	0.01	0.235	56.1	-4.74	-27	11
B042	13.59	9.12	31.7	6.34	174	39.89	3.6	13.5	2.51	3.73	15.5	0.273	18.0	0.006	0.02	0.304	63.4	-4.56	-26	11
B043	13.64	8.94	30.6	6.8	267	66.49	1.8	38.8	1.49	2.24	17.5	1.41	0.374	0.011	0.03	0.417	73.0	-3.91	-23	9
B044	13.53	8.98	31.2	6.87	479	78.81	3.8	59.3	0.770	9.34	35.5	2.21	0.750	0.005	0.01	0.163	55.8	-4.46	-27	9
B046	13.51	9.02	29.9	5.77	92	323.18	7.8	2.0	3.06	1.77	6.36	0.072	31.9	0.011	0.03	0.041	42.4	-4.04	-22	11
B049	14.23	9.01	31.2	7.15	620	500.38	3.7	39.5	19.0	18.6	66.0	9.15	59.9	0.020	0.01	0.277	50.5	-4.18	-23	10
B051	14.18	8.76	31.1	6.61	188	71	1.6	18.8	3.77	3.75	16.4	1.62	9.19	0.005	0.01	0.221	82.7	-4.51	-26	11
B053	14.17	8.67	31.5	6.62	1030	416.02	12.8	31.0	74.5	28.1	129	16.3	313	0.099	0.01	0.116	61.4	-4.47	-25	11
B055	13.86	9.78	30	7.8	610	608.29	2.3	76.8	21.9	23.5	44.6	13.3	1.73	0.037	0.05	1.26	48.8	-3.30	-19	7
W005	13.56	9.36	28.9	7.3	463	3.36	4.8	33.3	5.97	17.2	41.2	7.49	28.7	0.018	bdl	1.07	42.0	-4.30	-25	10
W006	13.51	9.39	28	7.17	804	7.99	2.1	60.9	20.8	35.7	72.4	16.6	46.6	0.045	bdl	1.38	56.1	-4.38	-24	11
W008	13.55	9.27	30	6.56	378	6.65	8.7	15.8	50.9	13.1	34.2	6.66	99.3	0.030	0.01	0.100	44.1	-4.51	-25	11
W009	13.52	9.28	29.3	6.84	765	17.02	14.1	22.1	47.6	23.2	84.5	9.21	214	0.086	0.02	0.197	56.3	-4.11	-24	9
W012	13.5	9.32	27.7	6.5	320	489.65	29.0	11.4	15.0	5.31	31.1	9.34	19.9	0.012	0.01	0.249	40.0	-4.01	-24	8
W014	13.45	9.3	28.9	6.83	160	1.77	14.9	4.0	8.01	3.16	11.2	0.348	62.9	0.029	0.02	0.029	31.0	-4.66	-27	11
W015	13.45	9.24	29.9	6.8	95	6.04	5.3	1.8	2.32	2.75	6.69	0.183	43.5	0.022	0.03	0.015	20.8	-4.82	-27	12
W016	13.39	9.29	25.5	6.81	638	0.79	50.5	47.0	44.9	9.01	48.5	26.6	7.91	0.048	bdl	0.518	27.9	-4.55	-26	11
W017	13.41	9.33	28.8	7	512	1.40	25.7	32.6	35.1	7.05	52.1	20.4	0.016	0.049	bdl	0.360	35.9	-4.52	-25	11
W020	13.42	9.35	29.5	6.5	44	0.24	6.2	1.2	0.455	0.360	1.46	0.012	14.5	0.008	bdl	0.027	29.5	-4.44	-24	12
W021	13.43	9.36	29.3	6.65	268	9.88	27.6	12.3	19.0	4.19	17.0	9.01	47.9	0.032	0.01	0.094	40.3	-4.36	-24	11
W022	13.44	9.36	31.5	6.65	374	1.77	41.8	10.9	17.9	6.04	32.0	7.83	54.6	0.050	0.03	0.261	34.6	-4.50	-25	11
W023	13.45	9.38	30.3	6.91	319	8.97	14.4	14.0	17.8	6.67	32.3	10.3	60.3	0.036	bdl	0.366	45.0	-4.52	-24	12
W024	13.42	9.37	26.7	6.96	228	7.20	15.9	16.4	17.3	3.28	14.5	5.03	30.7	0.034	0.02	0.101	25.6	-4.20	-22	11
W025	13.4	9.35	27.8	6.29	480	4.39	22.9	28.5	53.2	10.1	31.4	6.78	131	0.049	0.01	0.063	23.4	-4.02	-20	12
W028	13.36	9.3	28.8	6.72	367	524.54	23.0	30.8	34.9	5.59	15.1	30.6	91.7	0.072	0.03	0.393	53.9	-4.81	-25	14
W029	13.34	9.3	27	6.79	241	2.93	7.2	17.3	18.9	3.52	20.2	1.79	74.9	0.021	0.02	0.050	50.1	-4.30	-23	11
W033	13.13	9.35	30	6.03	310	20.86	0.2	3.9	0.9	5.68	91.2	78.0	3.46	0.008	0.01	0.141	13.7	-3.55	-16	12

W034	13.23	9.55	28.8	6.75	55	3.11	1.2	7.9	0.791	1.21	5.98	1.01	0.396	0.004	0.05	0.990	43.4	-5.37	-32	11
W036	13.97	9.76	26.8	6.54	1310	15.86	3.0	146	120	49.5	117	91.0	209	bdl	0.01	1.34	56.2	-3.65	-20	9
W038	13.96	9.75	29.9	6.22	1540	500.51	5.7	55.2	129	72.4	147	26.8	338	bdl	bdl	0.756	71.5	-3.74	-21	9
W041	13.96	9.78	29.2	6.77	1421	237.23	2.8	99.9	88.8	72.9	116	45.9	363	bdl	0.02	1.60	62.8	-3.94	-23	9
W049	14.16	9.94	28.4	7.28	743	104.68	0.3	66.7	13.1	36.9	49.8	11.2	39.9	0.021	0.01	1.43	58.9	-3.66	-20	9
W051	14.14	10.07	28	7.05	338	96.99	0.9	28.9	4.20	7.23	35.0	1.48	0.008	0.005	0.01	1.36	54.3	-3.50	-19	9
W052	14.13	10.07	29.1	7.15	670	186.66	2.2	58.7	19.5	19.5	61.2	17.4	65.1	0.030	0.01	2.68	71.4	-3.90	-23	8
W053	14.13	10.07	29.9	7.35	708	172.26	2.0	52.9	23.5	19.2	71.3	16.0	102	0.084	0.01	2.28	64.8	-4.07	-24	8
W054	13.89	9.81	27.9	6.55	655	187.51	2.8	24.8	18.5	24.9	78.1	17.6	79.9	0.005	0.01	1.12	60.6	-4.15	-23	10
W057	13.94	9.1	29.5	6.92	1967	164.03	5.1	28.2	162	76.9	254	89.6	556	0.194	0.01	0.484	79.8	-3.56	-19	9
W061	13.72	9.1	26.9	7.57	524	55.02	26.3	23.0	26.4	8.37	51.7	18.0	140	0.094	0.02	0.128	73.8	-4.32	-23	12
W062	13.74	9.12	30.5	6.65	368	100.41	16.2	13.1	6.86	6.84	44.5	7.28	41.9	0.019	0.04	0.243	60.1	-4.61	-24	12
W065	13.62	8.97	28.5	6.34	242	8.30	14.7	4.9	10.5	4.04	23.8	0.745	94.4	0.015	bdl	0.038	35.2	-4.89	-25	14
W067	13.5	8.98	29.5	7.04	225	49.29	8.6	18.5	17.1	8.56	30.1	1.47	79.1	0.018	0.06	0.318	108	-4.57	-24	13
W069	13.5	9.1	29.9	5.67	106	50.02	5.3	4.7	5.75	3.14	5.13	0.095	40.6	0.019	bdl	0.010	23.2	-4.74	-24	14
W071	13.55	9.05	30.3	5.83	356	10.49	26.0	11.8	19.9	7.60	26.4	7.96	126	0.059	0.09	0.042	29.9	-4.52	-23	13
W076	14.09	9.07	28.5	7.46	660	168.12	2.1	48.2	22.2	25.6	67.0	11.3	118	bdl	0.01	0.585	50.5	-4.12	-22	11
W077	13.64	9.46	28.8	6.9	1600	373.02	2.0	230	83.9	58.5	80.7	53.1	275	bdl	bdl	2.82	69.9	-4.32	-22	13
W081	13.86	9.78	29.8	7.07	2500	230.89	1.0	244	345	124	252	177	823	0.663	0.02	0.820	75.1	-4.23	-23	11
R001	13.59	9.3	26.1	8.04	115	43.68	3.5	6.7	0.68	3.77	13.2	0.234	0.547	0.004	0.02	0.207	11.8	0.55	3	-1
R003	13.55	9.27	25.7	7.81	50	21.84	2.5	4.5	0.48	2.04	6.21	0.114	0.680	bdl	0.01	0.129	9.4	-3.37	-18	9
R004 A	13.54	9.32	24.4	7.41	154	44.04	3.3	6.5	0.652	3.63	13.0	0.252	0.138	0.004	0.06	0.204	11.7	0.26	2	0
R004 B	13.53	9.32	24.1	7.2	63	20.74	2.3	3.8	0.281	2.03	6.16	0.095	0.218	bdl	bdl	0.130	9.6	-3.29	-18	9
R004 C	13.53	9.32	24.8	7.76	63	26.23	2.3	3.8	0.33	2.03	6.17	0.110	0.146	bdl	0.02	0.132	9.6	-3.12	-18	7
R005	13.4	9.29	24.8	6.4	65	24.83	2.4	3.9	0.345	2.09	6.54	0.124	0.422	bdl	0.02	0.133	9.8	-2.99	-17	7
R006 A	12.94	9.33	25.6	7.16	65	23.49	2.4	3.9	0.326	2.11	6.34	0.124	0.141	bdl	0.01	0.138	9.5	-2.97	-17	7
R006 B	12.92	9.34	28.8	6.86	90	35.01	1.9	5.2	0.321	3.28	8.95	0.364	0.011	bdl	0.07	0.165	23.1	-1.82	-7	7
R007	13.95	9.75	28.7	6.71	222	69.24	5.5	14.9	6.27	4.07	19.7	1.82	1.68	0.011	0.01	0.325	22.3	-0.77	-5	2

R008	13.96	9.85	30	8.2	193	56.06	3.8	16.5	3.96	4.55	24.8	2.65	2.08	0.009	0.01	0.297	27.4	-2.32	-10	8
R012	14.18	8.76	29.8	7.72	134	46.60	4.0	6.6	0.827	4.42	14.4	1.05	1.14	0.004	bdl	0.136	26.3	-1.71	-12	2
R013	14.17	8.65	32.2	8.92	139	50.51	2.5	10.9	1	4.34	12.7	0.709	1.80	0.004	0.01	0.308	32.5	-1.86	-11	4
R009	13.69	9.1	29.3	8.2	72	0.21	2.3	3.7	0.27	2.05	6.30	0.092	0.214	bdl	0.01	0.132	9.5	-3.01	-18	6
R010	13.67	9.05	28.7	8.81	65	0.24	2.4	3.7	0.322	2.06	6.35	0.101	0.039	bdl	0.01	0.135	9.3	-2.93	-17	6
Sp001	13.51	9.29	23.9	7.6	35	9.76	8.5	1.1	0.487	0.181	0.98	0.119	1.26	0.004	0.03	0.042	31.7	-5.10	-27	14
Rk	-	-	-	-	-	-	16673.3	9606.7	-	9520.0	8926.7	-	-	-	-	-	636686.7	-	-	-

B = borehole, W = dug-well, R = river or lake, Rk = rock, Temp. = Temperature, EC = electrical conductivity, n = number of samples, bdl = below detection limit, letter following R004 and R006 represent the sample station. Data for rocks (which are presented here as average) are from Ndjigui et al. (2014)

Table 1b

Sample ID	Long (dd.dd)	Lat (dd.dd)	Fe(II) (mg/l)	Mn (mg/l)	Al (mg/l)	As (µg/l)	Ba (µg/l)	BO2 (mg/l)	Br (mg/l)	Cd (µg/l)	Co (µg/l)	Cr (µg/l)	Cu (µg/l)	Li (µg/l)	Ni (µg/l)	Pb (µg/l)	V (µg/l)	Zn (µg/l)
B001	13.59	9.29	3.13	0.397	0.007	6.08	209	0.02	0.009	0.003	0.066	0.04	0.15	0.5	bdl	0.02	0.046	51.2
B002	13.6	9.29	0.005	0.024	bdl	0.54	166	0.06	0.017	0.005	0.549	0.03	1.71	1.0	1.1	0.09	19.3	61.9
B004	13.6	9.33	0.017	0.001	bdl	0.15	332	0.29	0.042	0.009	0.046	0.24	5.70	0.7	0.3	0.03	6.75	204
B005	13.5	9.39	bdl	bdl	bdl	0.27	245	bdl	bdl	0.004	0.026	0.10	0.48	0.2	0.2	0.03	0.486	9.61
B008	13.5	9.38	0.003	0.501	bdl	0.08	285	0.11	0.022	0.028	1.34	0.05	1.85	0.5	0.7	0.03	8.11	139
B009	13.55	9.27	bdl	bdl	0.003	0.08	397	0.12	0.040	0.014	0.030	0.21	2.60	4.7	0.4	0.02	6.84	139
B010	13.52	9.28	bdl	0.015	bdl	0.04	605	0.11	0.016	0.004	0.165	0.02	0.61	30.0	0.2	0.02	6.02	71.4
B011	13.5	9.32	bdl	0.001	bdl	0.16	762	0.10	0.010	0.015	0.112	0.08	1.76	2.4	0.7	0.02	0.694	182
B014	13.41	9.26	bdl	0.000	bdl	0.06	325	0.02	0.009	0.018	1.09	1.84	1.37	1.8	2.4	0.04	0.454	57.6
B015	13.39	9.3	0.021	0.023	bdl	0.05	720	0.26	0.206	0.063	3.12	0.63	0.64	2.2	4.5	0.02	0.316	319
B016	13.42	9.34	bdl	0.002	bdl	0.04	288	0.16	0.033	0.012	0.298	0.33	1.72	1.3	1.3	bdl	0.860	195
B019	13.42	9.37	bdl	0.001	bdl	0.02	363	0.18	0.005	0.016	0.829	0.16	0.21	2.0	1.1	bdl	0.835	173
B022	13.35	9.3	bdl	0.001	bdl	0.04	307	0.27	0.004	0.011	0.153	0.31	1.86	1.3	0.9	0.04	0.229	141
B025	12.97	9.35	0.087	0.013	0.098	0.18	401	0.86	0.028	0.017	0.774	2.92	11.6	4.2	2.5	4.80	1.90	404
B026	13.26	9.52	0.003	0.001	bdl	0.02	630	0.15	0.007	0.037	0.024	0.15	3.16	7.4	0.2	0.03	1.54	120
B028	14.1	9.87	bdl	0.001	bdl	0.05	87.4	0.07	0.038	0.004	0.035	0.05	2.82	2.7	0.2	0.04	12.4	58.3
B029	14.16	9.93	bdl	0.000	bdl	0.26	181	0.13	0.012	0.013	0.050	0.07	0.85	5.8	0.1	0.04	10.1	144
B031	14.14	10.06	0.330	0.026	bdl	0.03	255	0.11	0.017	0.010	0.053	0.04	0.78	14.5	0.1	0.12	0.658	131
B032	14.14	10.07	0.715	0.087	0.003	0.05	220	0.07	0.032	0.020	0.166	0.06	0.39	17.8	0.8	0.20	0.206	138
B034	13.93	9.94	0.001	0.001	0.003	0.13	309	0.09	0.022	0.007	0.033	0.47	0.39	8.6	0.2	0.04	37.7	105
B035	13.96	9.85	bdl	0.002	0.003	0.63	177	0.06	bdl	0.006	0.052	0.07	0.26	15.8	0.2	0.04	23.9	31.3
B036	13.66	9.06	bdl	0.098	0.003	0.05	171	0.14	0.039	0.206	0.070	0.30	1.49	22.4	0.4	0.29	6.76	130
B037	13.78	9.07	0.999	0.035	0.202	0.16	115	0.11	0.018	0.010	0.433	1.37	1.89	2.3	1.6	0.88	2.03	31.1
B039	13.67	9.05	bdl	0.082		0.03	207	0.16	0.043	0.025	0.040	0.04	0.56	86.2	0.1	0.02	1.75	140
B040	13.64	9.03	bdl	0.008	bdl	0.25	237	0.41	0.005	0.017	0.042	0.50	2.99	1.8	0.3	0.06	4.20	1369

B041	13.56	9.09	0.031	0.009	bdl	0.11	372	0.06	0.004	0.007	0.027	0.08	1.98	4.6	0.3	0.16	2.28	128
B042	13.59	9.12	0.078	0.003	bdl	0.15	358	0.20	0.006	0.010	0.029	0.15	1.65	14.9	0.4	0.16	3.37	141
B043	13.64	8.94	0.078	0.012	bdl	0.21	409	0.17	0.011	0.012	0.023	0.04	2.70	21.0	0.2	0.22	1.48	144
B044	13.53	8.98	bdl	0.001	0.003	0.37	880	0.09	0.005	0.004	0.014	0.02	7.17	14.1	0.1	0.35	8.22	64.7
B046	13.51	9.02	0.006	0.005	0.009	0.09	460	0.08	0.011	0.020	0.655	0.88	26.6	3.3	2.7	1.87	0.136	159
B049	14.23	9.01	bdl	0.119	bdl	0.55	428	0.09	0.020	0.043	0.080	0.03	0.33	19.3	0.1	0.21	5.66	110
B051	14.18	8.76	bdl	0.041	bdl	0.12	254	0.22	0.005	0.010	0.243	0.10	1.37	0.4	0.3	0.02	3.20	180
B053	14.17	8.67	0.013	0.001	bdl	0.13	1480	0.27	0.099	0.055	0.124	0.17	6.04	9.7	1.1	0.06	3.47	194
B055	13.86	9.78	0.045	0.040	0.004	0.43	123	0.41	0.037	0.000	0.037	bdl	0.08	9.1	0.4	bdl	2.23	68.0
W005	13.56	9.36	0.006	0.011	0.005	0.14	228	0.13	0.018	0.006	0.075	0.23	0.44	0.7	0.4	0.04	11.2	89.7
W006	13.51	9.39	bdl	0.011	bdl	0.09	298	0.12	0.045	0.005	0.082	0.03	0.22	3.0	0.2	bdl	19.0	95.1
W008	13.55	9.27	0.004	0.032	bdl	0.09	635	0.12	0.030	0.022	0.384	0.04	0.56	1.1	2.3	0.02	1.12	215
W009	13.52	9.28	bdl	0.033	bdl	0.20	1177	0.13	0.086	0.227	0.201	0.08	0.45	6.6	2.8	bdl	2.41	142
W012	13.5	9.32	0.003	0.004	0.011	0.22	320	0.47	0.012	0.008	0.108	0.06	1.12	0.2	0.4	0.05	2.56	145
W014	13.45	9.3	0.748	0.062	0.334	bdl	bdl	bdl	0.029	bdl	bdl	bdl	bdl	bdl	bdl	bdl	bdl	bdl
W015	13.45	9.24	bdl	0.025	bdl	0.03	547	0.19	0.022	0.012	4.15	0.19	0.48	2.3	5.8		0.105	126
W016	13.39	9.29	bdl	0.008	bdl	0.49	209	0.23	0.048	0.008	0.316	0.06	1.14	0.1	1.2		7.04	119
W017	13.41	9.33	0.003	0.273	bdl	0.35	439	0.16	0.049	0.004	1.26	0.03	0.42	1.0	0.7		0.215	116
W020	13.42	9.35	bdl	0.001	bdl	0.01	331	0.24	0.008	0.012	0.978	0.45	1.11	1.7	1.5	0.03	0.104	130
W021	13.43	9.36	0.006	0.007	0.003	0.10	268	0.18	0.032	0.020	0.087	0.06	1.14	1.2	1.2	0.03	0.983	136
W022	13.44	9.36	bdl	0.001	0.005	0.30	213	0.11	0.050	0.005	0.074	0.57	0.76	4.0	0.2	0.02	4.78	73.6
W023	13.45	9.38	0.006	0.011	0.005	0.03	433	0.04	0.036	0.013	0.153	0.11	0.66	0.9	2.0	0.02	0.490	64.6
W024	13.42	9.37	0.012	0.347	0.004	0.19	615	0.50	0.034	0.017	1.70	0.05	0.65	0.6	3.2	0.04	0.386	276
W025	13.4	9.35	bdl	0.037	0.004	0.16	1269	0.20	0.049	0.033	1.39	0.06	1.27	1.4	6.9	0.02	0.883	136
W028	13.36	9.3	0.167	0.607	0.031	0.18	583	0.46	0.072	0.052	33.3	0.08	13.9	39.3	39.2	0.04	0.667	217
W029	13.34	9.3	bdl	0.295	0.007	0.04	467	0.14	0.021	0.017	10.2	0.93	0.75	13.3	11.6	0.06	1.44	83.5
W033	13.13	9.35	bdl	0.001	bdl	0.01	74.3	0.13	0.008	0.008	0.031	0.04	0.48	0.2	0.2		0.691	141
W034	13.23	9.55	0.612	0.046	2.04	bdl	bdl	bdl	0.004	bdl	bdl	bdl	bdl	bdl	bdl	bdl	bdl	bdl

W036	13.97	9.76	bdl	0.160	bdl	0.19	250	0.15	bdl	0.045	0.244	0.07	1.21	16.1	4.0		8.10	96.5
W038	13.96	9.75	bdl	0.011	0.003	0.09	2058	0.14	bdl	0.008	0.184	0.04	0.49	6.5	0.3	0.04	13.5	109
W041	13.96	9.78	bdl	0.003	0.003	0.16	861	0.16	bdl	0.006	0.191	0.73	0.73	8.4	0.4	0.02	17.6	91.2
W049	14.16	9.94	bdl	0.018	bdl	0.56	131	0.11	0.021	0.005	0.042	0.10	0.29	2.9	0.3		21.3	87.5
W051	14.14	10.07	0.021	0.410	bdl	0.07	269	0.15	0.005	0.016	1.13	0.03	0.26	7.4	1.3		0.677	166
W052	14.13	10.07	bdl	0.042	bdl	0.06	213	0.19	0.030	0.009	0.078	0.02	0.34	17.8	0.5	0.02	6.98	120
W053	14.13	10.07	bdl	0.011	bdl	0.04	171	0.14	0.084	0.009	0.088	0.04	0.29	12.8	0.2	0.03	7.10	100
W054	13.89	9.81	bdl	0.001	bdl	0.07	324	0.11	0.005	0.004	0.071	0.23	0.47	2.0	0.2	0.03	20.6	94.3
W057	13.94	9.1	bdl	0.005	bdl	0.13	203	0.24	0.194	0.028	0.082	0.19	0.48	9.4	0.7	0.03	5.98	108
W061	13.72	9.1	bdl	0.006	0.004	0.20	692	0.17	0.094	0.011	0.113	0.46	0.74	1.3	1.1	0.03	2.59	101
W062	13.74	9.12	bdl	0.007	0.003	0.09	487	0.08	0.019	0.009	0.063	0.03	0.36	0.5	0.4	0.03	4.44	89.2
W065	13.62	8.97	0.140	0.063	0.129	bdl	bdl	bdl	0.015	bdl	bdl	bdl	bdl	bdl	bdl	bdl	bdl	bdl
W067	13.5	8.98	0.006	0.032	0.007	0.09	892	0.14	0.018	0.033	0.612	0.04	0.46	4.5	1.2	0.04	5.32	129
W069	13.5	9.1	0.021	0.056	0.010	0.05	725	0.30	0.019	0.032	9.02	2.05	1.60	3.4	6.7	0.15	0.083	130
W071	13.55	9.05	0.007	0.004	0.006	0.02	754	0.24	0.059	0.012	0.068	0.05	0.50	1.4	2.3	0.02	0.437	116
W076	14.09	9.07	0.004	0.004	0.004	0.10	236	0.11	bdl	0.009	0.100	0.03	0.38	9.3	0.4	0.03	11.2	95.9
W077	13.64	9.46	0.004	0.022	0.006	0.11	431	0.15	bdl	0.007	0.235	0.07	0.84	4.9	0.5	bdl	14.7	33.4
W081	13.86	9.78	0.004	0.006	0.003	0.20	132	0.10	0.663	0.017	0.248	0.29	0.43	8.6	4.0	bdl	19.2	73.4
R001	13.59	9.3	0.128	0.021	0.106	bdl	bdl	0.02	0.004	bdl	bdl	bdl	bdl	bdl	bdl	bdl	bdl	bdl
R003	13.55	9.27	0.009	0.001	0.010	0.28	257	0.18		0.007	0.038	0.09	0.46	0.2	0.3	0.08	0.465	40.4
R004 A	13.54	9.32	0.006	0.002	0.006	0.38	409	0.28	0.004	0.004	0.063	0.12	1.09	0.3	0.7	0.07	2.12	9.23
R004 B	13.53	9.32	0.009	0.001	0.006	0.20	214	0.21		0.004	0.024	0.06	0.36	0.2	0.2	0.02	0.532	12.9
R004 C	13.53	9.32	0.006	0.001	0.003	0.27	243	0.12		0.009	0.026	0.05	0.39	0.2	0.2		0.508	16.4
R005	13.4	9.29	0.222	0.051	0.107	bdl	bdl	bdl	bdl	bdl	bdl	bdl	bdl	bdl	bdl	bdl	bdl	bdl
R006 A	12.94	9.33	0.200	0.047	0.131	bdl	bdl	bdl	bdl	bdl	bdl	bdl	bdl	bdl	bdl	bdl	bdl	bdl
R006 B	12.92	9.34	0.389	0.031	0.381	bdl	bdl	bdl	bdl	bdl	bdl	bdl	bdl	bdl	bdl	bdl	bdl	bdl
R007	13.95	9.75	0.072	0.185	0.007	bdl	bdl	0.13	0.011	bdl	bdl	bdl	bdl	bdl	bdl	bdl	bdl	bdl
R008	13.96	9.85	0.122	0.837	0.006	bdl	bdl	0.17	0.009	bdl	bdl	bdl	bdl	bdl	bdl	bdl	bdl	bdl

R012	14.18	8.76	0.022	0.323	0.005	bdl	bdl	0.33	0.004	bdl	bdl	bdl	bdl	bdl	bdl	bdl	bdl	bdl	
R013	14.17	8.65	0.691	0.565	0.059	bdl	bdl	bdl	0.004	bdl	bdl	bdl	bdl	bdl	bdl	bdl	bdl	bdl	
R009	13.69	9.1	0.004	0.001	0.003	0.27	184	0.11		0.004	0.022	0.04	0.28	0.2	0.2	0.02	0.335	18.7	
R010	13.67	9.05	0.042	0.018	0.011	bdl	bdl	bdl	bdl	bdl	bdl	bdl	bdl	bdl	bdl	bdl	bdl	bdl	
Sp001	13.51	9.29	0.007	0.002	0.008	0.03	162	0.42	0.004	0.005	0.044	0.22	0.36	1.6	0.2	0.02	0.675	80.0	
Rk	-	-	67366.7	666.7	146286.7	-	720.8	-	-	-	18.4	99.3	46.2	11.4	46.1	14.5	90.6	55.4	

B = borehole, W = dug-well, R = river or lake, Rk = rock, Temp = Temperature, EC = electrical conductivity, n = number of samples, bdl = below detection limit, letter following R004 and R006 represent the sample station. Data for rocks (which are presented here only as average values) are from Ndjigui et al. (2014)

Table 1b cont`d:

Ref. code	Be (µg/l)	Ga (µg/l)	Hf (µg/l)	Mo (µg/l)	Nb (µg/l)	Rb (µg/l)	Sb (µg/l)	Sc (µg/l)	Sn (µg/l)	Sr (µg/l)	Ta (µg/l)	Te (µg/l)	Th (µg/l)	Ti (µg/l)	Tl (µg/l)	U (µg/l)	W (µg/l)	Y (µg/l)	Zr (µg/l)
B001	0.007	0.002	bdl	2.11	bdl	1.55		0.30	0.03	245	0.001	bdl	bdl	0.34	0.007	0.029	bdl	0.004	bdl
B002	bdl	bdl	bdl	1.61	bdl	0.79	0.037	0.59	0.02	422	bdl	bdl	bdl	0.17	0.008	0.426	bdl	0.007	bdl
B004	bdl	0.004	0.001	0.35	bdl	1.65	0.027	0.51	0.03	667	0.001	bdl	bdl	0.39	0.010	1.62	bdl	0.068	bdl
B005	bdl	0.012	0.001	0.25	bdl	0.99	0.019	0.10	0.04	89.9	0.001	0.01	bdl	0.32	0.008	0.013	bdl	0.013	bdl
B008	bdl	0.010	0.001	0.85	bdl	0.55	0.019	0.50	0.03	771	0.001	bdl	bdl	0.30	0.009	2.09	bdl	0.165	0.006
B009	bdl	bdl	bdl	0.15	bdl	12.9	0.006	0.42	bdl	718	bdl	bdl	bdl	0.42	0.014	1.07	bdl	0.022	bdl
B010	bdl	0.002	bdl	0.55	bdl	29.7	bdl	0.40	bdl	1897	0.001	0.03	bdl	0.10	0.015	21.0	bdl	0.043	bdl
B011	bdl	bdl	bdl	0.01	bdl	29.3	0.009	0.21	0.03	90.3	bdl	bdl	bdl	0.21	0.047	0.283	bdl	0.002	bdl
B014	0.109	bdl	bdl	0.04	bdl	31.0	bdl	0.29	0.04	80.9	bdl	bdl	bdl	0.25	0.126	0.097	bdl	0.018	bdl
B015	0.030	0.006	bdl	0.06	bdl	128	0.014	0.39	0.03	609	bdl	bdl	bdl	0.30	0.657	0.219	bdl	0.308	bdl
B016	0.024	0.002	bdl	0.15	bdl	49.1	0.006	0.44	0.02	344	bdl	0.02	bdl	0.24	0.056	0.236	0.08	0.022	bdl
B019	0.014	0.005	0.001	0.01	bdl	27.4	bdl	0.24	bdl	36.9	bdl	0.03	bdl	0.28	0.061	0.530	bdl	0.004	bdl
B022	0.013	0.002	bdl	0.04	bdl	12.7	bdl	0.25	0.04	60.5	bdl	bdl	bdl	0.34	0.011	0.093	bdl	0.005	bdl
B025	0.224	0.880	0.049	0.09	0.366	22.6	0.081	0.79	0.49	63.6	0.023	bdl	0.384	69.7	0.076	0.192	bdl	0.849	1.86
B026	0.019	0.005	bdl	1.15	bdl	13.1	bdl	0.53	0.03	383	bdl	bdl	bdl	0.28	0.006	3.13	bdl	0.020	bdl
B028	bdl	0.002	bdl	0.92	bdl	0.43	0.007	0.49	0.04	430	bdl	0.02	bdl	0.30	0.005	1.19	bdl	0.072	bdl
B029	bdl	0.010	0.001	1.67	bdl	0.39	0.006	0.65	bdl	333	0.001	bdl	bdl	0.39	0.004	1.20	bdl	0.241	bdl
B031	bdl	0.017	0.001	28.8	bdl	0.31	0.020	0.52	0.03	180	bdl	0.02	bdl	0.38	0.003	0.757	0.51	0.037	0.009
B032	bdl	0.008	0.001	9.73	bdl	0.47	0.008	0.54	0.04	173	bdl	0.02	bdl	0.51	0.005	0.918	bdl	0.015	bdl

B034	bdl	0.006	0.001	7.14	bdl	0.97	bdl	0.58	bdl	636	0.001	0.03	bdl	0.79	0.007	2.93	bdl	0.132	0.006
B035		0.017	0.003	10.7	0.021	5.92	0.328	0.42	bdl	1653	0.005	0.03	bdl	0.45	0.010	1.56	0.48	0.021	0.010
B036	0.008	0.008	bdl	23.3	bdl	6.19	0.007	0.36	0.01	1455	bdl	0.01	bdl	0.42	0.005	9.21	0.11	0.173	0.005
B037	0.300	1.15	0.075	0.13	0.407	7.08	0.007	0.78	0.15	39.8	0.034	bdl	0.543	60.2	0.034	0.334	bdl	2.63	1.65
B039	0.058	0.012	0.003	35.4	bdl	1.68	0.005	0.41	0.02	834	0.001	0.01	bdl	0.52	0.004	38.3	bdl	0.049	0.015
B040	0.028	0.005	bdl	0.22	bdl	0.98	0.054	0.75	0.04	221	bdl	bdl		0.58	0.004	0.451	bdl	0.006	bdl
B041	0.007	0.004	bdl	0.13	bdl	4.15	0.011	0.50	0.02	786	bdl	0.01	bdl	0.35	0.006	0.928	bdl	0.023	bdl
B042	0.023	0.006	bdl	0.07	bdl	1.62		0.40	0.02	636	bdl	bdl		0.37	0.004	0.111	bdl	0.009	bdl
B043	0.014	0.002	bdl	0.12	bdl	0.98	0.020	0.51	0.03	947	bdl	0.02	bdl	0.30	0.004	0.232	bdl	0.013	bdl
B044	bdl	0.006	bdl	0.22	bdl	5.34	0.014	0.51		1973	bdl	0.01	bdl	0.30	0.006	4.87	bdl	0.031	bdl
B046	0.289	0.005	0.001	0.01	bdl	19.0	0.051	0.33	0.03	103	bdl	0.02	bdl	0.37	0.080	0.059	bdl	0.016	bdl
B049	bdl	0.004	bdl	0.08	bdl	0.50	0.098	0.51	bdl	836	0.001	0.04	bdl	0.38	0.005	0.279	bdl	0.054	bdl
B051	bdl	bdl	bdl	0.14	bdl	0.85		0.66	0.03	336	0.001	0.01	bdl	0.40	0.003	0.074	bdl	0.011	bdl
B053	0.023	bdl	bdl	0.13	bdl	1.60	0.014	0.68	0.02	2989	0.001	0.04	bdl	0.23	0.013	1.52	bdl	0.088	bdl
B055	bdl	0.005	bdl	2.18	bdl	2.69	0.026	0.48	bdl	735	0.001	0.03	bdl	0.27	0.006	1.02	0.08	0.014	bdl
W005	bdl	0.005	bdl	1.45	bdl	1.29	0.016	0.47	0.04	840	0.001	0.02	bdl	0.52	0.006	4.26	bdl	0.028	bdl
W006	bdl	bdl	0.001	0.97	bdl	1.40	0.030	0.56	bdl	1771	0.001	0.01	bdl	0.18	0.006	1.86	0.07	0.038	bdl
W008	bdl	0.004	bdl	0.08	bdl	23.4	0.021	0.50	bdl	533	bdl	0.04	bdl	0.51	0.051	0.023	bdl	0.077	bdl
W009	0.016	bdl	bdl	0.08	bdl	25.2	0.048	0.57	bdl	1384	bdl	bdl	bdl	0.31	0.050	0.169	bdl	0.036	bdl
W012	bdl	0.018	bdl	1.44	bdl	41.3	0.069	0.40	0.04	333	bdl	0.01	bdl	0.26	0.045	0.059	bdl	0.088	0.006
W014	bdl	bdl	bdl	bdl	bdl	bdl	bdl	bdl	bdl	bdl	bdl	bdl	bdl	bdl	bdl	bdl	bdl	bdl	bdl
W015	0.021	0.001	bdl	0.02	bdl	18.8	0.014	0.11	0.03	152	bdl	0.06	bdl	0.20	0.020	0.004	bdl	0.020	bdl

W016	bdl	bdl	bdl	3.93	bdl	88.4	0.425	0.38	0.02	532	0.001	bdl	bdl	0.18	0.133	0.532	0.10	0.034	bdl	
W017	bdl	0.003	bdl	0.99	bdl	52.6	0.053	0.37	0.02	467	bdl	0.01	bdl	0.23	0.062	0.317	bdl	0.018	0.006	
W020	0.009	0.001	bdl	0.01	bdl	21.5	0.004	0.27	bdl	24.4	bdl	bdl	bdl	0.21	0.016	0.026	bdl	0.002	bdl	
W021	bdl	0.001	bdl	0.20	bdl	40.2	0.066	0.35	bdl	218	bdl	bdl	bdl	0.37	0.067	0.013	bdl	0.044	bdl	
W022	bdl	0.003	bdl	1.79	bdl	67.4	0.048	0.32	bdl	298	bdl	0.02	bdl	0.26	0.128	0.287	bdl	0.015	bdl	
W023	bdl	0.003	bdl	0.15	bdl	15.6	0.022	0.49	0.04	478	bdl	0.02	bdl	0.38	0.060	0.219	bdl	0.017	bdl	
W024	bdl	0.013	bdl	0.19	bdl	35.5	0.022	0.16	bdl	212	bdl	bdl	bdl	0.31	0.117	0.018	bdl	0.177	bdl	
W025	bdl	0.008	bdl	0.18	bdl	67.5	0.284	0.27	0.06	521	bdl	bdl	bdl	0.16	0.336	0.031	bdl	0.125	bdl	
W028	0.307	0.056	bdl	0.23	bdl	43.5	0.047	0.46	0.03	352	bdl	0.03	bdl	0.65	0.297	0.238	bdl	1.22	0.011	
W029	0.065	0.011	bdl	0.08	bdl	19.5	0.017	0.41	0.04	144	bdl	0.02	bdl	0.34	0.032	0.090	bdl	0.039	bdl	
W033	bdl	0.007	bdl	0.19	bdl	0.15	0.008	0.27	bdl	123	bdl	bdl	bdl	0.19	bdl	0.154	bdl	0.013	bdl	
W034	bdl	bdl	bdl	bdl	bdl	bdl	bdl	bdl	bdl	bdl	bdl	bdl	bdl	bdl	bdl	bdl	bdl	bdl	bdl	
W036	bdl	0.002	0.001	6.35	0.005	1.17	0.186	0.62	0.03	2483	0.002	0.04	bdl	0.38	0.006	1.47	0.09	0.035	0.005	
W038	bdl	0.003	bdl	0.44	bdl	0.72	0.013	0.84	0.02	2560	0.001	bdl	bdl	0.74	0.005	3.43	bdl	0.093	bdl	
W041	0.012	0.005	0.001	1.91	bdl	1.58	0.012	0.66	0.03	1601	bdl	bdl	bdl	0.54	0.004	2.75	bdl	0.045	0.008	
W049	bdl	0.002	bdl	1.24	bdl	0.52	0.020	0.60	bdl	349	0.002	0.03	bdl	0.26	0.003	0.157	bdl	0.011	bdl	
W051	bdl	0.007	bdl	1.07	bdl	0.65	0.008	0.46	0.03	349	bdl	bdl	bdl	0.64		0.369	bdl	0.017	0.005	
W052	0.008	0.002	0.001	7.77	bdl	0.65	0.007	0.66	0.03	564	bdl	0.03	bdl	0.54	0.005	5.06	bdl	0.020	0.008	
W053	0.016	0.002	bdl	5.81	bdl	0.69	0.008	0.62	0.03	599	0.001	bdl	bdl	0.40	0.003	7.00	bdl	0.045	0.005	
W054	bdl	0.003	0.001	0.98	bdl	0.75	0.013	0.62	0.02	662	0.001	bdl	bdl	0.39	0.006	0.470	bdl	0.026	0.006	
W057	bdl	0.003	0.001	0.88	bdl	3.61	0.045	1.15	0.03	2588	0.001	0.04	bdl	0.35	0.008	2.73	bdl	0.064	0.006	
W061	0.013	0.009	bdl	0.27	bdl	31.9	0.028	0.74	bdl	661	0.001	bdl	bdl	0.48	0.038	0.161	bdl	0.050	bdl	

W062	bdl	0.002	bdl	0.56	bdl	6.93	0.010	0.63	0.02	690	0.001	0.02	bdl	0.70	0.010	0.556	bdl	0.046	bdl
W065	bdl	bdl	bdl	bdl	bdl	bdl	bdl	bdl	bdl	bdl	bdl	bdl	bdl	bdl	bdl	bdl	bdl	bdl	bdl
W067	0.008	0.005	bdl	0.16	bdl	12.8	0.013	1.08	bdl	643	0.001	bdl	bdl	0.99	0.014	0.047	bdl	0.018	bdl
W069	0.085	0.021	bdl	0.01	bdl	19.9	bdl	0.15	0.04	158	bdl	bdl	0.20	0.024	1.04	bdl	0.327	bdl	
W071	0.020	0.006	bdl	0.01	bdl	38.5	bdl	0.27	0.03	510	0.001	bdl	bdl	0.29	0.043	0.013	bdl	0.054	bdl
W076	bdl	0.003	bdl	0.05	bdl	0.59	0.008	0.54	0.02	899	0.001	0.02	bdl	0.57	0.003	0.251	bdl	0.046	bdl
W077	bdl	bdl	0.007	2.84	0.017	1.10	0.036	0.82	0.27	1059	0.006	bdl	bdl	0.31	0.003	5.02	0.28	0.045	0.016
W081	bdl	bdl	0.001	0.71	bdl	0.72	0.009	1.13	bdl	2512	0.001	0.02	bdl	0.44	0.005	1.18	0.05	0.075	bdl
R001	bdl	bdl	bdl	bdl	bdl	bdl	bdl	bdl	bdl	bdl	bdl	bdl	bdl	bdl	bdl	bdl	bdl	bdl	bdl
R003	bdl	0.006	bdl	0.20	bdl	1.22	0.009	0.09	0.02	98.1	bdl	0.03	bdl	0.41	0.003	0.041	bdl	0.024	bdl
R004 A	bdl	0.023	bdl	0.56	bdl	0.65	0.023	0.09	bdl	156	0.001	bdl	bdl	0.37	bdl	0.142	bdl	0.038	0.006
R004 B	bdl	0.006	bdl	0.27	bdl	0.99	0.026	0.14	bdl	94.4	bdl	0.03	bdl	0.24	bdl	0.015	bdl	0.020	bdl
R004 C	bdl	0.006	bdl	0.29	bdl	1.05	0.012	0.08	0.02	99.1	bdl	0.02	bdl	0.32	bdl	0.014	bdl	0.014	bdl
R005	bdl	bdl	bdl	bdl	bdl	bdl	bdl	bdl	bdl	bdl	bdl	bdl	bdl	bdl	bdl	bdl	bdl	bdl	bdl
R006 A	bdl	bdl	bdl	bdl	bdl	bdl	bdl	bdl	bdl	bdl	bdl	bdl	bdl	bdl	bdl	bdl	bdl	bdl	bdl
R006 B	bdl	bdl	bdl	bdl	bdl	bdl	bdl	bdl	bdl	bdl	bdl	bdl	bdl	bdl	bdl	bdl	bdl	bdl	bdl
R007	bdl	bdl	bdl	bdl	bdl	bdl	bdl	bdl	bdl	bdl	bdl	bdl	bdl	bdl	bdl	bdl	bdl	bdl	bdl
R008	bdl	bdl	bdl	bdl	bdl	bdl	bdl	bdl	bdl	bdl	bdl	bdl	bdl	bdl	bdl	bdl	bdl	bdl	bdl
R012	bdl	bdl	bdl	bdl	bdl	bdl	bdl	bdl	bdl	bdl	bdl	bdl	bdl	bdl	bdl	bdl	bdl	bdl	bdl
R013	bdl	bdl	bdl	bdl	bdl	bdl	bdl	bdl	bdl	bdl	bdl	bdl	bdl	bdl	bdl	bdl	bdl	bdl	bdl
R009	bdl	0.007	bdl	0.25	bdl	1.20	0.015	0.13	0.03	102	bdl	0.03	bdl	0.10	bdl	0.012		0.006	bdl
R010	bdl	bdl	bdl	bdl	bdl	bdl	bdl	bdl	bdl	bdl	bdl	bdl	bdl	bdl	bdl	bdl	bdl	bdl	bdl

Sp001	0.013	0.008	0.001	0.04	bdl	16.9	0.006	0.31	bdl	12.4	bdl	bdl	bdl	0.27	0.009	0.005	bdl	0.017	bdl
Rk	1.0	17.5	5.3	3.4	11.6	36.6	-	10.9	1.2	115.5	0.8	-	29.9	8100.0	0.3	2.2	0.4	18.4	542.6

B = borehole, W = dug-well, R = river or lake, Rk = rock, Temp = Temperature, EC = electrical conductivity, n = number of samples, bdl = below detection limit, letter following R004 and R006 represent the sample station. Data for rocks (which are presented here only as average values) are from Ndjigui et al. (2014)

Table 1c

Click here to access/download;Table;Table 1c.docx

Table 1d :

Ref. code	La	Ce	Pr	Nd	Sm	Eu	Gd	Tb	Dy	Ho	Er	Tm	Yb	Lu	∑REE	LREE	HREE	MREE	LREE/HREE	$(Er/Nd)_N$	Eu/Eu*	Ce/Ce*	La/Yb	La/Sm	Gd/Dy
B001	0.002	0.002	0.001	-	0.003	0.050	0.002	-	-	-	0.001	-	-	-	0.061	0.005	0.001	0.055	5.000	-	96.119	0.326	-	0.667	-
B002	0.001	-	-	-	-	0.041	0.002	-	-	-	-	-	-	-	0.044	0.001	0.000	0.043	-	-	-	-	-	-	-
B004	0.014	0.010	0.002	0.012	0.007	0.086	0.007	0.001	0.003	0.001	0.002	-	0.002	0.001	0.148	0.038	0.009	0.101	4.222	1.982	57.852	0.436	7.000	2.000	2.333
B005	0.013	0.020	0.003	0.014	0.004	0.054	0.004	-	0.001	-	0.001	-	0.001	-	0.115	0.050	0.003	0.062	16.667	0.850	63.570	0.739	13.000	3.250	4.000
B008	0.047	0.051	0.008	0.045	0.007	0.074	0.010	0.002	0.014	0.004	0.007	0.001	0.004	-	0.274	0.151	0.030	0.093	5.033	1.850	41.648	0.607	11.750	6.714	0.714
B009	0.003	0.003	-	0.002	0.003	0.094	0.007		0.002	-		-	0.001	-	0.115	0.008	0.003	0.104	2.667	0.000	96.590	-	3.000	1.000	3.500
B010	0.010	0.028	0.002	0.008	0.010	0.156	0.008	0.001	0.003	-	0.001	-	0.001	-	0.228	0.048	0.005	0.175	9.600	1.487	82.129	1.445	10.000	1.000	2.667
B011	0.005	0.003	-	0.002	0.005	0.184	0.006	-	0.001	-	-	-	-	-	0.206	0.010	0.001	0.195	10.000	0.000	158.188	-	-	1.000	6.000
B014	0.007	0.004	0.001	0.002	0.005	0.081	0.006	-	0.001	-	0.001	-	-	-	0.108	0.014	0.002	0.092	7.000	5.947	69.637	0.349	-	1.400	6.000
B015	0.217	0.030	0.026	0.119	0.019	0.181	0.024	0.002	0.016	0.003	0.009	0.001	0.007	0.001	0.655	0.392	0.037	0.226	10.595	0.900	39.913	0.092	31.000	11.421	1.500
B016	0.007	0.006	0.001	0.005	0.005	0.067	0.007	-	0.001	0.001	0.002	-	0.006	0.001	0.109	0.019	0.011	0.079	1.727	4.758	53.328	0.523	1.167	1.400	7.000
B019	0.003	0.002	-	0.002	0.004	0.088	0.005	-	-	-	-	-	-	-	0.104	0.007	0.000	0.097	28.000	0.000	92.658	-	-	0.750	-
B022	0.008	0.009	0.002	0.009	0.003	0.081	0.002	-	-	-	0.001	-	-	-	0.115	0.028	0.001	0.086	17.145	1.322	155.710	0.519	-	2.667	-
B025	2.000	2.640	0.461	1.500	0.318	0.168	0.240	0.033	0.174	0.031	0.091	0.012	0.065	0.012	7.745	6.601	0.385	0.759	11.333	0.722	2.860	0.634	30.769	6.289	1.379
B026	0.009	0.013	0.002	0.010	0.008	0.153	0.009	-	0.002		0.001	-	-	-	0.207	0.034	0.003	0.170	4.000	1.189	84.910	0.707	-	1.125	4.500
B028	0.028	0.009	0.005	0.022	0.003	0.022	0.007	0.001	0.007	0.002	0.003	0.001	0.002	0.001	0.113	0.064	0.016	0.033	3.044	1.622	22.610	0.176	14.000	9.333	1.000
B029	0.041	0.014	0.015	0.067	0.013	0.049	0.014	0.003	0.018	0.004	0.013	0.001	0.008	0.001	0.261	0.137	0.045	0.079	28.000	2.308	17.100	0.130	5.125	3.154	0.778
B031	0.182	0.095	0.031	0.118	0.012	0.065	0.007	-	0.002	0.001	0.001	-	0.002	-	0.516	0.426	0.006	0.084	71.000	0.101	33.396	0.292	91.000	15.167	3.500
B032	0.036	0.038	0.006	0.021	0.003	0.057	0.003	-	0.001	-	0.001	-	0.001	0.001	0.168	0.101	0.004	0.063	25.250	0.566	89.468	0.597	36.000	12.000	3.000
B034	0.022	0.028	0.005	0.030	0.014	0.080	0.008	0.001	0.011	0.002	0.008	0.001	0.009	0.002	0.221	0.085	0.033	0.103	2.576	3.172	35.596	0.616	2.444	1.571	0.727
B035	0.003	-	-	-	-	0.045	-	-	0.001	-	-	-	-	0.001	0.050	0.003	0.002	0.045	1.500	-	-	-	-	-	0.000
B036	0.034	0.047	0.005	0.029	0.009	0.043	0.012	-	0.008	0.002	0.007	0.001	0.002	0.001	0.200	0.115	0.021	0.064	5.476	2.871	19.484	0.832	17.000	3.778	1.500
B037	3.300	4.960	0.870	3.310	0.674	0.146	0.600	0.084	0.474	0.078	0.225	0.039	0.219	0.037	15.016	12.44	1.072	1.504	11.604	0.809	1.081	0.675	15.068	4.896	1.266
B039	0.012	0.022	0.003	0.011	0.007	0.050	0.002	0.001	0.004	0.002	0.004	-	0.001	-	0.119	0.048	0.011	0.060	4.364	4.325	62.925	0.846	12.000	1.714	0.500
B040	0.005	0.008	0.001	0.005	0.007	0.059	0.003	-	0.001	-	-	-	0.001	-	0.090	0.019	0.002	0.069	9.500	0.000	60.626	0.825	5.000	0.714	3.000
B041	0.006	0.018	0.001	0.005	0.006	0.089	0.003	-	0.001	-	0.001	-	0.001	-	0.131	0.030	0.003	0.098	10.000	2.379	98.780	1.695	6.000	1.000	3.000
B042	0.004	0.005	-	0.003	0.006	0.083	0.004	-	-	-	-	-	0.001	-	0.106	0.012	0.001	0.093	12.000	0.000	79.779	-	4.000	0.667	-
B043	0.008	0.015	0.001	0.003	0.003	0.104	0.002	-	-	-	-	-	0.002	-	0.138	0.027	0.002	0.109	13.500	0.000	199.928	1.224	4.000	2.667	-
B044	0.007	0.012	-	0.003	0.004	0.224	0.010	-	-	-	0.002	-	0.001	-	0.263	0.022	0.003	0.238	7.333	7.930	166.776	-	7.000	1.750	-
B046	0.017	0.107	0.010	0.024	0.006	0.117	0.013	0.001	0.002	0.001	-	-	0.001	-	0.299	0.158	0.004	0.137	39.500	0.000	62.381	1.893	17.000	2.833	6.500
B049	0.032	0.032	0.007	0.021	0.005	0.112	0.007	-	0.002	0.001	0.004	-	0.002	-	0.225	0.092	0.009	0.124	10.222	2.266	89.146	0.493	16.000	6.400	3.500
B051	0.003	0.006	-	0.003	0.006	0.070	0.004	-	-	-	0.000	-		-	0.092	0.012	0.000	0.080	-	0.000	67.283	-	-	0.500	-
B053	0.024	0.026	0.005	0.011	0.019	0.400	0.019	0.001	0.003	0.001	0.002	-	0.005	0.001	0.517	0.066	0.012	0.439	5.500	2.163	99.134	0.548	4.800	1.263	6.333
B055	0.002	0.002	-		0.002	0.031	0.002	-	-	-	-	-	0.001	-	0.040	0.004	0.001	0.035	4.000	-	72.987	-	2.000	1.000	-
W005	0.014	0.026	0.002	0.008	0.000	0.063	0.002	0.001	0.002	0.001	0.001	-	-	0.001	0.121	0.050	0.005	0.066	10.000	1.487	-	1.134	-	-	1.000
W006	0.005	0.004	0.001	0.006	0.009	0.080	0.005	-	0.001	-	0.001	-	-	-	0.112	0.016	0.002	0.094	8.000	1.982	56.156	0.413	-	0.556	5.000
W008	0.047	0.014	0.012	0.075	0.014	0.177	0.015	0.001	0.006	0.001	0.004	0.001	0.002	-	0.369	0.148	0.014	0.207	10.571	0.634	57.515	0.136	23.500	3.357	2.500
W009	0.019	0.014	0.004	0.011	0.013	0.327	0.015		0.002		0.002		0.001	-	0.408	0.048	0.005	0.355	9.600	2.163	110.267	0.371	19.000	1.462	7.500
W012	0.070	0.048	0.020	0.092	0.011	0.089	0.016	0.002	0.013	0.003	0.014	0.002	0.016	0.003	0.399	0.230	0.051	0.118	4.510	1.810	31.590	0.296	4.375	6.364	1.231
W015	0.011	0.011	0.004	0.022	0.012	0.154	0.008	0.001	0.005	0.001	0.003		0.003	0.001	0.236	0.048	0.013	0.175	3.692	1.622	74.012	0.383	3.667	0.917	1.600
W016	0.004	-	-	-	0.006	0.054	0.002	-	0.003	0.001	0.006	0.002	0.024	0.006	0.108	0.004	0.042	0.062	0.095	-	73.404	-	0.167	0.667	0.667
W017	0.005	0.004	-	-	0.007	0.117	0.006	-	0.001	-	0.002	-	0.003	0.001	0.146	0.009	0.007	0.130	1.286	-	85.011	-	1.667	0.714	6.000
W020	0.006	0.005	0.001	0.002	0.008	0.099	0.003	-	-	-	-	-	-	-	0.124	0.014	0.000	0.110	-	0.000	95.158	0.471	-	0.750	-
W021	0.025	0.015	0.007	0.024	0.005	0.074	0.008	0.001	0.004	0.001	0.003	-	0.002	0.001	0.170	0.071	0.011	0.088	6.455	1.487	55.096	0.262	12.500	5.000	2.000
W022	0.009	0.017	0.003	0.003	0.006	0.062	0.008	-	0.001	-	-	-	0.001	-	0.110	0.032	0.002	0.076	16.000	0.000	42.139	0.755	9.000	1.500	8.000
W023	0.010	0.014	0.002	0.011	0.006	0.122	0.003	-	-	-	0.001	-	0.001	-	0.170	0.037	0.002	0.131	18.500	1.081	135.406	0.722	10.000	1.667	-
W024	0.076	0.073	0.023	0.103	0.035	0.174	0.030	0.005	0.021	0.005	0.019	0.002	0.017	0.004	0.587	0.275	0.068	0.244	4.044	2.194	25.285	0.403	4.471	2.171	1.429
W025	0.037	0.020	0.009	0.058	0.029	0.366	0.021	0.002	0.016	0.003	0.020	0.004	0.020	0.004	0.609	0.124	0.067	0.418	1.851	4.102	69.837	0.253	1.850	1.276	1.313
W028	0.109	0.411	0.085	0.505	0.131	0.195	0.164	0.025	0.164	0.037	0.125	0.020	0.126	0.022	2.119	1.110	0.494	0.515	2.247	2.944	6.265	0.985	0.865	0.832	1.000
W029	0.025	0.092	0.006	0.035	0.013	0.134	0.008	0.001	0.006	0.001	0.004	-	0.002	-	0.327	0.158	0.013	0.156	12.154	1.359	61.873	1.733	12.500	1.923	1.333
W033	0.007	0.018	0.001	0.003	0.002	0.020	0.002	-	0.002	0.001	0.002	-	0.001	-	0.059	0.029	0.006	0.024	4.833	7.930	47.089	1.570	7.000	3.500	1.000
W036	0.001	0.002	-	0.002	0.002	0.073	0.002	-	-	-	-	-	-	-	0.082	0.005	0.000	0.077	-	0.000	171.873	-	-	0.500	-
W038	0.046	0.022	0.005	0.021	0.025	0.591	0.027	0.002	0.007	0.001	0.002	-	0.001	0.002	0.752	0.094	0.013	0.645	7.231	1.133	107.115	0.335	46.000	1.840	3.857
W041	0.016	0.008	0.002	0.008	0.013	0.249	0.013	-	0.006	0.001	0.001	-	0.001	-	0.318	0.034	0.009	0.275	3.778	1.487	90.193	0.326	16.000	1.231	2.167
W049	0.003	-	-	0.001	0.004	0.036	0.003	-	0.001	-	0.001	-	0.001	-	0.050	0.004	0.003	0.043	1.333	11.895	48.936	-	3.000	0.750	3.000
W051	0.011	0.018	0.002	0.004	0.009	0.078	0.005	-	0.001	-	-	-	0.001	-	0.129	0.035	0.002	0.092	17.500	0.000	54.753	0.885	11.000	1.222	5.000
W052	0.010	0.010	0.001	0.007	0.002	0.059	0.003	-	0.001	0.001	0.002	-	0.001	-	0.097	0.028	0.005	0.064	5.600	3.398	113.421	0.730	10.000	5.000	3.000
W053	0.010	0.017	0.003	0.007	0.005	0.049	0.003	-	0.002	-	-	0.001	0.001	0.001	0.099	0.037	0.005	0.057	7.400	0.000	59.575	0.716	10.000	2.000	1.500
W054	0.014	0.069	0.005	0.017	0.012	0.099	0.009	-	0.001	-	0.002	-	-	-	0.228	0.105	0.003	0.120	35.000	1.399	44.858	1.903	-	1.167	9.000
W057	0.012	0.032	0.002	0.006	-	0.063	0.003	-	0.003	0.001	0.001	0.001	0.001	-	0.125	0.052	0.007	0.066	7.429	1.982	-	1.507	12.000	-	1.000
W061	0.024	0.015	0.004	0.023	0.006	0.218	0.014	0.001	0.007	0.001	0.004	-	0.003	-	0.320	0.066	0.015	0.239	4.400	2.069	112.004	0.353	8.000	4.000	2.000
W062	0.017	0.032	0.003	0.012	0.008	0.141	0.011	-	0.005	-	0.002	-	0.001	-	0.232	0.064	0.008	0.160	8.000	1.982	70.777	1.034	17.000	2.125	2.200
W067	0.014	0.026	0.004	0.006	0.017	0.270	0.012	-	0.004	-	0.001	-	-	-	0.354	0.050	0.005	0.299	10.000	1.982	89.015	0.802	-	0.824	3.000
W069	0.045	0.080	0.032	0.141	0.087	0.243	0.080	0.012	0.070	0.011	0.037	0.004	0.024	0.006	0.872	0.298	0.152	0.422	1.961	3.121	13.716	0.486	1.875	0.517	1.143
W071	0.028	0.023	0.009	0.029	0.019	0.229	0.017	0.001	0.004	0.001	0.004	0.001	0.004	0.001	0.370	0.089	0.015	0.266	5.933	1.641	60.000	0.334	7.000	1.474	4.250

W076	0.026	0.019	0.005	0.034	0.001	0.074	0.009	-	0.004	-	0.001	0.001	0.001	0.001	0.176	0.084	0.008	0.084	10.500	0.350	116.152	0.384	26.000	26.000	2.250
W077	0.010	0.002	0.001	0.011	0.010	0.134	0.007	0.001	0.003	-	0.003	0.001	0.001	0.001	0.185	0.024	0.009	0.152	2.667	3.244	75.417	0.146	10.000	1.000	2.333
W081	0.007	-	0.001	0.005	0.004	0.039	0.003	-	0.002	0.001	0.003	0.001	0.001	0.001	0.068	0.013	0.009	0.046	1.444	7.137	53.014	0.000	7.000	1.750	1.500
R003	0.032	0.071	0.006	0.025	0.008	0.076	0.008	0.001	0.003	-	0.002	-	0.001	-	0.233	0.134	0.006	0.093	22.333	0.952	44.734	1.182	32.000	4.000	2.667
R004 A	0.057	0.103	0.010	0.041	0.003	0.126	0.010	0.002	0.003	0.001	0.003	-	0.001	-	0.360	0.211	0.008	0.141	26.375	0.870	108.324	0.995	57.000	19.000	3.333
R004 B	0.012	0.024	0.004	0.012	0.004	0.065	0.004	-	0.002	-	0.002	-	0.002	0.001	0.132	0.052	0.007	0.073	7.429	1.982	76.519	0.799	6.000	3.000	2.000
R004 C	0.013	0.027	0.002	0.019	0.007	0.071	0.003	-	-	-	0.001	-	0.001	-	0.144	0.061	0.002	0.081	30.500	0.626	72.957	1.222	13.000	1.857	-
R009	0.008	0.014	0.001	-	0.002	0.056	0.003	-	0.001	-	0.001	-	-	-	0.086	0.023	0.002	0.061	11.500	-	107.653	1.142	-	4.000	3.000
Sp001	0.019	0.044	0.003	0.015	0.012	0.045	0.004	0.001	0.001	0.001	0.001	-	0.002	-	0.148	0.081	0.005	0.062	16.200	0.793	30.585	1.345	9.500	1.583	4.000
PAAS	38.2	79.6	8.83	33.9	5.55	1.08	4.66	0.77	4.68	0.990	2.85	0.41	2.82	0.43	184.770	160.530	12.180	12.060	13.180	1.000	1.000	1.000	13.546	6.883	0.996

Table 2:

	mean_Rock	mean_trend	Average	B025	B037	B044	B053	W028	W038	W061	W069	R004A	Sp001
Al	146286.67	79.46	0	0.01	0.02	0	NA	0	0	0	0	0	0
Th	29.93	0.46	0.01	0.15	0.3	NA	NA	NA	NA	NA	NA	NA	NA
Fe	67366.67	181.7	0	0.02	0.25	0	NA	0	NA	NA	0	0	0.01
Pb	14.53	0.19	0.01	3.96	1	0.02	0	0	0	0	0.03	0.01	0.07
Cu	46.16	1.81	0.03	3.02	0.68	0.16	0.04	0.51	0	0.02	0.11	0.06	0.41
Co	18.37	1.06	0.04	0.51	0.39	0	0	3.09	0	0.01	1.49	0.01	0.13
Cr	99.33	0.27	0	0.35	0.23	0	0	0	0	0.01	0.06	0	0.12
Ni	46.1	1.81	0.03	0.65	0.57	0	0.01	1.45	0	0.03	0.44	0.04	0.23
V	90.61	5.44	0.04	0.25	0.37	0.09	0.01	0.01	0.02	0.03	0	0.06	0.39
Mn	666.67	61.3	0.06	0.29	1.11	0	0	1.71	0	0.01	0.27	0.01	0.18
Zn	55.4	134.57	1.6	87.55	9.29	1.19	1.19	6.67	0.26	2.07	7.11	0.44	76.33
Ba	720.78	421.1	0.38	6.68	2.64	1.24	0.7	1.38	0.38	1.09	3.05	1.49	11.82
Sr	115.47	670.3	3.82	6.61	5.71	17.42	8.77	5.19	2.92	6.51	4.15	3.54	5.65
Li	11.38	7.19	0.42	4.43	3.35	1.26	0.29	5.88	0.08	0.13	0.91	0.07	7.39
Ca	8926.67	40312	2.98	5.04	5.68	0.4	4.9	2.88	2.17	6.59	1.74	3.82	5.77
Rb	36.58	15.28	0.28	7.42	3.2	0.15	0.01	2.02	0	0.99	1.65	0.05	24.3
K	16673.33	8024	0.32	8.35	1.89	0.23	0.26	2.35	0.04	1.79	0.96	0.52	26.81
Na	9606.67	31459	2.16	32.24	14.99	6.29	1.09	5.46	0.76	2.72	14.83	17.74	6.02
U	2.23	1.85	0.55	1.03	2.48	2.22	0.23	0.18	0.2	0.08	1.41	0.17	0.12
Mo	3.36	2.34	0.46	0.32	0.64	0.07	0.01	0.12	0.02	0.09	0.01	0.44	0.63
Mg	9520	14449	1	1	1	1	1	1	1	1	1	1	1

NA= not analysed. B0 = borehole. W0 = Hand dug wells. Sp = Spring. R = River. Rk= rocks (the average values for elements in rocks were calculated from the data of Ndjigui et al. 2014)